Pacific Northwest
NATIONAL LABORATORY

*Proudly Operated by* **Battelle** *Since 1965*

# Contaminant Attenuation and Transport Characterization of 200-DV-1 Operable Unit Sediment Samples

## May 2017

MJ Truex        CT Resch        SR Baum
JE Szecsody     BN Gartman      BB Christiansen
NP Qafoku       L Zhong         RE Clayton
CE Strickland   MK Nims         EM McElroy
JJ Moran        DL Saunders     D Appriou
BD Lee          BD Williams     KJ Tyrrell
MM Snyder       JA Horner       ML Striluk
AR Lawter       II Leavy

**DISCLAIMER**

This report was prepared as an account of work sponsored by an agency of the United States Government. Neither the United States Government nor any agency thereof, nor Battelle Memorial Institute, nor any of their employees, **makes any warranty, express or implied, or assumes any legal liability or responsibility for the accuracy, completeness, or usefulness of any information, apparatus, product, or process disclosed, or represents that its use would not infringe privately owned rights**. Reference herein to any specific commercial product, process, or service by trade name, trademark, manufacturer, or otherwise does not necessarily constitute or imply its endorsement, recommendation, or favoring by the United States Government or any agency thereof, or Battelle Memorial Institute. The views and opinions of authors expressed herein do not necessarily state or reflect those of the United States Government or any agency thereof.

PACIFIC NORTHWEST NATIONAL LABORATORY
*operated by*
BATTELLE
*for the*
UNITED STATES DEPARTMENT OF ENERGY
*under Contract DE-AC05-76RL01830*

Printed in the United States of America

Available to DOE and DOE contractors from
the Office of Scientific and Technical
Information,
P.O. Box 62, Oak Ridge, TN 37831-0062
www.osti.gov
ph: (865) 576-8401
fox: (865) 576-5728
email: reports@osti.gov

Available to the public from the National Technical Information Service
5301 Shawnee Rd., Alexandria, VA 22312
ph: (800) 553-NTIS (6847)
or (703) 605-6000
email: info@ntis.gov
Online ordering: http://www.ntis.gov

# Contaminant Attenuation and Transport Characterization of 200-DV-1 Operable Unit Sediment Samples

MJ Truex
JE Szecsody
NP Qafoku
CE Strickand
JJ Moran
BD Lee
MM Snyder
AR Lawter

CT Resch
BN Gartman
L Zhong
MK Nims
DL Saunders
BD Williams
JA Horner
II Leavy

SR Baum
BB Christiansen
RE Clayton
EM McElroy
D Appriou
KJ Tyrrell
ML Striluk

May 2017

# Summary

Contaminants disposed of at the land surface must migrate through the vadose zone before entering groundwater. Processes that occur in the vadose zone can attenuate contaminant concentrations during transport through the vadose zone. Thus, quantifying contaminant attenuation and contaminant transport processes in the vadose zone, in support of the conceptual site model (CSM) and fate and transport assessments, is important for assessing the need for, and type of, remediation in the vadose zone and groundwater. The framework to characterize attenuation and transport processes provided in U.S. Environmental Protection Agency (EPA) guidance documents was used to guide the laboratory effort reported herein.

The 200-DV-1 Operable Unit (OU) is in the process of characterizing the vadose zone to support a remedial investigation and feasibility study. Through a data quality objectives process, specific 200-DV-1 waste sites were selected for evaluation of attenuation and transport processes for mobile uranium, technetium-99 (Tc-99), iodine-129 (I-129), chromium, and nitrate contaminants. The specific elements of the laboratory effort were selected to provide data and associated interpretation to support the following three objectives:

- Define the contaminant distribution and the hydrologic and biogeochemical setting

- Identify attenuation processes and describe the associated attenuation mechanisms

- Quantify attenuation and transport parameters for use in evaluating remedies

These objectives are elements of the framework identified in EPA guidance for evaluating Monitored Natural Attenuation (MNA) of inorganic contaminants, and they directly support updating the CSM for these waste sites (and generally for the Hanford Central Plateau). Importantly, the information supports defining suitable contaminant transport parameters that are needed to evaluate transport of contaminants through the vadose zone and to the groundwater. This type of transport assessment supports a coupled analysis of groundwater and vadose zone contamination. The laboratory study information, in conjunction with transport analyses, can be used as input to evaluate the feasibility of remedies for the 200-DV-1 OU. This remedy evaluation will be enhanced by considering these study results that improve the understanding of controlling features and processes for transport of contaminants through the vadose zone to the groundwater.

The laboratory study described in this report was conducted using the samples shown in Table ES-1 for the selected waste sites in the S- and T-Complexes of the 200-DV-1 OU. The laboratory study included categories of individual analysis and experiments derived from EPA guidance for MNA of inorganic contaminants. Sediment characterization included determining contaminant concentrations (and oxidation state for some contaminants), concentrations of important geochemical constituents, microbial ecology relevant to contaminant attenuation, physical properties, and pore-water oxygen and hydrogen isotopes. Additional information to help assess attenuation processes included sequentially applying increasingly harsh extraction solutions to the sediment and measuring contaminants and geochemical constituents in the extractions (sequential-extraction analysis). This technique helps interpret the distribution of contaminants among mobile, partially mobile, and functionally immobile phases in the sediments. The character of iron and manganese phases in the sediments was also determined in relation to their role in redox reactions. Several types of methods were applied to evaluate

transport characteristics and to develop transport parameters for contaminants.  Where existing contaminant concentrations were high enough to enable testing, batch and soil-column leaching experiments were conducted that are used to evaluate and quantify contaminant release rates.  Because several samples had low existing contaminant concentrations, spiked-contaminant experiments were used in batch and soil-column tests to estimate the linear equilibrium partitioning coefficient ($K_d$), an important parameter for transport assessments.

**Table ES.1**.  Samples included in the laboratory study.

| Waste Site | Borehole | Geologic Unit | Nominal Depth Interval (ft bgs) |
|---|---|---|---|
| 216-T-19 (T-19) | C9507 | Cold Creek Unit silt | 92-96 |
| 216-T-19 (T-19) | C9507 | Cold Creek Unit caliche (high carbonate) | 102-106 |
| 216-T-19 (T-19) | C9507 | Ringold formation | 137-140 |
| 216-T-25 (T-25) | C9510 | Hanford Formation/Cold Creek Unit silt transition | 112-115 |
| 216-S-9 (S-9) | C9512 | Hanford Formation | 62-65 |
| 216-S-9 (S-9) | C9512 | Hanford Formation/Cold Creek Unit silt transition | 122-125 |

Interpretation of this laboratory study can be considered from several perspectives relevant to supporting 200-DV-1 OU activities.  Results for each contaminant were evaluated across all of the samples to identify contaminant-specific conclusions and to enable consideration of how results from this study may be relevant to other waste sites.  Results were also evaluated with respect to conclusions relevant to the specific waste sites included in the study.  Lastly, study results were evaluated with respect to updating CSMs and future evaluation of remedies, including the associated fate and transport assessment needed as a basis for remedy evaluation.

The data and information from this laboratory study were interpreted to support the following conclusions for each contaminant included in the study.

- Uranium

  – Uranium concentrations were low in most samples; therefore, a significant fraction of the uranium may be associated with natural background concentrations.

  – The dominant form of uranium was as U(VI), supporting the conclusion that little uranium reduction has occurred in these samples.

  – For samples where uranium concentrations were elevated, only a small fraction of the uranium was present in the aqueous phase or in a form that would be transported in the aqueous phase under equilibrium partitioning conditions.  Most of the uranium was associated with precipitates, and transport of uranium would be controlled by dissolution processes.  This type of slow-release transport behavior was observed in the batch and soil-column leaching experiments for samples with higher uranium concentration.

  – Uranium $K_d$ values were varied across the different samples tested, with the highest $K_d$ value associated with the sample of the high carbonate Cold Creek Unit (CCU) material.  Thus, in transport assessments, selection of a $K_d$ value for uranium should consider spatial variation of the $K_d$ value based on lithologic units and carbonate content.  The CCU samples show the highest $K_d$ values for uranium.  Thus, carbonate content and smaller particle sizes are important to consider for uranium $K_d$.  Organic carbon content did not appear to be important, but was generally low in

all samples.  In terms of desorption versus adsorption $K_d$ values, there was no clear trend across all of the samples.

- Iodine

  – I-129 concentrations in the vadose zone were non-detect for all samples.  Total iodine concentrations were moderate and suitable for conducting attenuation and transport studies.  Because total iodine and I-129 form the same chemical species, attenuation and transport behavior for total iodine and I-129 will be the same.

  – Total iodine speciation in the aqueous phase was mostly dominated by iodide.  However, sequential extractions showed only a small fraction of the iodine was present in the aqueous phase or in a form that would be transported in the aqueous phase under equilibrium partitioning conditions.  Most of the iodine was associated with precipitates (likely carbonates), and transport of iodine in these precipitates would be controlled by dissolution processes.  Speciation was not possible in the carbonate precipitate extractions for the sequential extraction procedure, but it is likely that the iodine present in these extractions was iodate because scientific literature has shown co-precipitation of iodate and carbonates.  The leaching experiments showed some slow-release behavior of iodine that may be associated with these carbonate precipitates.

  – Total iodine $K_d$ values show minimal sorption of iodide and moderate sorption of iodate.  Iodate $K_d$ values varied across the different samples tested, with the highest $K_d$ values associated with the samples with high carbonate concentrations.  Thus, in transport assessments, selection of a $K_d$ value for iodate should consider spatial variation of the $K_d$ value based on carbonate content.  Unlike uranium, the higher iodate $K_d$ values are not all associated with CCU material (smaller particle sizes).  Organic carbon content did not appear to be important, but was generally low in all samples.  Transport of iodide and iodate through the vadose zone will be different, and speciation should be considered when conducting transport assessments.  Desorption $K_d$ values were mostly higher than adsorption $K_d$ values in the batch experiments that were conducted.

- Tc-99

  – Tc-99 was not detected in any of the samples.

  – Tc-99 $K_d$ values determined in spiked-contaminant tests were minimal to low, and values varied slightly across the different samples tested.  However, the nominal retardation value for Tc-99 from these data would be close to 1.  In batch testing, some of the desorption $K_d$ values for Tc-99 were higher than the corresponding adsorption $K_d$ values.  Chemical reduction during the experimental timeframe (up to 56 days total) may have contributed to the higher apparent desorption $K_d$ values, noting that reduction of Tc-99 by Hanford sediments has been observed in the laboratory.

- Chromium

  – Cr(VI) was not detected in most samples and, when detected, was present at a low concentration.  Total chromium measured in acid extractions was likely from natural background.

  – Cr(VI) $K_d$ values determined in spiked-contaminant tests were low, and values varied slightly across the different samples tested.  The measured $K_d$ values generally increased with experiment time (from 1 to 28 days).  It is possible that all or some of this increase was due to Cr(VI) reduction, which has been observed in laboratory experiments with Hanford sediment.  Desorption $K_d$ values from batch experiments were all higher than adsorption values.  However,

some of the concentration changes in the batch desorption experiments (up to 56-day duration) may have been due to some Cr(VI) reduction.

- Nitrate

  – Nitrate concentrations were high in all of the samples. Two samples showed very low nitrite concentrations as a potential indicator of denitrification. However, nitrite concentrations were 4 to 5 orders-of-magnitude lower than nitrate concentrations, indicating that minimal reduction had occurred.

  – Nitrate behavior in leaching experiments showed rapid elution, consistent with a minimal $K_d$ value. The nominal retardation value for nitrate from these data would be close to 1.

The following conclusions were developed for the specific boreholes/waste sites analyzed in this study.

- T-19

  – Samples for the laboratory study from the T-19 waste site (borehole C9507) were of CCU silt, CCU caliche, and Ringold (silty, sandy gravel) materials. These samples were from locations well below the historical waste discharge and did not show signs of altered biogeochemistry induced by the waste discharge, other than the presence of contaminants. Nitrate concentrations were similar in all of the samples, indicating that waste fluids had penetrated to at least the depth of the lowest sample. The pore-water pH was consistent with a carbonate-saturated system. The highest uranium and (total) iodine concentrations were in the CCU caliche (high carbonate) material, suggesting that uranium and iodine accumulated in this zone as the waste solution passed through. Accumulation could be expected based on the observed high $K_d$ value in this unit and the potential formation of uranium- and iodine-carbonate precipitates. Thus, the CCU is an important unit at this waste site for controlling contaminant transport. Tc-99 was not detected in any of these samples. Cr(VI) was only detected at a very low concentration near the detection limit in the CCU caliche sample.

  – Based on the data collected in this laboratory study, the following attenuation processes are important at this waste site. Sorption processes are important for uranium and iodate, and to a lesser extent for chromate and Tc-99. Formation of uranium- and iodate-carbonate precipitates also appears to be an attenuation mechanism in T-19 borehole samples. Minor indications of reduction were observed in one T-19 sample, and the potential for reduction through biotic or abiotic (e.g., ferrous iron) mechanisms is present, though it would likely have limited effect on future contaminant migration.

- T-25

  – The sample for the laboratory study from the T-25 waste site (borehole C9510) was of CCU silt materials. The sample was from a location well below the historical waste discharge and did not show signs of altered biogeochemistry induced by the waste discharge, other than the presence of contaminants. The presence of high nitrate concentration indicates that waste fluids had penetrated to at least the depth of the sample. The pore-water pH was consistent with a carbonate-saturated system. The CCU silt had high carbonate content, though not as high as the CCU caliche sample from the T-19 site. Uranium and total iodine were present at low concentrations, though concentrations were sufficient for assessment of leachability. High $K_d$ values were measured for uranium and iodine, similar to the high $K_d$ values measured for the T-

19 CCU caliche sample that also had a large fraction of carbonate. Accumulation could be expected based on the high observed $K_d$ value in this unit and the potential formation of uranium- and iodine-carbonate precipitates. Thus, the CCU silt is an important unit at this waste site controlling contaminant transport. Tc-99 and Cr(VI) were not detected in any of the samples.

– Based on the data collected in this laboratory study, the following attenuation processes are important at this waste site. Sorption processes are important for uranium and iodate, and to a lesser extent for chromate and Tc-99. Formation of uranium- and iodate-carbonate precipitates also appears to be an attenuation mechanism in T-25 borehole samples. The potential for reduction through biotic or abiotic (e.g., ferrous iron) mechanisms is present, though it would likely have limited effect on future contaminant migration.

- S-9

– Samples for the laboratory study from the S-9 waste site (borehole C9512) were of sandy Hanford Formation and transition from Hanford to CCU silt materials. These samples were deep below the historical waste discharge and did not show significant signs of altered biogeochemistry induced by the waste discharge, other than the presence of contaminants. However, the upper sample showed indication of potential reductive activity that, along with the very high nitrate concentration, may indicate some waste solution effects at this depth. Nitrate concentration was very high in the upper sample (the highest concentration of all samples in the laboratory study), and was at a moderately high concentration in the lower sample, indicating that waste fluids had penetrated to at least the depth of the lowest sample. The pore-water pH was consistent with a carbonate-saturated system. The uranium concentration in the lower sample was low, but was an order of magnitude higher than the uranium concentration in the upper sample. Neither sample appeared to be elevated in carbonate. Tc-99 and Cr(VI) were not detected in any of the samples.

– Based on the data collected in this laboratory study, the following attenuation processes are important at this waste site. Sorption processes are important for uranium and iodate, and to a lesser extent for chromate and Tc-99. Formation of uranium- and iodate-carbonate precipitates also appears to be an attenuation mechanism in S-9 borehole samples. Minor indications of reduction were observed in one S-9 sample and the potential for reduction through biotic or abiotic (e.g., ferrous iron) is present, though it would likely have limited effect on future contaminant migration.

The study provided a set of data that addressed the study objectives and can support future evaluation of remedies, including MNA, and the associated fate and transport assessment that is needed as a basis for remedy evaluations. The first objective was to jointly evaluate contaminant concentrations and the biogeochemical and hydrologic setting for these data. This information provides a baseline for interpreting attenuation and transport studies. As noted, there were significant variations in transport parameter values and some attenuation mechanisms linked to specific sediment characteristics (e.g., carbonate content). For scaling and use of this information in fate and transport assessments, these variations should be considered in light of the sample properties. For this study, the sample properties were strongly linked to the sediment units sampled rather than waste stream properties. Thus, scaling and use in future efforts can translate the attenuation and transport information from this laboratory study to other waste sites based on the distribution of similar sediment units (e.g., the CCU silt and CCU caliche).

Another objective of the study was to identify attenuation processes that appear to be active in these samples and that will affect contaminant transport through the vadose zone. Sorption processes are important for uranium and iodate, and to a lesser extent for chromate and Tc-99. Carbonate content appeared to be important for uranium and iodate $K_d$. Accumulation in carbonate precipitates was identified as an attenuation mechanism for uranium and iodate. Slow release of uranium and total iodine was evident in leaching experiments. Geochemical signatures of reducing conditions were minimal or non-existent in the samples. However, there was indication of potential catalysts for reductive processes, including the presence of microbes and reduced iron and manganese phases. These reductive catalysts may be responsible for some of the difficult-to-extract contaminant phases (e.g., precipitated phases) observed in sequential extraction analysis. Attenuation mechanisms relevant to chromium and Tc-99 (other than sorption) could not be fully assessed because of the low/non-detect concentrations of these contaminants.

A key objective of the study was to quantify attenuation and transport parameters to support parameterization of fate and transport assessments. This type of assessment will be needed to evaluate transport of contaminants through the vadose zone, to evaluate the coupled vadose zone-groundwater system, and to assess the need for, magnitude of, and/or design of remediation. The contaminant- and sample-specific values from stop-flow portions of soil-column experiments, batch leaching, and $K_d$ experiments provide a set of information that can be directly used to develop transport parameters. Soil-column effluent concentration data can also be compared to one-dimensional simulations to assess fate and transport model configurations for $K_d$ or for surface complexation models.

Collectively, the information from this laboratory study can be considered in terms of updating the CSM for contaminants in the vadose zone. It can also provide input to describing the coupled vadose zone-groundwater system that needs to be considered for remedy determinations. CSM elements from this laboratory study are listed below. These elements will need to be incorporated with other data collected during the 200-DV-1 OU remedial investigation as part of updating the CSMs for the 200-DV-1 OU component waste sites.

- Sequential extraction experiments (and more coarsely indicated by comparison of water- and acid-extraction contaminant data) show that only a small fraction of the uranium and iodine mass in samples is in a mobile form that would transport under equilibrium-partitioning conditions. Leaching experiment results confirmed that slow-release processes affect the transport of these contaminants. The relative amount of uranium and iodine mass in the mobile versus functionally immobile phases affects the potential for future mass discharge from the vadose zone to the groundwater.

- Laboratory data suggest that formation and dissolution of uranium- and iodate-carbonate precipitates is a potential attenuation mechanism affecting the relative mobile and immobile mass fractions and the transport characteristics of uranium and iodine.

- Attenuation and sorption are not uniform in the vadose zone, especially for uranium and the iodate form of iodine. Lithology (e.g., the presence and extent of layers such as the CCU) and carbonate content affected the transport parameter values for these contaminants.

- For the waste sites included in this study, the effects of waste chemistry (e.g., altered sediment pH or biogeochemistry), other than contaminant concentrations, did not penetrate deep into the vadose zone. The biogeochemical signature of samples shows that transport evaluation at these waste sites will not need to include properties modified by waste chemistry for the deep portion of the vadose zone.

- While the CSM should acknowledge the potential for transformation processes (e.g., biotic or abiotic reduction), minimal evidence was observed that these processes are active. However, biotic and abiotic transformation may have occurred in the past and contributed to the currently observed contaminant distribution within the sediment and pore water.

- Oxygen and hydrogen isotope data were collected and primarily show correlation to regional precipitation with some variations from evaporative and condensation processes.

- It will be important to incorporate variations in physical property data into the CSM to augment existing data and correlate to indirect measures of lithology (e.g., geophysical logging). Some additional hydraulic property data were collected for this laboratory study and will be documented in a separate report.

This laboratory study extended the characterization of the 200-DV-1 OU to include identification and quantification of contaminant attenuation processes and parameters that will be needed to evaluate transport of contaminants through the vadose zone into the groundwater. The data generated in this laboratory study enable the site CSMs and transport analyses to be updated to reflect the observed contaminant behavior. In addition, the laboratory study was structured to address the information requirements for considering MNA as all or part of a remedy (i.e., EPA's guidance document *Use of Monitored Natural Attenuation for Inorganic Contaminants in Groundwater at Superfund Sites*[1]) and can be used as part of the technical defensibility for identifying attenuated transport through the vadose zone within the remedial investigation and feasibility study for the 200-DV-1 OU.

---

[1] EPA. 2015. *Use of Monitored Natural Attenuation for Inorganic Contaminants in Groundwater at Superfund Sites*. OSWER Directive 9283.1-36, U.S. Environmental Protection Agency, Office of Solid Waste and Emergency Response, Washington, D.C.

# Acknowledgments

# Acronyms and Abbreviations

| | |
|---|---|
| CAWSRP | *Conducting Analytical Work in Support of Regulatory Programs* |
| CCU | Cold Creek Unit |
| CHPRC | CH2M Hill Plateau Remediation Company |
| CSM | conceptual site model |
| DI | deionized |
| EPA | U.S. Environmental Protection Agency |
| ESL | Environmental Sciences Laboratory |
| MNA | Monitored Natural Attenuation |
| MPN | most probable number |
| OU | operable unit |
| PNNL | Pacific Northwest National Laboratory |
| QA | quality assurance |

# Contents

# Figures

# Tables

# 1.0   Introduction

Contaminants disposed of at the land surface must migrate through the vadose zone before entering groundwater.  Processes that occur in the vadose zone can attenuate contaminant concentrations during transport through the vadose zone.  Thus, quantifying contaminant attenuation and contaminant transport processes in the vadose zone, and the resulting temporal profile of contaminant discharge to the underlying groundwater, are important for assessing the need for, and type of, remediation in the vadose zone and groundwater.  This type of information will enhance the existing conceptual site models (CSMs) for the 200-DV-1 Operable Unit (OU) (Serne et al. 2010; CHPRC 2015a,b) in support of fate and transport analysis and remedy evaluation.

Contaminant transport through the vadose zone beneath aqueous waste disposal sites is affected by two types of attenuation processes:  (1) attenuation caused by advective and dispersive factors related to unsaturated water flow and (2) attenuation caused by biogeochemical reactions and/or physical/chemical interaction with sediments (e.g., phenomena such as sorption, solubility control, and decay/degradation that slow contaminant movement relative to water movement).  Figure 1 summarizes the types of attenuation mechanisms that may affect contaminant transport in the vadose zone.  Note that Figure 1 includes waste fluid properties and chemistry because wastes at Hanford were typically released directly to the vadose zone and attenuation may be affected by the nature of the waste material (e.g., Szecsody et al. 2013; Truex et al. 2014).
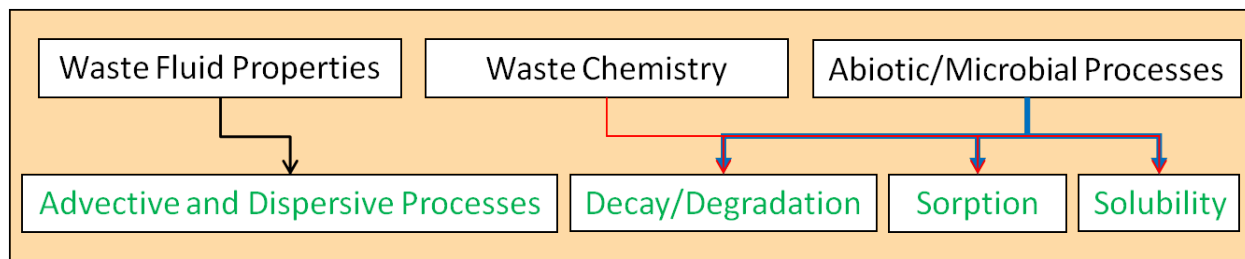


**Figure 1**.  Attenuation mechanisms (green font) for inorganic contaminants in the vadose zone and factors that can impact attenuation (black font) (Truex et al. 2015a).

A framework to characterize these attenuation and transport processes is provided by U.S. Environmental Protection Agency (EPA) guidance document *Use of Monitored Natural Attenuation for Inorganic Contaminants in Groundwater at Superfund Sites* (EPA 2015).  Additional information about vadose zone attenuation processes reported by Truex and Carroll (2013) and Truex et al. (2015a) is also relevant for characterization of the vadose zone.  These documents point to approaches that can be applied to identify and describe transport parameters for a vadose zone site.

The 200-DV-1 OU project is in the process of characterizing the vadose zone to support a remedial investigation and feasibility study (DOE 2012, 2016).  Through a data quality objectives process, specific 200-DV-1 waste sites were selected for evaluation of attenuation and transport processes for mobile uranium, technetium-99 (Tc-99), iodine-129 (I-129), chromium, and nitrate contaminants.  These waste sites were selected based on the following factors:

- Waste stream inventory (radiological and/or chemical component)
- Waste stream differentiation (acid/base, volume, unique characteristics)

- Disposal type (crib, trench, french drain, reverse well, etc.)

- Potential to obtain parameters from significant (site-specific) geologic units to fill data gaps in transport parameters

The data quality objectives process also identified that the characterization of attenuation and transport processes needed to include the following activities:

- Evaluate contaminant and geochemical constituents in the samples

- Identify interactions of contaminants with sediments

- Quantify contaminant mobility

- Evaluate factors controlling contaminant mobility

This report provides information for analyses on sediment samples from the S-Complex and T-Complex portions of the 200-DV-1 OU.  The samples were collected from the three borehole locations depicted in Figure 2.  Detailed description of these waste sites and boreholes is contained in the 200-DV-1 OU characterization planning documents (DOE 2012, 2016) and will be compiled in future 200-DV-1 characterization reports.  This report focuses only on description of the analyses conducted on the samples selected to assess attenuation and transport processes.
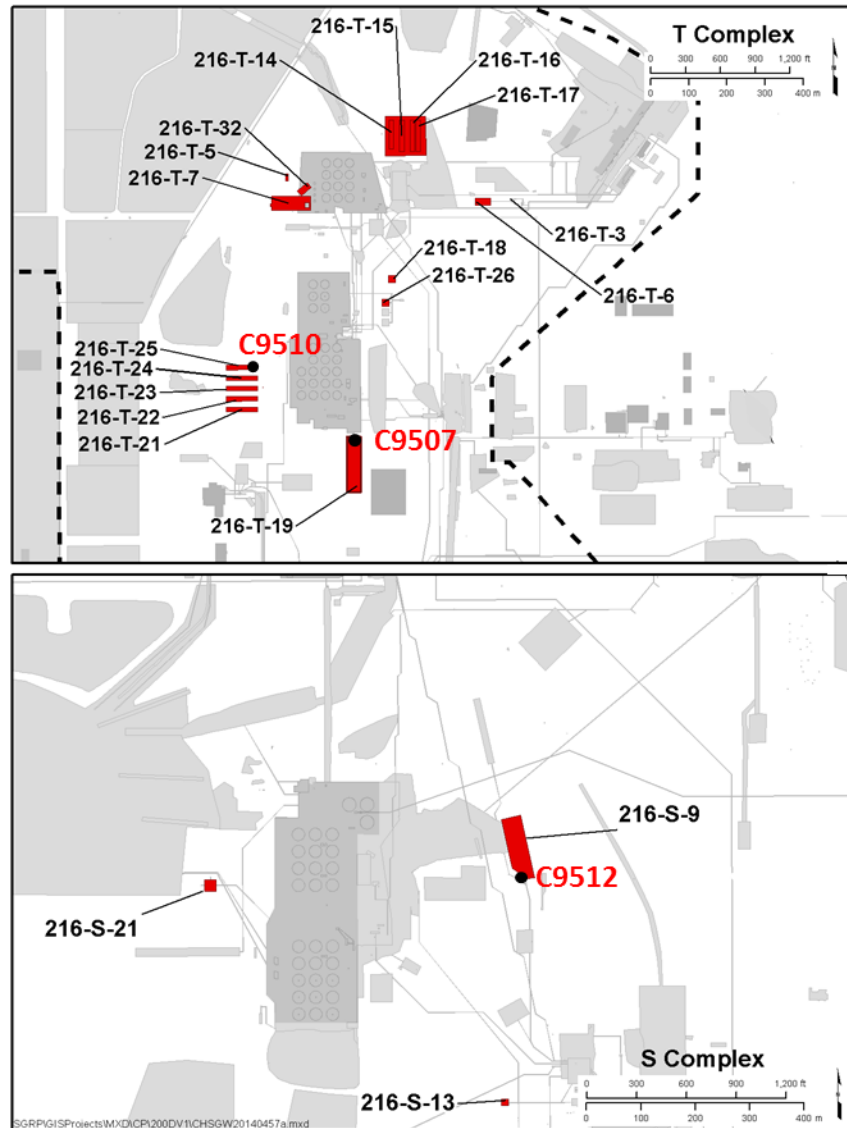
**Figure 2.** Location of waste sites and boreholes where samples were obtained for this laboratory study (adapted from DOE 2012).

This characterization information will be used to refine CSMs by enhancing the understanding of controlling features and processes for transport of contaminants through the vadose zone to the groundwater. The characterization approach was developed based on EPA (2015) guidance, identifying specific objectives (Section 2.0) and types of laboratory analyses (Section 3.0) to conduct on sediment samples. This report provides results and interpretation of these laboratory analyses from analysis of samples collected in fiscal year 2016 (Section 4.0), recommendations for future analyses on these and other samples (Section 5.0), and conclusions with respect to how these results are important for the remedial investigation/feasibility study for the 200-DV-1 OU and associated contaminant fate and transport assessment (Section 7.0). Quality assurance applied for this work is described in Section 6.0.

# 2.0   Objectives

The specific types of data identified for inclusion in the laboratory study reported herein will provide data and associated interpretation to support the following three objectives.  These objectives are elements of the framework identified in the EPA guidance (EPA 2015) for evaluating Monitored Natural Attenuation (MNA) of inorganic contaminants, which directly supports development of suitable contaminant transport parameters.

- Define the contaminant distribution and the hydrologic and biogeochemical setting

- Identify attenuation processes and describe the associated attenuation mechanisms

- Quantify attenuation and transport parameters for use in evaluating remedies

These overall objectives led to a series of laboratory analyses designed to provide suitable data and information.  A phased approach was used for this effort to progressively gather more detailed information based on initial results.  This progressive/tiered approach is consistent with EPA MNA guidance.

The information from these analyses will be used as input to evaluate the feasibility of MNA and other remedies for the 200-DV-1 OU.  The information from these analyses will also be used as input to refine the CSM for the targeted vadose zone sites.

# 3.0   Approach

Samples for the laboratory analyses were collected by CH2M Hill Plateau Remediation Company (CHPRC) as part of the drilling campaign for the 200-DV-1 OU remedial investigation.  Sets of samples for each borehole included multiple sample intervals as potential targets for the analyses.  The sample handling procedures used upon sample delivery to the laboratory are described in Section 3.1.  This section also describes the selection of the specific sample intervals and the analyses selected for these sample intervals.  Laboratory and experimental methods were derived from the approaches described in *Use of Monitored Natural Attenuation for Inorganic Contaminants in Groundwater at Superfund Sites* (EPA 2015).  The laboratory analysis methods are presented in Section 3.2.

## 3.1   Sample Handling and Selection of Samples Intervals and Associated Analyses

Pacific Northwest National Laboratory (PNNL) and CHPRC jointly selected samples for testing through meetings that were held after all of the samples for a borehole were collected.  The selected samples from boreholes C9507, C9510, and C9512 are listed in Table 1.  The samples were in 12-inch-long liners within a 5-ft-long sonic core, except for samples B35461 and B35463 from the C9507 borehole (at the T-19 waste site).  Sample B35461 was from the Ringold unit, where the sample recovery was poor.  CHPRC and PNNL identified a 5-ft liner with approximately 2 ft of the liner containing sample material suitable for the laboratory analyses.  The 2-ft section of this liner was received by PNNL.  This 2-ft-long portion of liner was cut into four 6-in. lengths and distributed for different types of analyses.  CHPRC and PNNL identified another 5-ft liner, sample B35461, with approximately 2 ft of the liner containing an apparently intact sample suitable for intact hydraulic property measurement.  The 5-ft liner was received by PNNL.  This liner was processed for intact hydraulic property assessment (along with another sample), which will be described in a separate report.

The liner samples were shipped from the drilling site to the PNNL 331 Building, where they were inspected, the chain of custodies were completed, and the samples were placed in a refrigerator (4°C).  Once selected, the sample liner for use in isotopic analyses was frozen, except as noted in Table 1 where a subsample of liquid from a liner containing saturated sediment and free liquid was collected and frozen as the sample for isotopic analysis.  The nominal liner sample disposition plan within a 5-ft core sample is shown in Figure 3.  Target 5-ft cores selected for testing generally divide liners for specific types of tests according to this plan.  However, the plan was modified in some cases depending on the observed sample recovery and initial inspection of material type within the liners by the PNNL-CHPRC technical team.

**Table 1**.  Sediment samples selected for analyses.

| Borehole and Liner Designation | Borehole ID | Sample ID | Nominal Geologic Unit | Depth Interval (ft bgs) | Analysis (report section) |
|---|---|---|---|---|---|
| T19 core 14A | C9507 | B35432 | CCUz | 92.1-93.1 | 3.2.6 |
| T19 core 14C | C9507 | B35434 | CCUz | 94.1-95.1 | 3.2.2, 3.2.3, 3.2.4, 3.2.5 |
| T19 core 14D | C9507 | B35435 | CCUz | 95.1-96.1 | 3.2.1 (intact analysis, separate report) |
| T19 core 16A | C9507 | B35441 | CCUc | 102.4-103.4 | 3.2.6 |
| T19 core 16B | C9507 | B35442 | CCUc | 103.4-104.4 | 3.2.1 |
| T19 core 16C | C9507 | B35443 | CCUc | 104.4-105.4 | 3.2.2, 3.2.3, 3.2.4, 3.2.5 |
| T-19 Ringold | C9507 | B35461/B36H08 | Ringold | 137.6-138.1 | 3.2.3, 3.2.4, 3.2.5 |
| T-19 Ringold | C9507 | B35461/B36H08 | Ringold | 138.1-138.6 | 3.2.3, 3.2.4, 3.2.5 |
| T-19 Ringold | C9507 | B35461/B36H08 | Ringold | 138.6-139.1 | 3.2.1 |
| T-19 Ringold | C9507 | B35461/B36H08 | Ringold | 139.1-139.6 | 3.2.2, 3.2.6 |
| T-19 Ringold | C9507 | B35463 | Ringold | 142.6-147.7 | 3.2.1 (intact analysis, separate report) |
| T-25 core 14A | C9510 | B361M7 | H2/CCUz transition | 112.3-113.3 | 3.2.6 |
| T-25 core 14B | C9510 | B361M9 | H2/CCUz transition | 113.3-114.3 | 3.2.1 |
| T-25 core 14C | C9510 | B361N1 | H2/CCUz transition | 114.3-115.3 | 3.2.2, 3.2.3, 3.2.4, 3.2.5 |
| S-9 core 8A | C9512 | B36173 | H1/H2 | 62.2-63.2 | 3.2.6 |
| S-9 core 8B | C9512 | B36175 | H1/H2 | 63.2-64.2 | 3.2.1 |
| S-9 core 8C | C9512 | B36177 | H1/H2 | 64.2-65.2 | 3.2.2, 3.2.3, 3.2.4, 3.2.5 |
| S-9 core 20A | C9512 | B361D9 | H2/CCUz transition | 122-123 | 3.2.6 |
| S-9 core 20B | C9512 | B361F1 | H2/CCUz transition | 123-124 | 3.2.1 |
| S-9 core 20C | C9512 | B361F3 | H2/CCUz transition | 124-125 | 3.2.2, 3.2.3, 3.2.4, 3.2.5 |
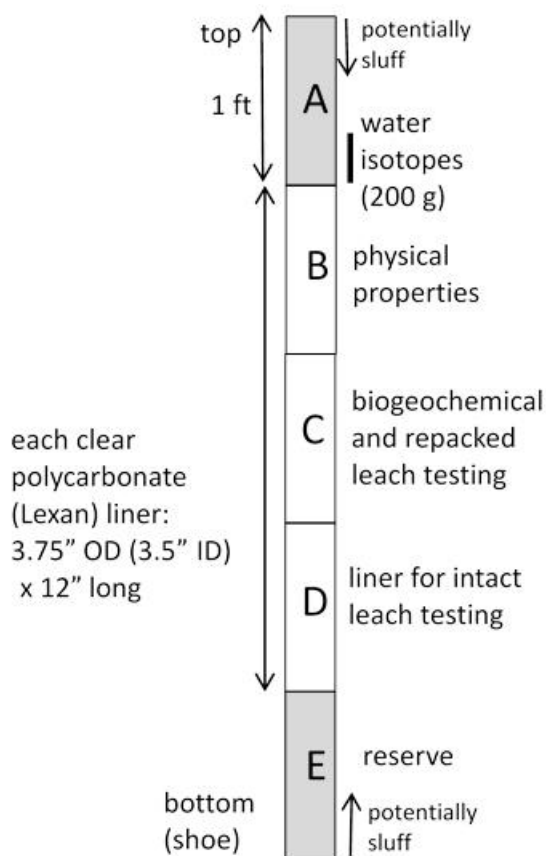


**Figure 3**.  Nominal schematic of analysis on specific core intervals.

## 3.2   Laboratory Methods

Laboratory analyses were selected to evaluate attenuation processes and other factors affecting fate and transport of contaminants in the vadose zone. These analyses were based on the characterization approaches described for evaluating MNA of inorganic contaminants (EPA 2007a,b, 2010, 2015). The analyses were selected to provide data to support interpretation of contaminant behavior in the vadose zone, and will be used in conjunction with additional information produced by CHPRC as part of their related characterization efforts at these and other vadose zone boreholes. The laboratory experimental effort was organized using the following specific analysis objectives, which are related to the overall objectives described in Section 2.0. The subsequent sections describe the laboratory methods applied for each of the analysis objectives.

**Analysis Objectives**

1.  Characterize the physical aspects of the sample that are used to evaluate pore water flow and provide the sediment information needed to interpret and scale biogeochemical analysis results.

2.  Characterize the microbial ecology in the samples, focusing on identification of the microbial phenotypes that are present. This information will be used to interpret (1) microbial processes that can directly affect the chemical form of the contaminant, (2) the microbial community's relation to geochemical processes affecting sediment surface phases and contaminant chemical form, and (3) microbial processes related to sequestration or accumulation of contaminants.

3.  Characterize the contaminant concentration, distribution, and, where appropriate, the oxidation-reduction state and chemical form in the pore water and on sediment surfaces. This information allows interpretation of contaminant mobility in the context of the biogeochemical system data.

4.  Characterize the geochemical conditions in the pore water and on sediment surfaces to facilitate interpretation of attenuation and transport processes. Information about elements and compounds in the samples enables evaluation of biogeochemical processes related to the contaminant chemical form and mobility.

5.  Characterize the contaminant mobility using tests that impose specific conditions, and collect temporal data for interpreting the mobility of the contaminant (e.g., by quantifying the rate of contaminant transfer to the aqueous phase).

6.  Determine the oxygen and hydrogen isotopic signature of the pore water for use in comparing to existing data that may enable the source of the pore water within the sample to be evaluated.

### 3.2.1   Analysis Objective 1:  Physical Characterization

Standard physical sediment analysis methods shown in Table 2 were applied as needed to meet analysis objective number 1. Because of the long duration required for determining unsaturated hydraulic properties, results of the hydraulic property evaluation will be presented in a separate report.

**Table 2**. Physical sediment analysis methods.

| Required Data | Method Basis |
|---|---|
| Moisture content | ASTM D2216-10 |
| Intact-core dry bulk density, particle density and porosity | ASTM D7263-09, D854-14 |
| Intact-core air permeability | ASTM D6539-13 |
| Core particle size by sieve (4, 2, 1, 0.5 mm sieves) | ASTM D6913-04 |
| Core particle size by laser diffraction (< 0.5 mm) | ASTM D4464-15 |
| Lithology, texture, petrologic composition (sand, gravel, basalt, quartz) and photos | Geologist inspection of borehole samples |

### 3.2.2    Analysis Objective 2:  Microbial Ecology

Microbiological and molecular analyses performed on the soil samples are listed in Table 3.  Two categories of analyses were applied to evaluate the microbial ecology of the samples.  The first category is based on applying an extract of the sample to different types of microbial culturing media.  Microbial growth for these culturing media is measured and used to interpret the phenotypes of microbes present in the sample.  The second category is based on extracting genetic material from the sample, identifying the genetic sequences present, and comparing these sequences to sequences in published databases to identify the microbes present at the genus or species level.

Methods for enumeration of total microbial numbers, bacterial density, and total heterotrophs were based on methods contained in the *Standard Methods for the Examination of Water and Wastewater*, 22nd Edition (Rice et al. 2012).  Modifications for methods included verification of electron acceptor utilization using methods from the literature.  The quality approach used for gene quantification was based on a guidance document from the EPA (2004).

**Table 3**. Microbiological and molecular methods.

| Required Data | Method Basis |
|---|---|
| Total microbial numbers | APHA SM 9216A |
| Total heterotrophs | APHA SM 9221C<br>Nitrate – Callos et al. 1999<br>Iron  – Gould et al. 2003<br>Manganese  – Grebel et al. 2016 |
| Bacterial density<br>Total heterotrophs<br>Anaerobic heterotrophs<br>Nitrate-reducing bacteria<br>Iron-reducing bacteria<br>Manganese-reducing bacteria | APHA SM 9215A |
| Overall phylogenetic diversity<br>Gene sequence information<br>Bacterial identification | Argonne National Lab Next Generation Sequencing Core Facility Quality Assurance Policy<br>Benson et al. 2015; Rehm et al. 2013; O'Leary et al. 2015; Cole et al. 2013 |
| APHA is American Public Health Association. | |

### 3.2.3 Analysis Objective 3: Contaminant Concentration, Distribution and Oxidation-Reduction State

Contaminant data were interpreted based on the elements and compounds present in the sample pore water or on sediment surfaces. Contaminant information was obtained by the analyses listed in Table 12 (Section 3.2.7). However, specific types of extractions were applied to provide material for analysis. The type of extraction and the concentration of the contaminant were both needed to interpret the contaminant conditions. Extractions applied to evaluate the contaminant conditions are listed in Table 4. In addition, alkaline extraction was conducted on sediment samples by EPA Method 3060A to provide material for analysis of chromium.

**Table 4**. Extraction methods for contaminant analysis.

| Required Data | Method Basis |
|---|---|
| Water extraction (1:1 sediment:$H_2O$) | Um et al. 2009 and Zachara et al. 2007 |
| Acid extraction (1:3 sediment:$H_2O$, 8M $HNO_3$) | Um et al. 2009 and Zachara et al. 2007 |
| Sequential extractions: <br>     Artificial groundwater <br>     Ion exchangeable <br>     pH 5.0 acetate <br>     pH 2.3 acetic acid <br>     Oxalate, oxalic acid <br>     8M $HNO_3$, 95°C | Gleyzes et al. 2002; Beckett 1989; Larner et al. 2006; Sutherland and Tack 2002; Section 3.2.3.1 |
| 1000-hour carbonate extraction | Zachara et al. 2007; Kohler et al. 2004; Section 3.2.3.2 |

#### 3.2.3.1 Sequential Extractions

Six sequential liquid extractions were conducted on a sediment sample. Extraction 1 is the aqueous contaminant fraction, extraction 2 is the adsorbed contaminant fraction (ion exchangeable), extraction 3 is the "rind-carbonate" contaminant fraction, extraction 4 is the total carbonate contaminant extraction fraction, extraction 5 is the Fe-oxide contaminant fraction, and extraction 6 is defined as the hard-to-extract contaminant fraction. These sequential extractions were conducted at a 1:2 sediment:liquid ratio at room temperature (20°C to 25°C). The extractions used reagents 1 through 6 defined below.

- **Reagent 1 - Artificial groundwater:**

| Constituent | Concentration (mM) |
|---|---|
| $H_2SiO_3*nH_2O$, silicic acid | 0.2 |
| KCl, potassium chloride | 0.11 |
| $MgCO_3$, magnesium carbonate | 0.15 |
| NaCl, sodium chloride | 0.26 |
| $CaSO_4$, calcium sulfate | 0.49 |
| $CaCO_3$, calcium carbonate | 1.5 |

Once the chemicals dissolved, an excess of calcium carbonate ($CaCO_3$) was added to the solution and allowed to mix. After approximately 1 week, excess $CaCO_3$ was filtered out using a 0.45-µm filter.

- **Reagent 2 - 0.5 mol/L $Mg(NO_3)_2$:** 128.2 g $Mg(NO_3)_2 \cdot 6H_2O$ + 30 µL 2 mol/L NaOH to pH 8.0, balance deionized (DI) $H_2O$ to 1.0 liter

- **Reagent 3 - Acetate solution:** 136.1 g sodium acetate•3$H_2O$ + 30 mL glacial acetic acid (17.4 mol/L), pH 5.0, balance DI $H_2O$ to 2.0 liters

- **Reagent 4 - Acetic acid solution:** concentrated glacial acetic acid, pH 2.3; 50.66 mL glacial acetic acid (17.4 mol/L) + 47.2 g $Ca(NO_3)_2$*4$H_2O$, pH 2.3, balance DI $H_2O$ to 2.0 liters

- **Reagent 5 - Oxalate solution:** 0.1 mol/L ammonium oxalate, 0.1 mol/L oxalic acid; 9.03 g anhydrous oxalic acid + 14.2 g ammonium oxalate*$H_2O$, balance DI $H_2O$ to 1.0 liter

- **Reagent 6 - 8.0 mol/L $HNO_3$:** 502 mL conc. $HNO_3$ (15.9 mol/L) + 498 mL DI $H_2O$

In the first extraction, 6 mL of artificial groundwater (reagent 1) is mixed with 3.0 (±0.5) g of sediment for 50 minutes in a centrifuge tube. The tube is then centrifuged at 3000 rpm for 10 minutes, and liquid is drawn off the top of the sediment and filtered (0.45 µm) for analysis. Extractions 2 and 3 are conducted with the same procedure except using reagents 2 and 3, respectively. The fourth extraction uses the same procedure except with a contact time of 5 days and with use of reagent 4. The fifth extraction is conducted the same as extraction 1 except using reagent 5. In the sixth extraction, 6 mL of nitric acid (reagent 6) is added to the sediment and mixed for 2 hours at 95°C. The tube is then centrifuged at 3000 rpm for 10 minutes, and liquid is drawn off the top of the sediment and filtered (0.45 µm) for analysis.

### 3.2.3.2    1000-hour Carbonate Extraction

A carbonate solution (0.0144M $NaHCO_3$ + 0.0028M $Na_2CO_3$ (pH 9.3); 2.42 g $NaHCO_3$ + 0.592 g $Na_2CO_3$ + balance DI $H_2O$ to 2.0 liters) is used for the 1000-hour carbonate extractions (Kohler et al. 2004). Sediment (3.0 ± 0.5 g) and 6.0 mL of the carbonate solution were placed in 45-mL Teflon or polycarbonate centrifuge tubes, mixed for 1000 hours at 6 rpm, and centrifuged at 3000 rpm for 10 minutes, and liquid was drawn off the top of the sediment and filtered (0.45 µm) for analysis.

### 3.2.4    Analysis Objective 4:  Geochemical Conditions

Geochemical conditions were interpreted based on the elements and compounds present in the sample pore water or on sediment surfaces. The geochemical information was obtained by the analyses listed in Table 12 (Section 3.2.7). However, specific types of extractions are applied to provide material for analysis. The type of extraction and the concentration of the element/compound were both needed to interpret the data in terms of the geochemical conditions. Extractions applied to evaluate the geochemical conditions are listed in Table 5.

**Table 5**. Extraction methods for geochemical analysis.

| Required Data | Method Basis |
|---|---|
| Water extraction (1:1 sediment: $H_2O$) | Um et al. 2009 and Zachara et al. 2007 |
| Acid extraction (1:3 sediment:$H_2O$, 8M $HNO_3$) | Um et al. 2009 and Zachara et al. 2007 |
| Sequential extractions:<br>    Artificial groundwater<br>    Ion exchangeable<br>    pH 5.0 acetate<br>    pH 2.3 acetic acid<br>    Oxalate, oxalic acid<br>    8M $HNO_3$, 95°C | Gleyzes et al. 2002; Beckett 1989; Larner et al. 2006; Sutherland and Tack 2002; Section 3.2.3.1 |
| 1000 h carbonate extraction | Zachara et al. 2007; Kohler et al. 2004; Section 3.2.3.2 |
| Iron/Mn phase extractions:<br>    Ion exchangeable Fe(II), Mn,<br>    Oxide/sulfide,<br>    Total Fe(II), Fe(III), Mn,<br>    Amorphous- Fe(III), Mn-oxides,<br>    Crys.-Fe(III), Mn-oxides | Heron et al. 1994; Chao and Zhou 1983; and Hall et al. 1996; Section 3.2.4.1 |

### 3.2.4.1    Iron and Manganese Extractions

Iron extractions were conducted to quantify ferrous iron, ferric iron, and manganese, which are solubilized by different solutions.  These extractions were conducted in an anoxic chamber.

- For the first extraction, sediment samples ($2.0 \pm 0.5$ g) were mixed with 10.0 mL of ion exchange (1.0 M $CaCl_2$) solution for 50 minutes at 6 rpm, centrifuged (3000 rpm, 10 minutes), and filtered (0.45 µm).  The solution was then analyzed for Fe(II) and Mn.

- For the second extraction, sediment samples ($2.0 \pm 0.5$ g) were mixed with 10.0 mL of 0.5M HCl for 24 hours at 6 rpm, centrifuged (3000 rpm, 10 minutes), and filtered (0.45 µm).  The solution was then analyzed for Fe(II) and Mn.

- For the third extraction, sediment samples ($2.0 \pm 0.5$ g) were mixed with 10.0 mL of 5M HCl for 24 hours at 6 rpm, centrifuged (3000 rpm, 10 minutes), and filtered (0.45 µm).  The solution was then analyzed for Fe(II) and Mn.  The solution was also analyzed for total Fe.

- For the fourth extraction, sediment samples ($2.0 \pm 0.5$ g) were mixed with 10.0 mL of 0.25M $NH_2OH \bullet HCl$ solution for 30 minutes at 50°C, centrifuged (3000 rpm, 10 minutes), and filtered (0.45 µm).  The solution was then analyzed for total Fe and Mn.

- For the fifth extraction, sediment samples ($2.0 \pm 0.5$ g) were mixed with 10.0 mL of dithionite-citrate-bicarbonate solution (0.3 mol/L Na-citrate, 1.0 mol/L $NaHCO_3$, and 0.06 mol/L sodium dithionite), mixed for 30 minutes at 80°C, centrifuged (3000 rpm, 10 minutes), and filtered (0.45 µm).  The solution was then analyzed for total Fe and Mn.

### 3.2.5 Analysis Objective 5: Contaminant Release Rate from Sediment and Mobility

Contaminant mobility was evaluated for some sediment samples (B35434, B35443, and B361N1; Table 1) in batch and soil-column leaching tests that impose specific conditions and collect temporal data. These tests expose contaminated sediment to an aqueous solution (simulated groundwater) and measure changes in contaminant concentration over time under flowing or quiescent (batch) conditions (Table 6). For the column tests, sequential extractions for contaminants (Section 3.2.3) were conducted on the post-test sediments from the column for comparison to the pre-leaching results obtained on the sediments. Because contaminant concentrations in some of the samples were low, and to augment the batch and column leaching data, spiked contaminant experiments (batch and column) were also conducted for all of the samples (Table 6). Contaminant and other geochemical constituent information from samples collected during the tests were obtained by the analyses listed in Table 12 (Section 3.2.7).

**Table 6**. Contaminant mobility tests.

| Required Data | Method Basis |
|---|---|
| Batch-leaching test | Szecsody et al. 1994; Section 3.2.5.1 |
| 1-D soil-column test | Qafoku et al. 2004; Szecsody et al. 2013; Section 3.2.5.2 |
| Spiked-contaminant tests | Section 3.2.5.3 |

#### 3.2.5.1 Batch-Leaching Test

Batch experiments used 50 g of sediment and 200 mL of air-saturated artificial groundwater placed in a 250-mL polyethylene centrifuge bottle. The bottle was placed on a slow (12-rpm) linear mixer with supernatant samples taken at 1, 10, 30, 100, 300, 1000 hours for analysis of the target contaminants. Sampling consisted of (a) centrifuging the bottle at 3000 rpm for 10 minutes, (b) removing 5.0 mL from the bottle, and (c) filtering the liquid (0.45 µm).

#### 3.2.5.2 Soil-Column Test

Soil-column experiments were conducted with one-dimensional, vertical, bottom-up flow of injected simulated groundwater solution through contaminated sediment. The concentration of contaminant in the effluent was measured. A non-sorbing, non-reactive tracer (bromide ion) was included in the injection solution and its breakthrough was measured to assess column flow dynamics. The flow rate was set to achieve a residence time of between 1 and 4 hours. Sampling frequency in the effluent was varied based on typical contaminant elution dynamics with more dynamics present at earlier times (fewer pore volumes).

Stop-flow events ranging from 10 to 1000 hours were conducted, during which the flow rate of solution through the column was stopped to provide time for contaminants present in one or more surface phases on the sediment surface to partition into pore water (i.e., diffusion from intraparticle pore space, or time-dependent dissolution of precipitated phases, and/or desorption). Operationally, initiating a stop-flow event involves turning off the pump and plugging both ends of the column (to prevent water movement out of the sediment column). Ending a stop-flow event involves reconnecting the column to the pump, turning on the effluent sample collector, and then turning on the pump. The calculation of the

contaminant release rate from sediment (µg contaminant/g of sediment/day) uses the contaminant effluent concentration before and after the stop-flow event, and the duration of the stop-flow event.

### 3.2.5.3    Spiked-Contaminant Tests

One objective of the 200-DV-1 OU vadose zone characterization program is to determine the attenuation/transport parameters that can be used to evaluate contaminant transport.  In some cases, contaminants were present in samples in sufficient concentration that batch and column leaching experiments (Sections 3.2.5.1 and 3.2.5.2) could be used to estimate transport parameters such as the linear equilibrium partitioning coefficient ($K_d$) or other types of parameters that describe contaminant transport behavior (e.g., based on modeling analysis of the results).  However, some samples lacked sufficient contaminant concentrations to conduct these leaching tests.  For this reason, PNNL and CHPRC determined that batch and column tests using samples spiked with contaminants should be conducted on all of the sediment samples to provide a dataset useful for estimating the $K_d$ value or other types of parameters that describe contaminant transport behavior (e.g., based on modeling analysis of the results).  Samples selected for the spiked-contaminant tests are listed in Table 7.

**Table 7**.  Samples selected for spiked-contaminant analyses.

| Borehole and Liner Designation | Borehole ID | Sample ID | Geologic Unit | Depth Interval (ft bgs) |
|---|---|---|---|---|
| Spiked-Contaminant Batch Testing | | | | |
| T19 core 14C | C9507 | B35434 | CCUz | 94.1-95.1 |
| T19 core 16C | C9507 | B35443 | CCUc | 104.4-105.4 |
| T-19 137-139 | C9507 | B35461/B36H08 | Ringold | 137.6-138.6 |
| T-25 core 14C | C9510 | B361N1 | H2/CCUz transition | 114.3-115.3 |
| S-9 core 8C | C9512 | B36177 | H1/H2 | 64.2-65.2 |
| S-9 core 20C | C9512 | B361F3 | H2/CCUz transition | 124-125 |
| Spiked-Contaminant Soil-Column Testing | | | | |
| T19 core 14C | C9507 | B35434 | CCUz | 94.1-95.1 |
| T-19 137-139 | C9507 | B35461/B36H08 | Ringold | 137.6-138.6 |
| S-9 core 20C | C9512 | B361F3 | H2/CCUz transition | 124-125 |

Specific chemical species of the contaminants were used in the adsorption/desorption $K_d$ measurements.  For Tc-99, $TcO_4^-$ was used.  For iodine, both $I^-$ and $IO_3^-$ were used.  Uranyl nitrate was added to provide uranium.  For Cr, $CrO_4^{2-}$ was used.  Stable I-127 at low concentrations was used as a surrogate for I-129 in these experiments.

Batch experiments used the solutions listed in Table 8 and Table 9.

**Table 8**. Vadose zone pore-water simulant recipe (from Serne et al. 2015).  Adjust pH to 7.0 to 7.2 with sodium hydroxide or sulfuric acid.

| Constituent | Concentration (mM) |
|---|---|
| $CaSO_4*2H_2O$ | 12 |
| NaCl | 1.7 |
| $NaHCO_3$ | 0.4 |
| $NaNO_3$ | 3.4 |
| $MgSO_4$ | 2.6 |
| $MgCl_2*6H_2O$ | 2.4 |
| KCl | 0.7 |
| Adjust pH to 7.0 to 7.2 with sodium hydroxide or sulfuric acid | |

**Table 9**.  Artificial (Hanford) groundwater.

| Constituent | Conc. (mM) |
|---|---|
| $H_2SiO_3*nH_2O$, silicic acid | 0.20 |
| KCl, potassium chloride | 0.11 |
| $MgCO_3$, magnesium carbonate | 0.15 |
| NaCl, sodium chloride | 0.26 |
| $CaSO_4$, calcium sulfate | 0.49 |
| $CaCO_3$, calcium carbonate | 1.50 |

For the Table 9 solution, the reagents were added to DI water.  Once the chemicals dissolved, an excess of calcium carbonate ($CaCO_3$) was added to the solution to equilibrate with calcite while stirring.  After approximately 1 week, excess $CaCO_3$ was filtered out using a 0.45-µm filter.  The final pH was 7.5. 85,000, 170,000, and 850,000

After the solutions are prepared, they were spiked to reach targeted concentrations of contaminants (Table 10).  Additional concentrations were tested for sediments B35434 and B35461 (see parentheses, Table 10).  For Tc-99, 5, 10, and 50 µg/L equate to 85,000, 170,000, and 850,000 pCi/L, respectively.

**Table 10**.  Contaminants and spike concentrations.

| Contaminant | Contaminant Concentration in Simulated Pore Water | Contaminant Concentration in Simulated Groundwater |
|---|---|---|
| Tc-99 | 50 µg/L (5, 10 µg/L) | 50 µg/L (5, 10 µg/L) |
| Cr | 500 µg/L (100, 1000 µg/L) | 500 µg/L (100, 1000 µg/L) |
| U | 500 µg/L (100, 1000 µg/L) | 500 µg/L (100, 1000 µg/L) |
| $I^-$ | 100 µg/L (500, 1000 µg/L) | 100 µg/L (500, 1000 µg/L) |
| $IO_3^-$ | 100 µg/L (500, 1000 µg/L) | 100 µg/L (500, 1000 µg/L) |

Spiked-contaminant batch adsorption/desorption experiments were conducted in 50-mL polypropylene centrifuge tubes at room temperature (~22°C). The experiments were performed at a solid-to-solution ratio of 2:3. The supernatant was sampled (filtered through a 0.45-μm filter membrane) for contaminant analysis (Table 11) at 1, 7, and 28 days of equilibration, with the experimental tubes mounted horizontally on an orbital shaker at the slowest rotation speed possible. Batch experiments were conducted in duplicate for each sampling time, each contaminant ($^{99}TcO_4^-$, $I^-$, $IO_3^-$, U, and $CrO_4^{2-}$), and each of the two solutions.

**Table 11**. Batch test supernatant analyses (specific methods per Table 12, Section 3.2.7).

| Data and Instrumentation | Constituents Analyzed |
|---|---|
| Metals by ICP-OES | Al, Ba, Ca, Fe, K, Mg, Mn, Na, Si, Sr, Cr |
| U, Tc-99 by ICP-MS | U, Tc-99 |
| Iodine by ICP-MS | Iodide, iodate, and total iodine |
| Anions by ion chromatography | Br-, Cl-, F-, $NO_3^-$, $NO_2^-$, $PO_4^{-3}$, $SO_4^{-2}$ |
| Aqueous pH by electrode | pH |
| ICP is inductively coupled plasma; MS is mass spectrometry; OES is optical emission spectroscopy. | |

The desorption portion of the experiment was conducted by adding an amount of unspiked solution to each of the centrifuge tubes that was equal to the amount of supernatant removed. The tube was vortexed to mix well, equilibrated on an orbital shaker, and resampled at 28 days.

Soil-column experiments were conducted with one-dimensional, vertical, bottom-up flow of injected simulated groundwater solution through the sediment. The breakthrough of contaminant concentration at the effluent was compared to the influent contaminant concentration and the breakthrough of a non-sorbing, non-reactive tracer (bromide ion). These data can be analyzed by one-dimensional flow analysis to estimate an adsorption $K_d$. After contaminant breakthrough, the influent solution was switched to contaminant-free solution. The subsequent elution of contaminant and decrease of the contaminant concentrations in the effluent were then tracked. These data can be analyzed by one-dimensional flow analysis to estimate a desorption $K_d$. One duplicate column experiment (using the same sediment) was conducted for each batch of 20 samples.

### 3.2.6    Objective 6: Oxygen and Hydrogen Isotopic Signature of the Pore Water

Isotopic analysis for oxygen and hydrogen can be applied for water samples. Within the vadose zone, however, much of a sample's water remains bound to the surfaces of soil particles or contained within pore spaces, making isotope measurement challenging. An extraction procedure was used to quantitatively remove water from solid soil samples and ensure minimal isotopic fractionation during the extraction and collection process.

A vacuum distillation apparatus was applied for extraction. This apparatus was constructed based on slightly modified versions of those discussed in West et al. (2006) and Goebel and Lascano (2012). In brief, a soil sample is added to one end of the system and then frozen to prevent water migration out of the material. Once a vacuum is established, the sample is heated to drive off the native water, which is collected into a cryogen trap cooled by liquid nitrogen. Once the extraction is complete, the water is removed from this cryogen trap and its isotopic content can be analyzed on a separate instrument, offline

from the extraction system. Extracted water extracted was analyzed for isotopic ratios using a PNNL operating procedure (OP-DVZ-AFRI-002) for the analytical instrument.

## 3.2.7    Chemical Analysis Methods

Standard chemical analytical methods were applied to quantify elements and compounds that are present in extraction solutions and temporal samples from the tests described in Section 3.2, as shown in Table 12.

**Table 12**.  Chemical analyses.

| Analysis[a] | Hold Time | Constituents Analyzed | Method Basis |
|---|---|---|---|
| Metals by ICP-OES | 6 months | Al, Ba, Ca, Fe, K, Mg, Mn, Na, Si, Sr, Cr | EPA 6010D |
| U, Tc-99 by ICP-MS | 6 months | U, Tc-99 | EPA 6020B |
| Iodine species by ICP-MS | 6 months | Iodide, iodate | PNNL-ESL-ICPMS-iodine |
| Kinetic phosphorescence analysis | 6 months | U(VI) | Brina and Miller 1992 |
| Cr(VI) | 24 hrs | Cr(VI) | Hach 8023 |
| Fe(II) | 24 hrs | Fe(II) | Hach 8147 |
| $Br^-$ by electrode | 28 days | $Br^-$ | EPA 9211 |
| Anions by ion chromatography | Nitrate, nitrite: each 48 hr; $PO_4$: 48 hr | $Cl^-$, $F^-$, $Br^-$, $NO_3^-$, $NO_2^-$, $PO_4^{3-}$, $SO_4^{2-}$ | EPA 9056A |
| pH by electrode | Immediate (12 hr) | pH | EPA 9040C |
| Specific conductance (SpC) by electrode | Immediate (12 hr) | SpC | EPA 9050A |
| Total carbon (TC) and total inorganic carbon (TIC)[b] | 28 days | TC and TIC | EPA 9060A |

(a)  Analyses were for aqueous samples except as noted footnote b.
(b)  TC and TIC were also analyzed directly on sediment samples as an information-only analysis using manufacturer procedures (SHIMADZU SSM-5000A procedure).

# 4.0   Results

The laboratory analysis data are described below and interpreted in relation to the three main objectives of the work (Section 2.0).  These objectives were developed to be consistent with EPA guidance for evaluating natural attenuation of contaminants, and to provide data and parameters that support contaminant fate and transport assessments.  The sections below present the data for each of the three objectives.  Quantification of hydraulic properties for selected samples is also being conducted to support these objectives.  However, because of the long-term nature of those tests, results of hydraulic property evaluation will be provided in a separate report.

In Section 4.1, contaminant distribution data are presented in the context of the hydrologic and biogeochemical setting.  This information enables the data collected in this effort to be linked with the 200-DV-1 OU characterization data compiled by CHPRC.  Collectively, this information is a foundation for interpreting contaminant distribution, correlations between contaminant data and other types of data, and the sediment conditions relevant for interpreting attenuation and transport parameters.

Section 4.2 presents and interprets data in terms of identifying contaminant attenuation processes and the types of attenuation mechanisms that are suggested by these data.  Some of these data quantify how contaminants are distributed in different phases within the vadose zone.  This distribution provides input to interpretation of attenuation processes and contaminant mobility.  Other data quantify contaminant mobility based on batch or column experiments that measure the release rate of contaminants from a sediment sample.  Data quantifying the type and content of iron and manganese in the sediment are also provided because several of the targeted contaminants are sensitive to redox reactions and iron oxides are important for contaminant sorption.

Section 4.3 presents data and interpretations that support quantification of attenuation and transport parameters.  Batch and column experimental data provide information to estimate contaminant partitioning and kinetically controlled release rates from sediments.  Because contaminant concentrations were low in many of the sediment samples, results of spiked-contaminant experiments (batch and column tests) are presented with quantification of contaminant partitioning from these tests.  This report provides an initial interpretation of attenuation and transport parameters.  The data will also be useful for additional interpretation by others through modeling of the results.

## 4.1   Contaminant Concentrations and Hydrologic and Biogeochemical Setting

Several types of data provide information about the contaminant concentrations and the hydrologic and biogeochemical setting for the sediment samples.  Contaminant and geochemical constituent concentrations were measured for sediments using water, acid, and/or alkaline extractions, where appropriate.  Microbial ecology was evaluated to identify the number and types of organisms present and to provide information about the types of reactions they may catalyze.  Characterization of iron and manganese was conducted to assess the potential for redox reactions and iron-oxide sorption.  Oxygen and hydrogen isotopes were measured as a potential means to distinguish different sources of pore water.  Sediment physical properties were measured, photographs of the sediments were taken, and geologic

material was classified.  Collectively, this information defines the foundation for scaling and interpreting attenuation and transport parameters for field applications.

### 4.1.1    Contaminants and Geochemical Constituents

Baseline analyses and associated sediment extractions are shown in Table 13.  In these samples, analyses for Tc-99 and I-129 were all non-detect with nominal detections limits of 17 and 1.25 pCi/g, respectively.  The full set of contaminant data collected for the sediment samples is shown in Table 14. Note that for the purpose of evaluating iodine attenuation and transport behavior, this project used total iodine data because its concentration is above the method detection limit.  The samples were also analyzed to determine the iodide and iodate concentrations in the sample because the transport properties of iodide and iodate are different (e.g., Zhang et al. 2013; Truex et al. 2016).  Unfortunately, matrix interferences rendered determination of the speciation difficult, with results only reportable for two of the samples.  Chromium concentrations as measured by alkaline extraction or water extraction were low. Only one sample had detectable Cr(VI) in the water extract and this value was near the detection limit. Total chromium measurements for the water extract were non-detect for this same sample, although the detection limit was higher than for the Cr(VI) measurement; dilution had to be applied for total chromium measurement because of the high nitrate concentration in the samples.  Data for geochemical constituents are listed in Table 15.

**Table 13**.  Baseline contaminant concentrations.

| Sample Name | Sample Location | Technetium-99 pCi/g dry (acid) | Uranium ug/kg dry (acid) | Iodine-129 pCi/g dry (water) | Chromium ug/kg dry (alkaline) | Nitrate ug/kg dry (water) |
|---|---|---|---|---|---|---|
| C9507-B35434 | T19 14C (CCUz) | ND | 784 | ND | 848 | 77,200 |
| C9507-B35443 | T19 16C (CCUc) | ND | 3890 | ND | ND | 83,600 |
| C9507-B35461 | T19 138' (Ringold) | ND | 320 | ND | ND | 95,800 |
| C9510-B361N1 | T25 14C (H2/CCU) | ND | 490 | ND | ND | 6330 |
| C9512-B36177 | S-9 8C (H1/2) | ND | 268 | ND | 657 | 235,000 |
| C9512-B361F3 | S-9 20C (H2) | ND | 293 | ND | ND | 9350 |

**Table 14**.  Contaminant data.

| | | Water Extracts | | | | | | | | |
|---|---|---|---|---|---|---|---|---|---|---|
| Sample Name | Sample Location | Technetium-99 pCi/g dry | Uranium ug/kg dry | U(VI) ug/kg dry | Total Iodine ug/kg dry | Iodate ug/kg dry | Iodide ug/kg dry | Chromium ug/kg dry | Cr(VI) ug/kg dry | Nitrate ug/kg dry |
| C9507-B35434 | T19 14C (CCUz) | ND | 5.78 | 6.14 | 2 | 1.09 | 1.07 | ND | ND | 77,200 |
| C9507-B35443 | T19 16C (CCUc) | ND | 114 | 98.57 | 42.5 | NR | NR | ND | 14.20 | 83,600 |
| C9507-B35461 | T19 138' (Ringold) | ND | 0.15 | 0.22 | 7.88 | NR | NR | ND | ND | 95,800 |
| C9510-B361N1 | T25 14C (H2/CCU) | ND | 3.57 | 4.26 | 10.2 | NR | NR | ND | ND | 6330 |
| C9512-B36177 | S-9 8C (H1/2) | ND | 0.0568 | ND | 2.21 | ND | ND | ND | ND | 235,000 |
| C9512-B361F3 | S-9 20C (H2) | ND | 0.461 | 0.63 | 2.17 | 1.09 | 1.04 | ND | ND | 9350 |
| | | Acid Extracts | | | | | | | | |
| Sample Name | Sample Location | Technetium-99 pCi/g dry | Uranium ug/kg dry | U(VI) ug/kg dry | Chromium ug/kg dry | -- | -- | -- | -- | -- |
| C9507-B35434 | T19 14C (CCUz) | ND | 784 | 946 | 5640 | -- | -- | -- | -- | -- |
| C9507-B35443 | T19 16C (CCUc) | ND | 3890 | 3335 | 5920 | -- | -- | -- | -- | -- |
| C9507-B35461 | T19 138' (Ringold) | ND | 320 | 310 | 3650 | -- | -- | -- | -- | -- |
| C9510-B361N1 | T25 14C (H2/CCU) | ND | 490 | 420 | 4020 | -- | -- | -- | -- | -- |
| C9512-B36177 | S-9 8C (H1/2) | ND | 268 | 279 | 4520 | -- | -- | -- | -- | -- |
| C9512-B361F3 | S-9 20C (H2) | ND | 293 | 302 | 7130 | -- | -- | -- | -- | -- |
| | | Alkaline Extraction | | | | | | | | |
| Sample Name | Sample Location | Chromium ug/kg dry | -- | -- | -- | -- | -- | -- | -- | -- |
| C9507-B35434 | T19 14C (CCUz) | 848 | -- | -- | -- | -- | -- | -- | -- | -- |
| C9507-B35443 | T19 16C (CCUc) | ND | -- | -- | -- | -- | -- | -- | -- | -- |
| C9507-B35461 | T19 138' (Ringold) | ND | -- | -- | -- | -- | -- | -- | -- | -- |
| C9510-B361N1 | T25 14C (H2/CCU) | ND | -- | -- | -- | -- | -- | -- | -- | -- |
| C9512-B36177 | S-9 8C (H1/2) | 657 | -- | -- | -- | -- | -- | -- | -- | -- |
| C9512-B361F3 | S-9 20C (H2) | ND | -- | -- | -- | -- | -- | -- | -- | -- |

**Table 15**. Geochemical constituents.

| | | | | | | Ba ug/g dry | Ca ug/g dry | Fe ug/g dry | Mg ug/g dry | Mn ug/g dry | K ug/g dry | Si ug/g dry | Na ug/g dry | Sr ug/g dry | Cl ug/g dry | Fl ug/g dry | Nitrite ug/g dry | PO4 ug/g dry | SO4 ug/g dry | TOC ug/g dry | TIC ug/g dry |
|---|---|---|---|---|---|---|---|---|---|---|---|---|---|---|---|---|---|---|---|---|---|
| | | | | | | | | | | | | | | | | | | | | | |

### Water Extracts

| Sample Name | Sample Location | pH | SpC mS/cm | Al ug/g dry | Ba ug/g dry | Ca ug/g dry | Fe ug/g dry | Mg ug/g dry | Mn ug/g dry | K ug/g dry | Si ug/g dry | Na ug/g dry | Sr ug/g dry | Cl ug/g dry | Fl ug/g dry | Nitrite ug/g dry | PO4 ug/g dry | SO4 ug/g dry | TOC ug/g dry | TIC ug/g dry |
|---|---|---|---|---|---|---|---|---|---|---|---|---|---|---|---|---|---|---|---|---|
| C9507-B35434 | T19 14C (CCUz) | 8.6 | 0.257 | ND | ND | 4.19 | ND | 0.652 | ND | ND | 3.02 | 17.5 | ND | ND | ND | 5.52 | ND | ND | ND | 11.2 |
| C9507-B35443 | T19 16C (CCUc) | 9.36 | 0.699 | ND | ND | 0.862 | ND | 0.461 | ND | ND | 12.2 | 64.5 | ND | ND | 4.68 | ND | ND | 12.1 | ND | 55.1 |
| C9507-B35461 | T19 138' (Ringold) | 8.13 | 0.288 | ND | ND | 4.97 | ND | 1.68 | ND | ND | 4.13 | 19.5 | ND | ND | 1.4 | ND | ND | 10.2 | ND | 9.4 |
| C9510-B361N1 | T25 14C (H2/CCU) | 8.38 | 0.124 | ND | ND | 6.28 | ND | 1.51 | ND | ND | 4.05 | 3.51 | ND | 0.544 | 0.506 | ND | ND | 6.02 | ND | 11.8 |
| C9512-B36177 | S-9 8C (H1/2) | 8.3 | 0.516 | ND | ND | 8.92 | ND | 1.7 | ND | 4.11 | 4.49 | 88.7 | ND | ND | ND | 9.73 | ND | ND | ND | 10.8 |
| C9512-B361F3 | S-9 20C (H2) | 8.39 | 0.126 | ND | ND | 4.32 | ND | 1.35 | ND | 2.24 | 7.43 | 20.1 | ND | ND | 0.798 | ND | ND | 4.45 | ND | 7.6 |

### Acid Extracts

| Sample Name | Sample Location | Al ug/g dry | Ba ug/g dry | Ca ug/g dry | Fe ug/g dry | Mg ug/g dry | Mn ug/g dry | K ug/g dry | Si ug/g dry | Na ug/g dry | Sr ug/g dry | -- | -- | -- | -- | -- | -- | -- | -- | -- |
|---|---|---|---|---|---|---|---|---|---|---|---|---|---|---|---|---|---|---|---|---|
| C9507-B35434 | T19 14C (CCUz) | 3600 | 36.2 | 8740 | 6560 | 2900 | 176 | 829 J | ND | 132 | 21.9 | -- | -- | -- | -- | -- | -- | -- | -- | -- |
| C9507-B35443 | T19 16C (CCUc) | 5530 | 75.7 | 142,000 | 6020 | 15,000 | 112 | 655 J | ND | 1040 | 200 | -- | -- | -- | -- | -- | -- | -- | -- | -- |
| C9507-B35461 | T19 138' (Ringold) | 3200 | 38.4 | 2810 | 8340 | 2050 | 136 | 400 J | ND | 447 | 16.2 | -- | -- | -- | -- | -- | -- | -- | -- | -- |
| C9510-B361N1 | T25 14C (H2/CCU) | 3460 | 53.6 | 42,200 | 5690 | 2670 | 125 | 452 J | 27.9 | 136 | 52.9 | -- | -- | -- | -- | -- | -- | -- | -- | -- |
| C9512-B36177 | S-9 8C (H1/2) | 3030 | 33.9 | 7920 | 6020 | 2880 | 160 | 654 | ND | 209 | 21.4 | -- | -- | -- | -- | -- | -- | -- | -- | -- |
| C9512-B361F3 | S-9 20C (H2) | 3760 | 36.9 | 6830 | 6490 | 2920 | 142 | 1020 | ND | 118 | 22.1 | -- | -- | -- | -- | -- | -- | -- | -- | -- |

### TOC Sediment and Water Extract

| Sample Name | Sample Location | TC-sed ug/g dry | TIC-sed ug/g dry | TOC-sed ug/g dry | TOC-WE ug/g dry | TIC-WE ug/g dry | Moisture wt% | -- | -- | -- | -- | -- | -- | -- | -- | -- | -- | -- | -- | -- |
|---|---|---|---|---|---|---|---|---|---|---|---|---|---|---|---|---|---|---|---|---|
| C9507-B35434 | T19 14C (CCUz) | 3400 | 3220 | ND | ND | 11.2 | 5.79 | -- | -- | -- | -- | -- | -- | -- | -- | -- | -- | -- | -- | -- |
| C9507-B35443 | T19 16C (CCUc) | 50900 | 49100 | 1740 | ND | 55.1 | 15.7 | -- | -- | -- | -- | -- | -- | -- | -- | -- | -- | -- | -- | -- |
| C9507-B35461 | T19 138' (Ringold) | 287 | ND | ND | ND | 9.4 | 4.3 | -- | -- | -- | -- | -- | -- | -- | -- | -- | -- | -- | -- | -- |
| C9510-B361N1 | T25 14C (H2/CCU) | 16100 | 16200 | ND | ND | 11.8 | 6.49 | -- | -- | -- | -- | -- | -- | -- | -- | -- | -- | -- | -- | -- |
| C9512-B36177 | S-9 8C (H1/2) | 2960 | 2710 | 249 | ND | 10.8 | 2.69 | -- | -- | -- | -- | -- | -- | -- | -- | -- | -- | -- | -- | -- |
| C9512-B361F3 | S-9 20C (H2) | 2750 | 2350 | 402 | ND | 7.6 | 5.8 | -- | -- | -- | -- | -- | -- | -- | -- | -- | -- | -- | -- | -- |

Note: J flag for potassium acid extract results denotes an estimated value because the blank spike recovery was 78.2%, which is outside the target range of 80-120%.

4.4

Contaminant concentrations in all of the samples were low except for moderate uranium concentrations in one sample and high nitrate concentrations in all samples (although some samples had much higher nitrate concentrations than other samples). Total iodine concentrations were moderate. Although total iodine is not an identified contaminant of potential concern, its transport behavior is expected to be the same as I-129 and was of interest to enable evaluation of transport behavior and parameters in these samples. Cr(VI) concentrations were low or not detectable. Chromium (total) was measured in acid extractions and is likely natural chromium present in the sediment.

Because of the very low contaminant levels in three of the samples (B35461, B361F3, and B36177), soil-column leaching studies were not conducted on these samples. Even though it was determined that soil-column leaching could provide useful information for the other three samples (B35434, B35443, and B361N1), contaminant concentrations in these samples were low to moderate. Thus, spiked-contaminant studies were conducted for all of the samples. The sample with moderate uranium concentration was from a portion of the CCU with a high carbonate concentration. High carbonate concentration may have acted to retain uranium contamination as it migrated into this unit through formation of uranium carbonate compounds. Sequential extraction tests described in Section 4.2 provide more information in relation to the phase distribution of uranium contamination and other contaminants.

Geochemical indicators identified by the EPA MNA guidance are those associated with formation of categories of precipitates that may affect contaminants, those associated with contaminant sorption (e.g., iron oxides), and those associated with redox processes. Geochemical indicators are also used for joint interpretation with biological characterization data (see Section 4.1.2). Geochemical data show similar conditions in all samples except for higher carbonate content in samples B35443 (the highest content by a significant amount) and B361N1, as indicated by high calcium concentrations in the acid extractions (and high magnesium for B35443) and by the high total inorganic carbon in the sediment analyses. Contaminants affected by carbonate concentration include uranium, iodine (iodate species), and Cr(VI) (in the form of chromate). Two of the samples (B35434 and B36177) showed minor indications of geochemically reduced conditions due to low sulfate concentrations and the presence of nitrite. Iron and manganese concentrations in the water extracted for these samples were non-detect, although iron and manganese could have been oxidized and precipitated as oxides during sample collection and handling. Nitrite and sulfides would be more resistant to oxidation and may be remnant indicators of geochemically reduced conditions in these samples. Reductive processes affect the fate and transport of uranium, Tc-99, Cr(VI), iodine, and nitrate. Organic carbon was present in samples B35443, B361F3, and B36177, though at generally low concentration. Organic carbon is important to consider in conjunction with the biological system. These geochemical data will be considered with respect to interpreting the other types of characterization data discussed below.

## 4.1.2    Microbial Ecology

The microbial ecology in the samples was evaluated using several types of analyses. Culturing techniques provide information about the phenotype of microbes that are present and able to actively use specific types of electron acceptors when electron donors are present. The data provide an estimate of the population of each phenotype (i.e., nitrate reducers). However, the data do not indicate how active the microbes are in situ, but indicate what types and existing populations of microbes can be active (i.e., are present and alive). This information is important because use of electron acceptors such as nitrate, iron,

and manganese by microbes changes the redox state and related chemical form of these materials. These changes affect how these chemicals interact with contaminants or, in the case of nitrate, reduce its concentration as a contaminant. Many microbes capable of using these electron acceptors have also been shown to transform radionuclides, such as TC-99, uranium, and iodate. Genetic evaluation tools were also applied. These tools compare genetic material from the sample to known bacterial phyla to identify the microbes in the samples. By knowing the microbial phyla, literature information can be used to assess what general type of reactions these microbes may catalyze.

Table 16 shows the results of sediment characterization using culturing techniques. Overall distribution of phyla within four of the samples is shown in Figure 4. Two of the samples, both from borehole S-9, did not show a response in the genetic analysis.

**Table 16**.  Microbial phenotype results showing ability of bacteria to grow on a variety of electron acceptors.  Values indicate number of cells/g of sediment tested.

| Sample ID | Borehole Designation | Depth (ft bgs) | Oxygen | Nitrate | Iron | Manganese | Colony Forming Units |
|---|---|---|---|---|---|---|---|
| C9507-B35434 | T19 14C (CCUz) | 94.1-95.1 | 1,100 | > 1,100,000 | > 1,100,000 | 460 | 0 |
| C9507-B35443 | T19 16C (CCUc) | 104.4-105.4 | 460,000 | > 1,100,000 | 1,100,000 | 20,000 | 4,100,000 |
| C9507-B35461 | T19 138' (Ringold) | 138 | 240 | 11,000 | > 1,100,000 | > 1,100 | 0 |
| C9510-B361N1 | T25 14C (H2/CCU) | 114.3-115.3 | > 1,100 | > 1,100,000 | 1,100,000 | > 1,100 | 172,667 |
| C9512-B36177 | S-9 8C (H1/2) | 64.2-65.2 | > 1,100,000 | 210,000 | 1,100,000 | 240 | 117,000 |
| C9512-B361F3 | S-9 20C (H2) | 124-125 | 2,100 | 240,000 | 21,000 | 43,000 | 1,776,667 |
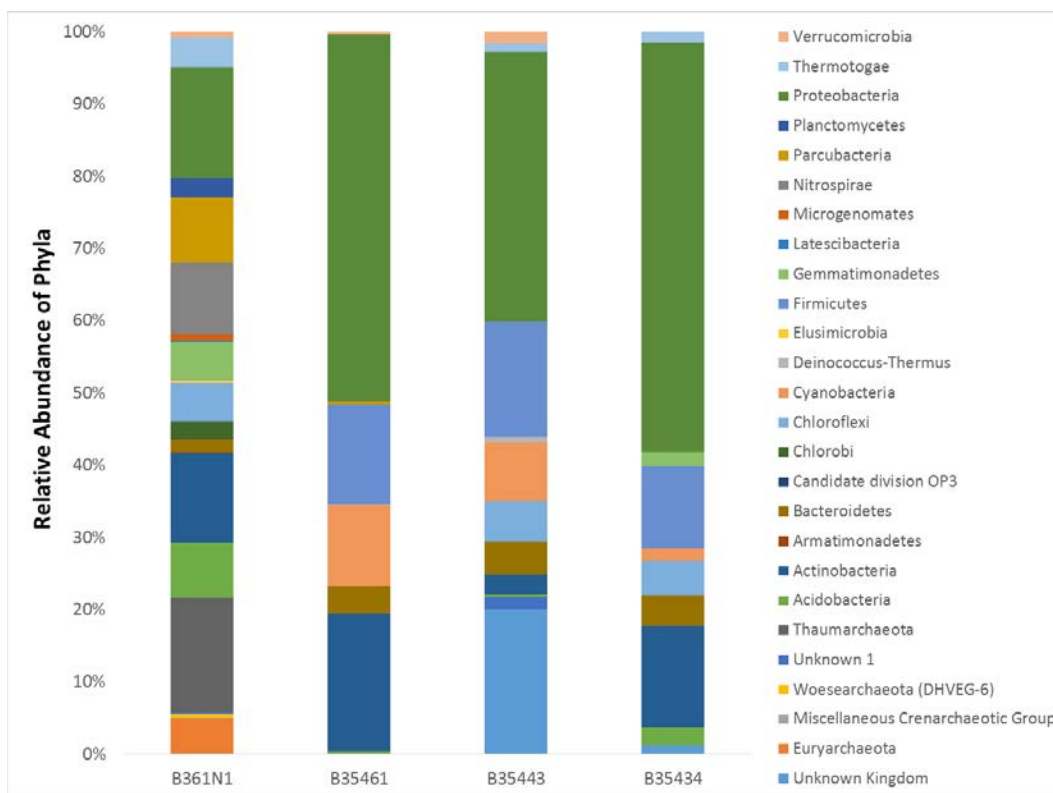
**Figure 4**.  Relative abundance of bacterial phyla based on the 16S rRNA gene.

Most probable number (MPN) analysis was performed using a range of common electron acceptors that may be found in the Hanford vadose zone, either as natural constituents of the minerals present (e.g., iron and manganese) or as contaminants (nitrate) introduced to the environment during waste disposal activities.  Total heterotrophs (provided as colony forming units) are another measure of aerobic bacteria that may grow better on a solid surface.  Bacteria in sediment from sample B35434 showed low numbers, while in sample B35443, numbers of aerobic bacteria were high ($4 \times 10^5$ to $4 \times 10^6$).  Number of aerobic heterotrophs in the Ringold sediments (sample B35461) dropped to zero for total heterotrophs and $2.4 \times 10^2$ for MPN.  Bacterial numbers in sample B35434 and sample B35461 may be low compared to the number in sample B35443 because more moisture was present in sample B35443 (see Table 16).  In addition, TOC was highest in sample B35443, indicating bacteria may have had a potential carbon source or that bacteria may have already grown on these sediments.  Low bacterial numbers in sample B35461 may have also been affected by the non-standard core handling (e.g., storage at room temperature for a period before shipment to the laboratory).

When compared to negative controls to which no sediment was added, sediment samples from boreholes T19 (B35434 and B35443) and T25 (B361N1) showed cell densities for bacteria using nitrate as the electron acceptor in numbers greater than $1 \times 10^6$ bacteria/g of sediment.  Samples from the S9 borehole (B36177 and B361F3) showed slightly lower cell density at ~$2.3 \times 10^5$ cells/g of sediment.  High numbers of bacteria able to grow in the presence of nitrate as a potential electron acceptor is not surprising because high concentrations of nitrate were found in the sediments when extracted with water (Table 14).

In addition, growth was noted in treatments containing ferric iron as the electron acceptor, with bacterial numbers exceeding $1 \times 10^6$ cells/g of sediment in most cores. Numbers of bacteria were only $2.1 \times 10^4$ for sample B361F3. Chemical analysis used to determine whether growth was associated with reduction of the electron acceptor present indicated that bacteria were able to grow using nitrate as an electron acceptor, but reduction to ferrous iron did not occur during growth on ferric iron with the exception of sample B361F3, indicating that the bacteria may have been growing under fermentative conditions. Extraction of ferrous and ferric iron (Table 17) showed higher levels of ferrous iron, indicating that reduction events may have occurred previously. These results may explain why iron reduction was not noted in most of the MPN tests containing ferric iron. Of the electron acceptors tested, treatments with manganese showed the least growth, but the number of manganese reducers was the highest in sample B35443, which also showed the highest moisture. In addition, this sample contained the most Mn(IV) (Table 18), compared to the other samples tested.

Figure 4 shows that samples from all depths for borehole T19 (samples B35434, B35443, and B35461) show a microbial community dominated by Proteobacteria, indicating that there is likely a range of facultative anaerobes that should have the ability to use various inorganic, metal, and radionuclides as electron acceptors. There are also significant numbers of *Actinobacteria* and *Firmicutes*, which also contain facultative members. These phyla are also significant because when adverse conditions such as decreased water are encountered, they can form spores that allow for survival for long periods. Facultative anaerobes are able to grow in oxic as well as anoxic environments using alternate electron acceptors such as nitrate. Phyla found in the samples also contain many bacterial species that are capable of contaminant transformation, which ultimately could affect fate and transport. A diverse, more evenly distributed community was present in the sample analyzed from borehole T25 (sample B361N1). This sample also had Proteobacteria, which represented approximately 15% of the total community. Interestingly, the T25 sample (B361N1) also contained a significant percentage of Archaea, which have not commonly been encountered in Hanford sediments.

## 4.1.3    Iron and Manganese Characterization

Iron and manganese exist in multiple redox states and chemical forms in the subsurface. The relative distribution of iron and manganese in different forms provides insight into the sorptive and reactive capacity of the sediments. A series of extractions with measurement of iron and manganese was conducted to characterize the sediments using extraction techniques identified in scientific literature (and referred to in EPA MNA guidance [EPA 2015]).

Table 17 and Table 18 show the results of the extractions and iron and manganese analyses, respectively. For context, the information is also plotted, showing the relative portions of different iron forms and the relative amount of redox-active iron and ferrous iron phases (Figure 5a) and Mn phases (Figure 5b).

**Table 17**.  Ferrous and ferric iron phases in sediments based on liquid extractions.

| Sample Name | Sample Location | ads. Fe$^{II}$ (mg/g) | Fe$^{II}$CO$_3$, FeS (mg/g) | Other Fe$^{II}$ (mg/g) | am. Fe$^{III}$ (mg/g) | crys. Fe$^{III}$ (mg/g) | Other Fe$^{III}$ (mg/g) | Total Fe$^{II+III}$ (mg/g) |
|---|---|---|---|---|---|---|---|---|
| C9507-B35434 | T19 14C (CCUz) | < 1.20E-3 | 0.316 | 5.25 | 0.0195 | 0.549 | 13.8 | 19.4 |
| C9507-B35443 | T19 16C (CCUc) | < 1.20E-3 | < 1.20E-3 | 7.24 | < 1.20E-3 | 0.061 | 6.90 | 14.1 |
| C9507-B35461 | T19 138' (Ringold) | < 1.20E-3 | 3.92 | 5.50 | 0.1852 | 0.327 | 19.2 | 28.6 |
| C9510-B361N1 | T25 14C (H2/CCU) | < 1.20E-3 | < 1.20E-3 | 9.57 | 0.0086 | 0.286 | 13.8 | 23.4 |
| C9512-B36177 | S-9 8C (H1/2) | < 1.20E-3 | 0.991 | 4.18 | 0.0414 | 0.228 | 11.1 | 16.3 |
| C9512-B361F3 | S-9 20C (H2) | < 1.20E-3 | 1.22 | 4.98 | 0.0382 | 0.640 | 14.6 | 20.8 |
| C9512-B361F3 | S-9 20C (H2) | < 1.20E-3 | 1.22 | 4.80 | 0.0351 | 0.632 | 13.9 | 19.9 |

ads. = adsorbed, am. = amorphous, crys. = crystalline

**Table 18**.  Manganese phases in sediments based on liquid extractions.

| Sample Name | Sample Location | ads. Mn$^{II}$ (mg/g) | Mn$^{II}$CO$_3$ (mg/g) | am. Mn$^{II+IV}$ (mg/g) | crys. Mn$^{II+IV}$ (mg/g) | Other Mn$^{II+IV}$ (mg/g) | Total Mn$^{II+IV}$ (mg/g) |
|---|---|---|---|---|---|---|---|
| C9507-B35434 | T19 14C (CCUz) | 4.71E-03 | 0.155 | 9.20E-02 | 1.35E-02 | 0.045 | 0.306 |
| C9507-B35443 | T19 16C (CCUc) | < 1.20E-3 | 2.78E-03 | 1.93E-03 | 5.66E-03 | 0.153 | 0.163 |
| C9507-B35461 | T19 138' (Ringold) | 1.86E-03 | 0.133 | 7.89E-02 | < 1.20E-3 | 0.117 | 0.328 |
| C9510-B361N1 | T25 14C (H2/CCU) | < 1.20E-3 | 3.07E-02 | 6.02E-02 | 1.91E-03 | 0.140 | 0.232 |
| C9512-B36177 | S-9 8C (H1/2) | < 1.20E-3 | 0.145 | 1.52E-01 | < 1.20E-3 | < 1.20E-3 | 0.246 |
| C9512-B361F3 | S-9 20C (H2) | < 1.20E-3 | 0.120 | 7.02E-02 | < 1.20E-3 | 0.077 | 0.267 |
| C9512-B361F3 | S-9 20C (H2) | < 1.20E-3 | 0.116 | 6.73E-02 | < 1.20E-3 | 0.072 | 0.255 |

ads. = adsorbed, am. = amorphous, crys. = crystalline
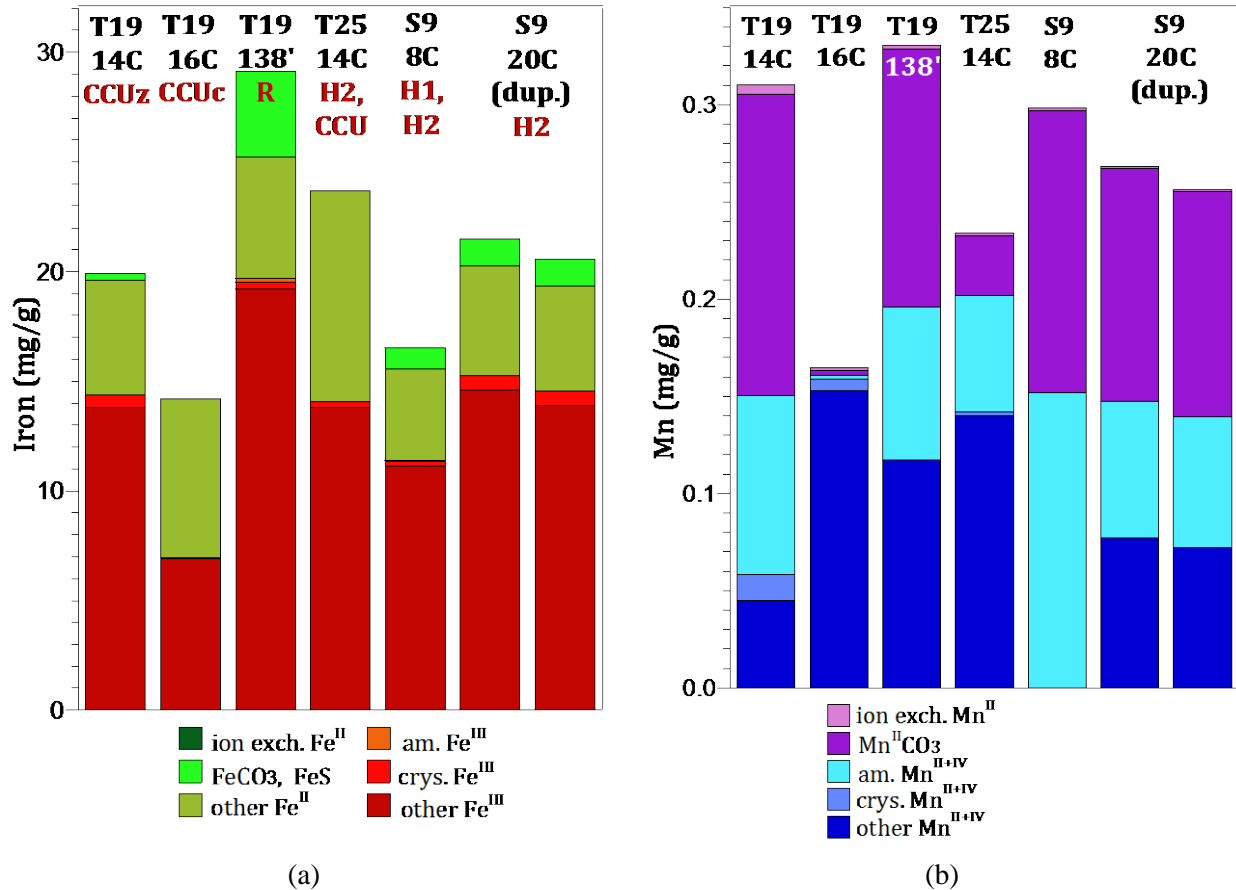
**Figure 5**. Iron (a) and manganese (b) surface phase distributions in sediments, based on liquid extractions.

Iron and manganese extractions were conducted to characterize the potential for contaminant redox reactions in the sediments. Sediments contained a total of 14 to 28 mg/g extractable iron, based on a 3-week 5M HCl extraction. Hanford, Ringold, and Cold Creek formation sediments contain a mixture of mafic (i.e., sediments derived from basalt) and granitic minerals, with mafic minerals (pyroxenes, amphiboles) and clay minerals containing significant Fe and Mn phases (Table 19). The amorphous and crystalline ferric iron oxide extractions (orange and light red, Figure 5a) show that a small fraction of the total ferrous iron in the sediment is more readily dissolved oxides (and available for microbial iron reduction), whereas the majority of ferrous iron was likely in pyroxene and amphibole phases. Ferrous phases accounted for 25% to 40% of the total iron (green bars in Figure 5a), with little adsorbed ferrous iron (dark green, see Table 17), minor ferrous iron in carbonates/sulfides (light green), some of which is redox reactive, and the remaining ferrous iron in unidentified phases (likely in clays). Although all of these sediments are from the vadose zone, some abiotic reduction can occur under water-saturated conditions (Szecsody et al. 2014) due to the availability of ferrous iron from carbonates/sulfides.

**Table 19**.  Summary of Hanford mineralogy (after Xue et al. 2003).

| Mineral | Formula | Both Fm (% wt) | Hanford Fm (% wt) | Ringold Fm (% wt) |
|---|---|---|---|---|
| Quartz | $SiO_2$ | $37.7 \pm 12.4$ | $38.4 \pm 12.8$ | $37.03 \pm 12.4$ |
| Microcline | $KAlSi_3O_8$ | $17.0 \pm 6.7$ | $15.3 \pm 4.4$ | $18.7 \pm 8.0$ |
| Plagioclase | $NaAlSi_3O_8$-$CaAl_2Si_2O_8$ | $18.7 \pm 7.7$ | $22.2 \pm 7.2$ | $15.5 \pm 6.8$ |
| Pyroxenes | $(Ca,Mg,Fe)Si_2O_6$ | $3.03 \pm 5.99$ | $5.01 \pm 7.83$ | $1.14 \pm 2.52$ |
| Calcite | $CaCO_3$ | $4.97 \pm 7.19$ | $1.91 \pm 1.71$ | $0.68 \pm 0.92$ |
| Magnetite | $Fe_3O_4$ | $5.09 \pm 4.37$ | $4.46 \pm 4.12$ | $5.68 \pm 4.63$ |
| Amphiboles | $Ca_2(Mg, Fe, Al)_5 (Al, Si)_8O_{22}(OH)_2$ | $5.55 \pm 5.97$ | $5.46 \pm 5.67$ | $5.64 \pm 6.40$ |
| Apatite | $Ca_{10}(PO_4)_6(OH)_2$ | $0.60 \pm 1.04$ | $0.52 \pm 0.92$ | $0.67 \pm 1.16$ |
| Mica[a] | $(K, Na,Ca)(Al, Mg, Fe)_{2-3}$ $(Si,Al)_4O_{10}(O, F, OH)_2$ | $2.07 \pm 4.47$ | $2.46 \pm 3.74$ | $1.71 \pm 5.15$ |
| Ilmenite | $FeTiO_3$ | $2.51 \pm 2.66$ | $1.28 \pm 1.51$ | $3.67 \pm 3.00$ |
| Epidote | $\{Ca_2\}\{Al_2Fe^{3+}\}[O|OH|SiO_4|Si_2O_7]$ | $1.65 \pm 2.98$ | $1.78 \pm 3.75$ | $1.52 \pm 2.14$ |
| (a)  Muscovite, biotite, phlogopite, lepidolite, clintonite, illite, phengite | | | | |

Although the total manganese (II and IV) extracted from the sediment (0.16 to 0.33 mg/g) was ~1-2% of the total iron in the sediment, there was a greater fraction of potentially redox reactive $Mn^{II}$.  The fraction of ion exchangeable $Mn^{II}$ was small (ranging from below detection limits to 4.7 µg/g), but the $Mn^{II}$ associated with carbonates (0.003 to 0.16 mg/g) was significant.  $Mn^{II}$ phases were 20% to 55% of the total Mn.

### 4.1.4    Oxygen and Hydrogen Isotopes

Isotopic analysis for oxygen and hydrogen are developed and applied for multiple purposes (Prudic et al. 1997).  For instance, the stable isotopes of water ($\delta^2H$ [deuterium] and $\delta^{18}O$ [18-oxygen]) can be used to assist with tracking of underground contaminant plumes or linking a source to a measured water sample.  For the 200-DV-1 OU, the pore water in the vadose zone is a mixture of water from previous natural recharge and the anthropogenic water discharges of waste streams.  Isotopic data was collected to assess whether the signatures from different areas can be correlated to mixtures of different types of water sources.  As shown in Table 20, this section includes data for sediment samples collected from the S- and T-Complexes (borehole C9507 [T-19 waste site], borehole C9510 [T-25 waste site], and borehole C9512 [S-9 waste site]).  To assist interpretation, plots include data for sediment samples from the B-Complex (Szecsody et al. 2017, borehole C9552 [BY Cribs waste site], borehole C9487 [B7-AB waste site], and borehole C9488 [B-8 waste site]) and for water samples from the perched-water aquifer in the B-Complex (Lee et al. 2017).

**Table 20**. Sediment samples selected for analyses and isotope data values (outliers removed).

| Borehole and Liner Designation | Borehole ID | Sample ID | Nominal Geologic Unit | Depth Interval (ft bgs) | Data Source | $\delta^{18}O$ (‰) | $\delta^2H$ (‰) |
|---|---|---|---|---|---|---|---|
| T19 14A | C9507 | B35432 | CCUz | 92.1-93.1 | This report | -19.36 (2.0) | -145.5 (7.8) |
| T19 16A | C9507 | B35441 | CCUc | 102.4-103.4 | This report | -17.54 (1.0) | -135.1 (6.0) |
| T-19 Ringold | C9507 | B35461 | Ringold | 139.1-139.6 | This report | -15.33 (0.3) | -123.9 (1.1) |
| T-25 14A | C9510 | B361M7 | H2/CCUz | 112.3-113.3 | This report | -17.16 (0.2) | -138.0 (0.9) |
| S-9 8A | C9512 | B36173 | H1/H2 | 62.2-63.2 | This report | -21.05 (2.7) | -146.7 (11.5) |
| S-9 20A | C9512 | B361D9 | H2/CCUz | 122-123 | This report | -20.54 (1.1) | -143.5 (6.2) |
| BY Cribs 13A | C9552 | B341B1 | H2 | 102.2 – 103.2 | Szecsody et al. (2017) | -13.48 (0.2) | -128.3 (1.0) |
| BY Cribs 18A | C9552 | B341C1 | H2 | 127.3 – 128.3 | Szecsody et al. (2017) | -15.13 (1.1) | -134.9 (3.3) |
| BY Cribs 19A | C9552 | B341C3 | H2 | 132.1 – 133.1 | Szecsody et al. (2017) | -14.18 (0.4) | -130.3 (0.9) |
| BY Cribs 30A | C9552 | B34H74 | CCUg | 192.2 – 193.2 | Szecsody et al. (2017) | -16.43 (0.9) | -145.0 (5.7) |
| B7-AB 17A | C9487 | B34WB1 | H2 | 132.1 – 133.1 | Szecsody et al. (2017) | -19.24 (0.1) | -143.3 (0.1) |
| B7-AB 35D | C9487 | B34WH8 | H2/CCUz | 220.0 – 221.0 | Szecsody et al. (2017) | -18.11 (1.8) | -141.8 (9.7) |
| B7-AB Opt. 12C | C9487 | B354L1 | CCUz | 227.2 – 227.7 | Szecsody et al. (2017) | -16.19 (0.5) | -127.0 (1.4) |
| B7-AB Opt. 14C | C9487 | B354M3 | CCUz | 232.0 – 233.0 | Szecsody et al. (2017) | -17.73 (0.9) | -135.4 (3.5) |
| B-8 37B | C9488 | B355L8 | CCUz | 222.5 – 225.5 | Szecsody et al. (2017) | -16.09 (0.9) | -129.4 (5.6) |
| Perched Water | NA | NA | Well Samples | NA | Lee et al. (2017) | Lee et al. (2017) | Lee et al. (2017) |

Isotopic ratios for deuterium and 18-oxygen are reported in delta (δ) notation, defined as

$$\delta = \left(\frac{Rsa}{Rstd} - 1\right) \times 1000$$

where R is the ratio of the abundance of the heavy to light isotope (i.e. $^2H/^1H$, $^{18}O/^{16}O$), *sa* denotes the sample, and *std* indicates the standard (McKinney et al. 1950). Delta values are reported in per mil (‰), with $\delta^2H$ and $\delta^{18}O$ values relative to Vienna Standard Mean Ocean Water ($\delta^2H$ = 0‰, $\delta^{18}O$ = 0‰).

Isotopic analysis for oxygen and hydrogen are typically plotted as shown in Figure 6, which also shows the global meteoric water line (Craig 1961), an assembled regional meteoric water line (Graham 1983), and the rough isotope region reported for Columbia River surface water at this location (Spane and Webber 1995) for comparison to the values of water extracted and measured in this study. Error bars correlate to the standard deviation resulting from a minimum of triplicate extraction replicates each isotopically analyzed using multiple analytical replicates (n≥9). All data is shown in Figure 6a while Figure 6b contains a culled data set in which a Modified Thompson Tau test was used to eliminate outliers in the data that may have resulted from a combination of inherent sample heterogeneity and/or inefficient water extraction. Note that while this statistical application may have reduced the size of associated error bars, the overall trends discussed below remain intact. As such, the additional data discussion is based on the revised data set resulting from the statistical rejection of outlier data points (at the 95% confidence interval). In addition to the vadose zone sediment samples analyzed, isotopic ratios are plotted for water extracted from the perched-water aquifer in the B-Complex (errors bars correlate to the standard deviation of the analytical replicates, n≥9).

The global meteoric water line (Craig 1961) shows the average relationship, worldwide, between $\delta^2$H and $\delta^{18}$O in natural terrestrial waters (e.g., rivers, lakes) and precipitation. The deviation between the local and global meteoric water lines is attributed to evaporative processes coupled to the typically short precipitation durations and semi-arid nature of the local region (Graham 1983). There is overlap between the local meteoric water correlation for each of the extracted water samples and nearly all of the perched water samples, suggesting close connection between regional precipitation and the samples. There is also an interesting relationship between the data from boreholes containing three or more data points (C9507, C9552 [Szecsody et al. 2017], and C9487 [Szecsody et al. 2017]). In each of these cases, the data show strong correlation between the two isotopes ($R^2$ of 1.00, 0.97, and 0.91 respectively) as would be expected, and the linear fit to each of these data sets show a show respective slopes of 5.46, 5.74, and 5.62. These relationships show strong connection to both previous measurements of vadose zone water (DePaolo et al. 2004; identified a slope of ~5) and to the regional meteoric precipitation line (slope of ~5.8). More revealing, however, is the offset between sample data sets whereby samples from C9552 (Szecsody et al. 2017) are noticeably shifted to the right in the isotope plots, likely indicating more extensive evaporation history in these samples than in the others.

A trend was observed between the measured vadose zone samples and depth (Figure 7), but there are different behaviors of this trend in different boreholes. For instance, in the T- and S-Complex samples, the total data set displayed a correlation with $R^2$ of only 0.42; removal of just point B361D9 increased this correlation to $R^2$ of 0.96 and the three samples within core C9507 T19 also showed a strong correlation with depth ($R^2$ of 0.96). The trend toward isotopic enrichment (less negative values) with increased sample depth apparent in the vadose zone samples is qualitatively consistent with the observations of Hearn et al. (1989), who cited upwelling of isotopically enriched deeper waters for this trend in their analyses. However, the much shallower nature of these samples (<45 m compared to >1200 m) combined with the nature of vadose versus groundwater samples make it difficult to invoke a similar mechanism here. It is possible, however, that barometric mixing effects (similar to those described by Spane [1999]) induced mixing of underlying groundwater vapor with overlaying vadose zone water.

In contrast, DePaolo et al. (2004) suggest that strong evaporative effects in upper Hanford soil columns can create significant (e.g., 2-6 ‰ shift in $\delta^{18}$O) isotopic enrichment in resulting vadose zone moisture. This mechanism likely helps explain the enriched isotope values observed in samples from C9552 and C9488 (Szecsody et al. 2017). This effect is generally confined to only the upper couple meters (or less) of soil. While slight isotopic enrichment may be expected compared to precipitation values below this surface enrichment, that process would not account for the more depleted values being found at shallow depths within the C9507 (T19) borehole. In a core exhumed from the 200 West Area in 1999, DePaolo et al. (2004) also observed a negative isotopic anomaly in water extracted from a surface to groundwater depth profile. They attributed this excursion to leaking industrial process water that subsequently focused at the boundary of a coarser grained layer underlain by a finer grained layer. While a similar mechanism considered here would be consistent with the negative isotopic values observed in sample B35432, a more continuous depth profile would be required to validate this hypothesis. Interestingly, samples B35441 (Szecsody et al. 2017), B35461/B36H08, and B361M7 (Szecsody et al. 2017) are consistent with the absolute isotopic values DePaolo et al. (2004) observed in their study, but samples including B36173 and B361D9 (both from borehole C9512 S9) are isotopically depleted in comparison to this previous study. Winter precipitation is known to have a more depleted isotopic composition but ranges around a $\delta^{18}$O of ~ -18‰ and $\delta^2$H of ~ -138‰ (DePaolo et al. 2004), so seasonality on its own cannot explain these data.

These observations are more confounding in that evaporative enrichment (e.g., observed by DePaolo et al. [2004] and Singleton et al. [2004]) typically propagates down core, thus isotopically enriching the entire core. Evidence of this is seen in the perched water data whereby these samples show isotopic enrichment consistent with near-surface evaporative processes (Lee et al. 2017). A potential hypothesis for explaining the depletion of the C9512 S9 samples may rest in release of industrial condensate generated from intentional evaporitic enrichment of wastes to reduce their volumes. As noted in DOE/RL-92-93 (DOE 1992), such condensate would exhibit an isotopic depletion as an inverse to the enrichment observed in residual fluid following evaporation (as would be required by conservation of mass). Discharge of industrial condensate in the vicinity of C9512 S9 could potentially explain both the inherent depleted isotopic content of these samples as well as the deviation of these samples from the more generalized correlation between $\delta^{18}O$ versus depth; large-scale release of industrial condensate would likely overprint existing isotopic trends within the vadose depth profile. In support of this, there is noted historical release of process condensate from the D-2 receiver tank within the 202-S Building that resulted from condensation of evaporate used to concentrate decontamination waste at this location (DOE 2016). The sharp negative isotope deviation in vadose zone water within this location could represent an isotopic signature of this process that may be a useful for tracking regional migration of the resulting plume. A similar process may also contribute to the most extreme isotopic signature within the C9507 T19 borehole, notably B35432, as there was noted release of process and steam condensate from the 242 T evaporator in this region but also release of additional tank waste and waste supernate (DOE 2016). It is unclear whether a similar mechanism can explain the depleted isotope signatures in C9487 (specifically B34WB1 [Szecsody et al. 2017]), but it remains a leading hypothesis regarding the extracted water in this sample having an isotopic composition more depleted than annual precipitation extremes or observed groundwater.

The isotope measurements of the S- and T-Complex samples were plotted against measured nitrate concentrations (Figure 8). Two immediate features were observed. First, there is a linear relationship between the nitrate concentration and isotope data that also correlates to increasing depth in the borehole. The patterns seen in C9507 T19 are in contrast to the data from C9512 S9, however, which shows minimal variation in isotope values or nitrate over a fairly large vertical column (~60 ft).

Taken together, the stable isotope data provide a few interesting observations on these systems. First, most boreholes having multiple data points show covariance of the two measured isotopes, suggesting strong input from regional precipitation (e.g., C9507 T19, C9487 [Szecsody et al. 2017], C9552 [Szecsody et al. 2017], and the suite of perched water samples [Lee et al. 2017]). While each of these data sets shows isotopic signatures associated with evaporation, samples from C9552 (Szecsody et al. 2017) show a significant increase in this feature, suggesting a stronger evaporative history than in the other samples. In contrast to evaporative enrichment, some samples show negative isotope excursions suggestive of inclusion of condensate-derived moisture in the vadose zone. While this is most notable in samples B36173 and B361D9, the mechanism may also help explain observations from samples from the C9507 T19 and C9487 (Szecsody et al. 2017) boreholes.
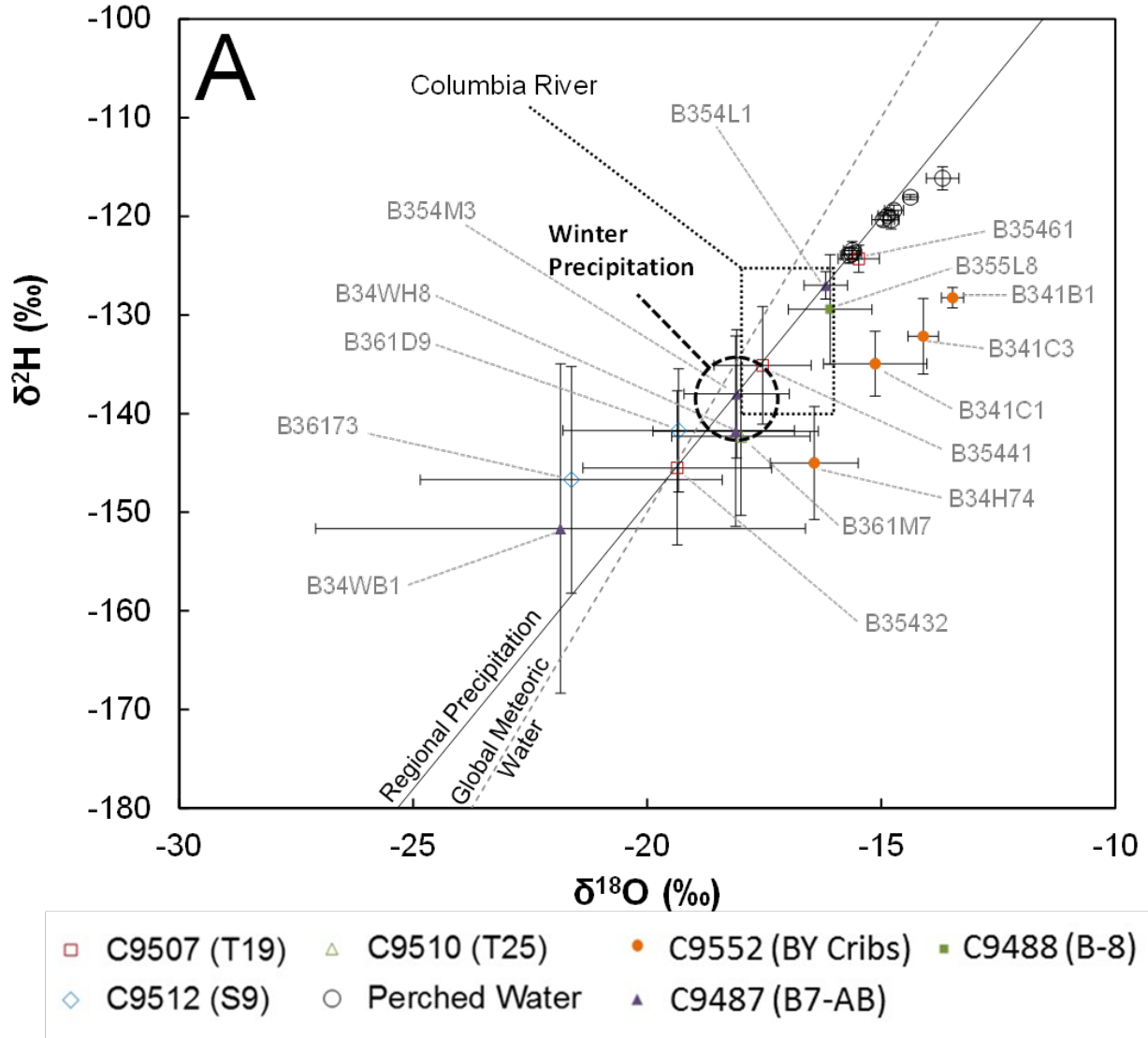
**Figure 6.** Isotope data for vadose zone sediment and perched water analyses. (A) Data resulting from the full data set. (B) Data refined by a Modified Thompson Tau test to remove outlier points (continued on next page). Depiction of winter precipitation is after DePaolo et al. (2004) with a nominal value of δ18O of ~ -18‰ and δ2H of ~ -138‰.
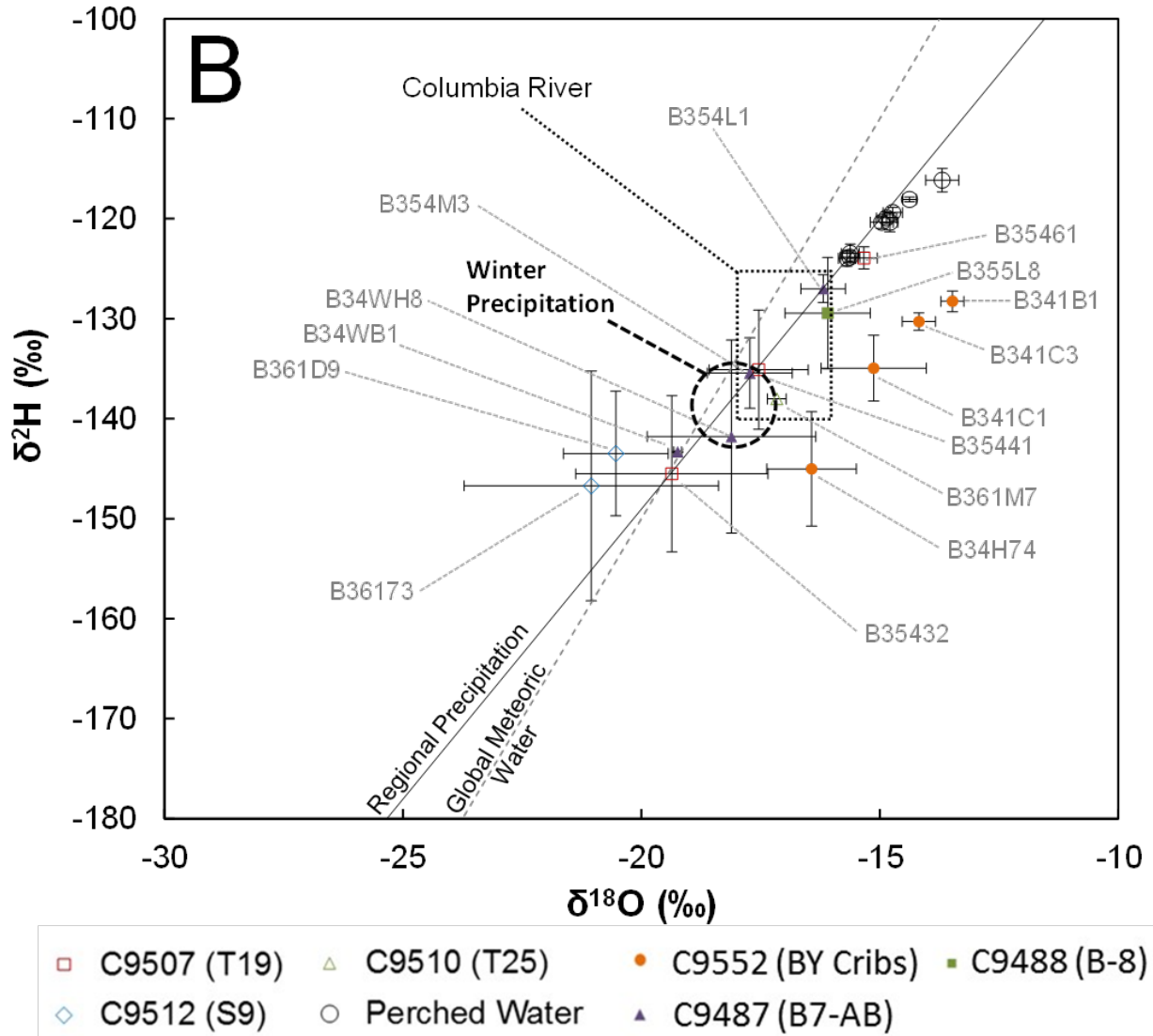
**Figure 6 (continued).** Isotope data for vadose zone sediment and perched water analyses. (A) Data resulting from the full data set. (B) Data refined by a Modified Thompson Tau test to remove outlier points. Depiction of winter precipitation is after DePaolo et al. (2004) with a nominal value of δ18O of ~ -18‰ and δ2H of ~ -138‰.
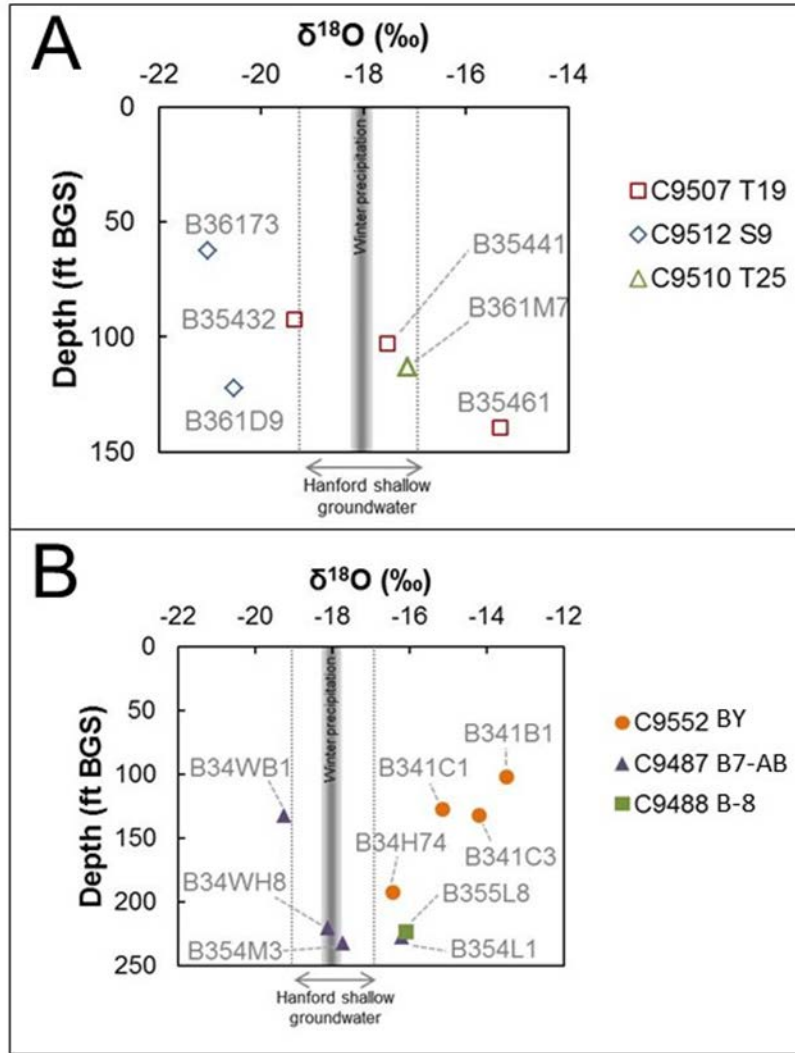
**Figure 7**. $\delta^{18}O$ relating to sample depth, average local winter precipitation, and local shallow groundwater within the Hanford Site: (A) sample data from the T- and S-Complexes, and (B) sample data from the B-Complex.
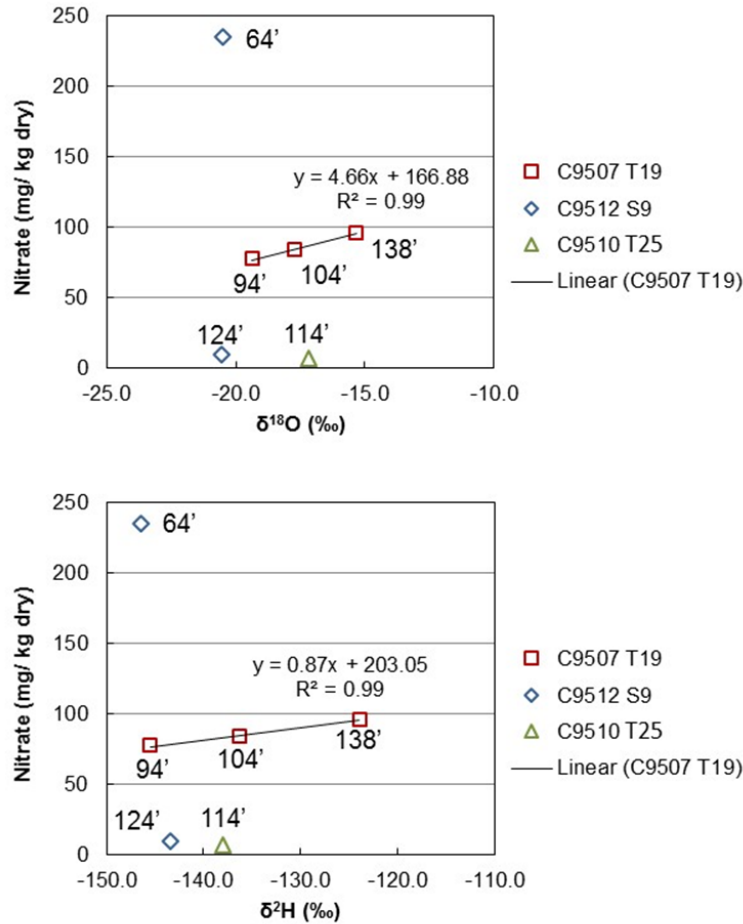
**Figure 8.** Correlation of isotopic ($\delta^2$H and $\delta^{18}$O) analysis and measured nitrate concentration from T- and S-Complex samples.

### 4.1.5 Sediment Physical Characterization

Physical characterization was conducted to define the hydrogeologic context for the observed contaminant and biogeochemical data. Fundamental information includes a geologist log and associated core pictures, and sediment physical properties (particle size distribution, particle and bulk density, moisture content, and porosity). Air permeability was measured to provide an indication of relative differences in permeability between samples. Detailed hydraulic characterization, including saturated and unsaturated hydraulic properties, was also conducted, but will be described in a separate report. The physical data reported here are descriptive for each individual sample. However, full interpretation is best conducted by considering the data for these samples in the context of data from other samples in the vadose zone. That broader interpretation will be conducted by CHPRC as part of their overall CSM efforts for the 200-DV-1 OU.

Core pictures are shown in Figure 9 through Figure 13. The geologist logs for these samples are included in Appendix A. Table 21 is a summary of the physical sediment characterization for these samples. Plots of the particle size distributions are shown in Figure 14 through Figure 18. Note that the

physical properties for two additional samples (B35435 and B35463, Table 1) will be determined and reported as part of the hydraulic property analysis report



**Figure 9**.  Photograph of sample B35442 (Core C9507, liner 16B, CCUc sediment sample).
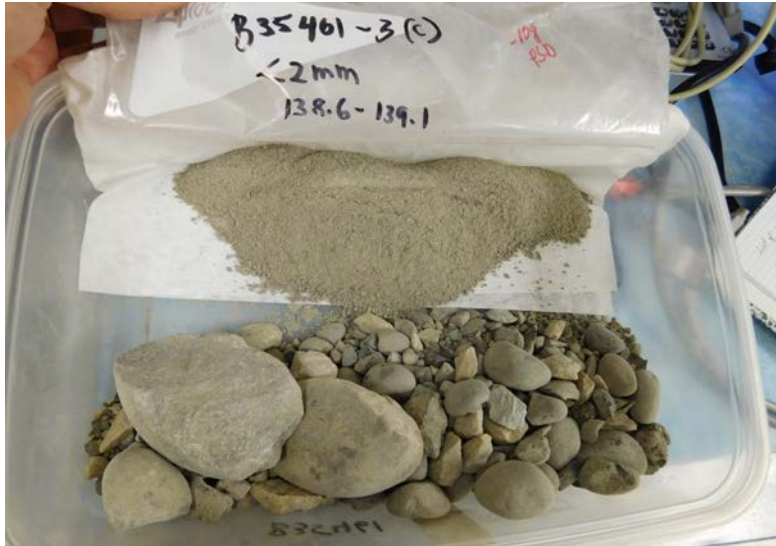


**Figure 10**.  Photograph of sample B35461 (Core C9507, Ringold sediment sample).

**Figure 11**.  Photograph of sample B361M9 (Core C9510, liner 14B, H2/CCUz sample).



**Figure 12**.  Photograph of sample B36175 (Core C9512, liner 8B, H1/H2 sample).

**Figure 13**. Photograph of sample B361F1 (Core C9512, liner 20B, H2/CCUz sample).

**Table 21**. Summary of measured physical properties.

| Column Parameters | Units | T19 16B (CCUc) C9507-B35442 | T19 138' (Ringold) C9507-B35461 | T25 14B (H2/CCU) C9510-B361M9 | S-9 8B (H1/2) C9512-B36175 | S-9 20B (H2) C9512-B361F1 |
|---|---|---|---|---|---|---|
| Diameter | cm | 8.89 | 8.89 | 8.89 | 8.89 | 8.89 |
| Length | cm | 30.897 | 15.75 | 30.4754 | 30.685 | 29.257 |
| Core volume | mL | 1917.833 | 977.631 | 1891.663 | 1904.674 | 1816.035 |
| Gravimetric moisture content | g/g | 0.154 | 0.027 | 0.064 | 0.025 | 0.030 |
| Volumetric moisture content | $m^3/m^3$ | 0.270 | 0.059 | 0.132 | 0.044 | 0.050 |
| Bulk density | $g/cm^3$ | 1.754 | 2.215 | 2.066 | 1.747 | 1.639 |
| Particle density | $g/cm^3$ | 2.739 | 2.754 | 2.739 | 2.624 | 2.652 |
| Porosity | $m^3/m^3$ | 0.360 | 0.196 | 0.246 | 0.334 | 0.382 |
| Air permeability | darcy | 0.053 | ---- | 0.059 | 3.935 | 0.779 |
| Gravel | % | 36.317 | 77.589 | 11.545 | 1.308 | 0.530 |
| Sand | % | 40.309 | 15.729 | 59.354 | 90.109 | 81.081 |
| Silt | % | 16.612 | 5.601 | 21.647 | 8.569 | 18.328 |
| Clay/mud | % | 6.763 | 1.082 | 7.456 | 0.015 | 0.062 |
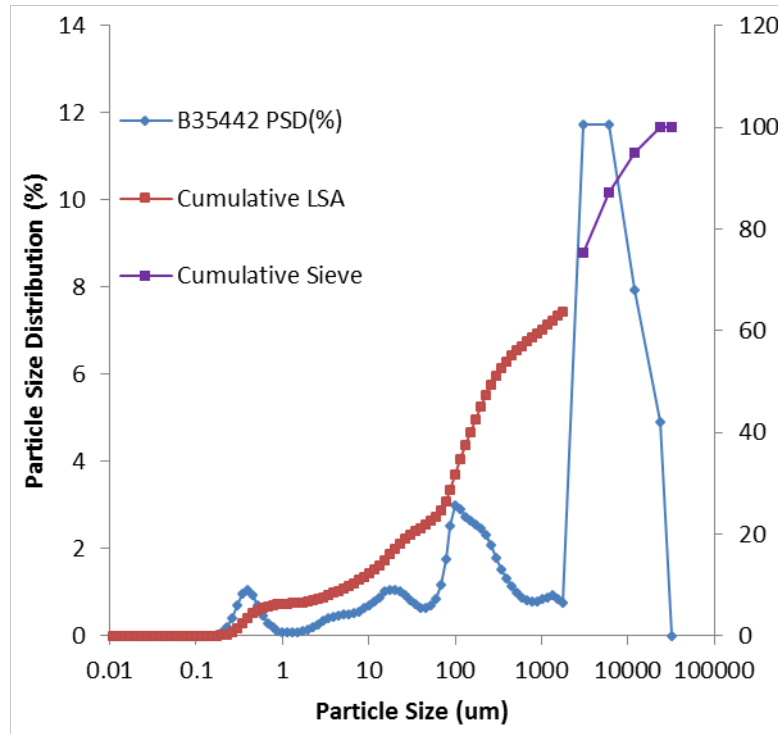
**Figure 14**. Particle size distribution of sample B35442 (Core C9507, liner 16B, CCUc sediment sample).
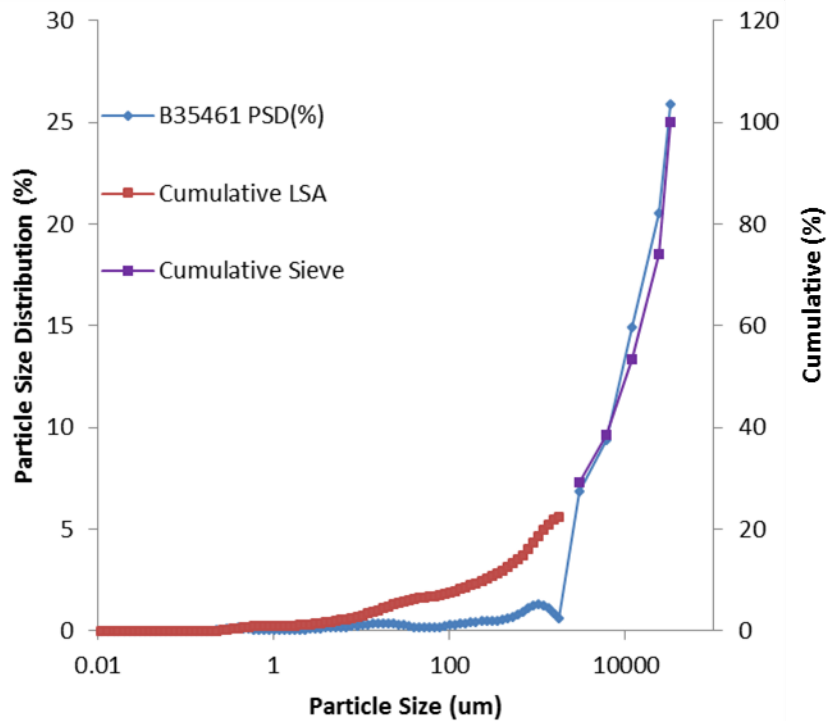


**Figure 15**. Particle size distribution of sample B35461 (Core C9507, Ringold sediment sample).
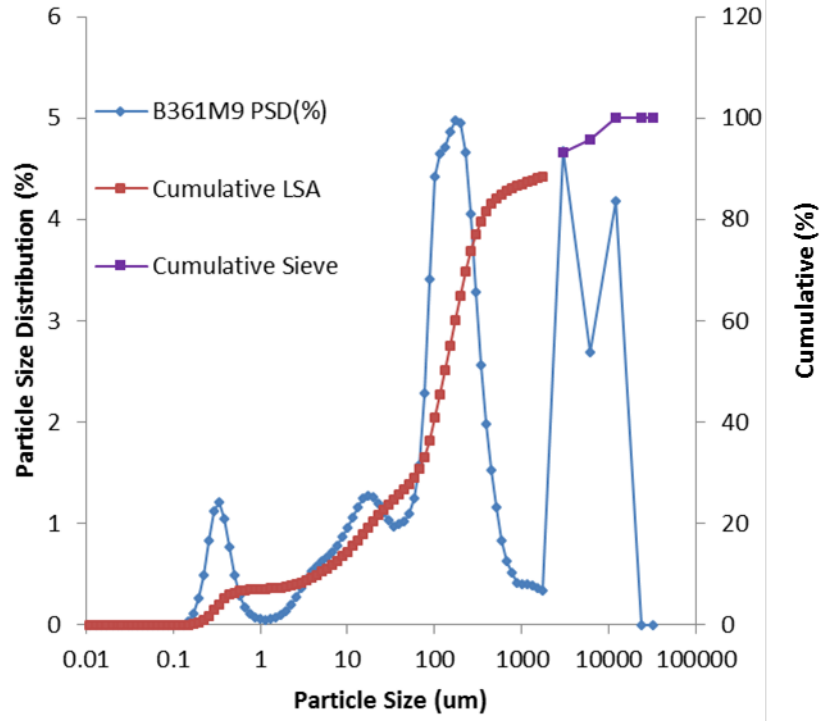
**Figure 16**. Particle size distribution of sample B361M9 (Core C9510, liner 14B, H2/CCUz sample).
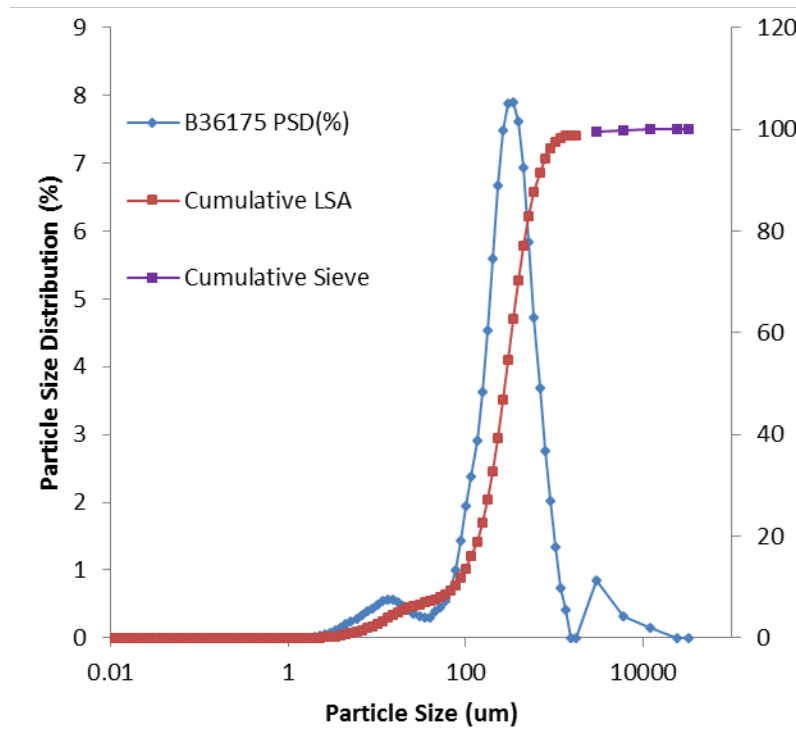


**Figure 17**. Particle size distribution of sample B36175 (Core C9512, liner 8B, H1/H2 sample).
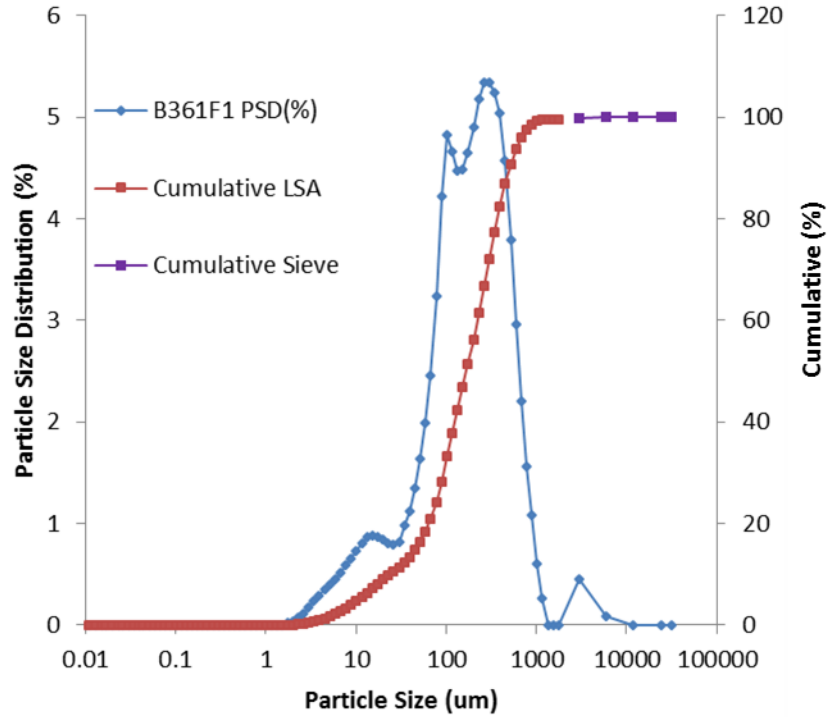
**Figure 18**. Particle size distribution of sample B361F1 (Core C9512, liner 20B, H2/CCUz sample).

The physical data characterize the basic hydrogeologic setting for each sample. The set of samples analyzed for this report represents a diverse set of hydrogeologic settings relevant to contaminant attenuation and transport in the Hanford Central Plateau vadose zone and important lithologic features for each targeted borehole (waste site). Additional information on hydraulic properties and physical properties for two additional samples will be reported separately.

## 4.2 Observation of Attenuation Processes

Identifying attenuation processes involves collecting data that can be used to demonstrate whether contaminants have interacted with sediments in a way that changes their mobility. One type of data is from sequential extractions (Table 22). In this process, a sediment sample is sequentially exposed to harsher extraction solutions and the contaminant concentration in each solution is measured. These data show how the contaminant mass in a sediment sample is distributed among water and different sediment-associated phases. Analysis for geochemical constituents was also conducted for each extraction solution to help interpret the types of sediment constituents mobilized or dissolved by each solution for the specific sediment sample. Speciation of iodine as iodide and iodate was also measured. However, interference from the matrix hindered iodine speciation analyses other than from the first extraction solution.

**Table 22**.  Sequential extraction of contaminants from sediment samples.

| Extraction Solution | Hypothesized Targeted Sediment Components | Interpreted Contaminant Mobility of Extracted Fraction | Color Code |
|---|---|---|---|
| Aqueous: artificial Hanford groundwater | Contaminants in pore water and a portion of sorbed uranium | Mobile phase | |
| Ion exchange: 1M Mg-nitrate | Readily desorbed contaminants | Readily mobile through equilibrium partitioning | |
| Acetate pH5: 1 hour in pH 5 sodium acetate solution | Contaminants associated with surface exposed carbonate precipitates and other readily dissolved precipitates | Moderately mobile through rapid dissolution processes | |
| Acetate pH 2.3: 1 week in pH 2.3 acetic acid | Dissolution of most carbonate compounds, and sodium boltwoodite (a hydrous uranium silicate) | Slow dissolution processes for contaminant release from this fraction; mobility is low with respect to impacting groundwater | |
| Oxalic acid: 1 hour | Dissolution of iron and manganese oxides | Slow dissolution processes are associated with contaminant release; mobility is very low with respect to impacting groundwater | |
| 8M HNO$_3$: 2 hours in 8M nitric acid at 95°C | Dissolves most phases that contained anthropogenic contaminants | Very slow dissolution processes are associated with contaminant release; functionally immobile; some or all of the contaminants in this phase may be naturally occurring. | |

Table 23 and associated Figure 19 through Figure 21 show the sequential extraction contaminant results for each sample for uranium, total iodine, and chromium.  There was no extractable Tc-99 contamination in these samples.  Iodine speciation for the first extraction is shown in Table 24. Geochemical constituents released in each extraction solution are shown in Figure 22 and in Figure 23. Interpretation of geochemical constituents accounted for the types of ions added as part of some of the extraction solutions (e.g., magnesium) and the effect of acidic conditions on some of the chemical analyses (e.g., iodine).

**Table 23**. Tabulated sequential extraction results for uranium, iodine, and chromium.

| Sample ID | Sample | µg/g Ext. 1 | µg/g Ext. 2 | µg/g Ext. 3 | µg/g Ext. 4 | µg/g Ext. 5 | µg/g Ext. 6 | µg/g Total | µg/g 1000h ext. | fraction Ext. 1 | fraction Ext. 2 | fraction Ext. 3 | fraction Ext. 4 | fraction Ext. 5 | fraction Ext. 6 |
|---|---|---|---|---|---|---|---|---|---|---|---|---|---|---|---|
| **Uranium** | | | | | | | | | | | | | | | |
| C9507-B35434 | T19 14C (CCUz) | 0.029 | 0.036 | 0.165 | 0.168 | 0.153 | 0.222 | 0.771 | 0.072 | 0.037 | 0.047 | 0.213 | 0.217 | 0.198 | 0.287 |
| C9507-B35443 | T19 16C (CCUc) | 0.155 | 0.095 | 0.550 | 0.523 | 0.019 | 1.719 | 3.061 | 0.427 | 0.051 | 0.031 | 0.180 | 0.171 | 0.006 | 0.562 |
| C9507-B35461 | T19 138' (Ringold) | 0.002 | 0.003 | 0.017 | 0.032 | 0.040 | 0.171 | 0.266 | 0.167 | 0.007 | 0.011 | 0.066 | 0.121 | 0.150 | 0.644 |
| C9510-B361N1 | T25 14C (H2/CCU) | 0.007 | 0.023 | 0.099 | 0.082 | 0.029 | 0.163 | 0.403 | 0.052 | 0.017 | 0.057 | 0.245 | 0.203 | 0.071 | 0.406 |
| C9512-B36177 | S-9 8C (H1/2) | 0.002 | 0.003 | 0.016 | 0.028 | 0.022 | 0.205 | 0.275 | 0.016 | 0.007 | 0.010 | 0.057 | 0.101 | 0.081 | 0.745 |
| C9512-B361F3 | S-9 20C (H2) | 0.004 | 0.005 | 0.031 | 0.035 | 0.044 | 0.118 | 0.237 | 0.025 | 0.019 | 0.019 | 0.133 | 0.147 | 0.186 | 0.496 |
| **Iodine** | | Ext. 1 | Ext. 2 | Ext. 3 | Ext. 4 | Ext. 5 | Ext. 6 | Total | 1000h ext. | Ext. 1 | Ext. 2 | Ext. 3 | Ext. 4 | Ext. 5 | Ext. 6 |
| C9507-B35434 | T19 14C (CCUz) | 0.002 | 0.002 | 0.108 | 0.082 | 0.024 | 0 | 0.219 | 0.023 | 0.011 | 0.009 | 0.495 | 0.376 | 0.109 | 0 |
| C9507-B35443 | T19 16C (CCUc) | 0.039 | 0.016 | 0.260 | 0.377 | 0.198 | 0 | 0.891 | 0.107 | 0.044 | 0.018 | 0.292 | 0.423 | 0.222 | 0 |
| C9507-B35461 | T19 138' (Ringold) | 0.010 | 0.004 | 0.016 | 0.038 | 0.030 | 0 | 0.097 | 0.021 | 0.102 | 0.044 | 0.160 | 0.387 | 0.306 | 0 |
| C9510-B361N1 | T25 14C (H2/CCU) | 0.012 | 0.017 | 0.217 | 0.292 | 0.196 | 0 | 0.734 | 0.068 | 0.016 | 0.023 | 0.296 | 0.397 | 0.267 | 0 |
| C9512-B36177 | S-9 8C (H1/2) | 0.003 | 0.001 | 0.008 | 0.009 | 0.004 | 0 | 0.025 | 0.006 | 0.102 | 0.051 | 0.310 | 0.368 | 0.170 | 0 |
| C9512-B361F3 | S-9 20C (H2) | 0.002 | 0.002 | 0.010 | 0.008 | 0.006 | 0 | 0.028 | 0.012 | 0.085 | 0.084 | 0.344 | 0.275 | 0.212 | 0 |
| **Chromium** | | Ext. 1 | Ext. 2 | Ext. 3 | Ext. 4 | Ext. 5 | Ext. 6 | Total | 1000h ext. | Ext. 1 | Ext. 2 | Ext. 3 | Ext. 4 | Ext. 5 | Ext. 6 |
| C9507-B35434 | T19 14C (CCUz) | 0.039 | 0 | 0 | 0 | 0 | 2.976 | 3.014 | -- | 0.013 | 0 | 0 | 0 | 0 | 0.987 |
| C9507-B35443 | T19 16C (CCUc) | 0.021 | 0 | 0 | 0 | 0 | 3.303 | 3.324 | -- | 0.006 | 0 | 0 | 0 | 0 | 0.994 |
| C9507-B35461 | T19 138' (Ringold) | 0.039 | 0 | 0 | 0.707 | 0.748 | 1.969 | 3.464 | -- | 0.011 | 0 | 0 | 0.204 | 0.216 | 0.569 |
| C9510-B361N1 | T25 14C (H2/CCU) | 0 | 0 | 0 | 0 | 0 | 2.813 | 2.813 | -- | 0 | 0 | 0 | 0 | 0 | 1.000 |
| C9512-B36177 | S-9 8C (H1/2) | 0 | 0 | 0 | 0 | 0 | 3.851 | 3.851 | -- | 0 | 0 | 0 | 0 | 0 | 1.000 |
| C9512-B361F3 | S-9 20C (H2) | 0 | 0 | 0 | 0 | 0 | 4.2494 | 4.249 | -- | 0 | 0 | 0 | 0 | 0 | 1.000 |
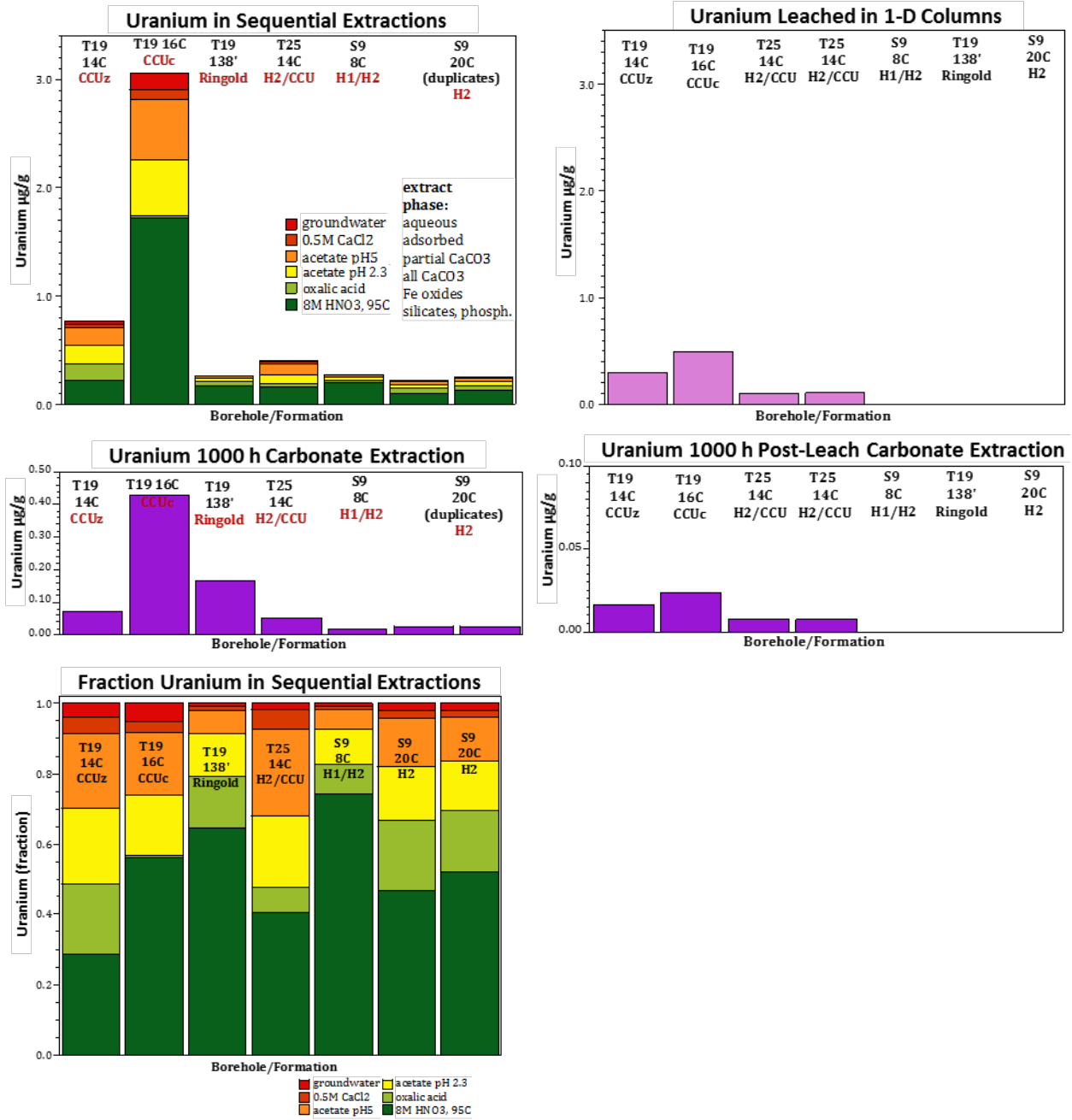
**Figure 19**. Uranium sequential extraction results. Note that leaching experiments were not conducted for samples T-19 Ringold (C9507-B35461), S-9 8C (C9512-B36177), or S-9 20C (C9512-B361F3).
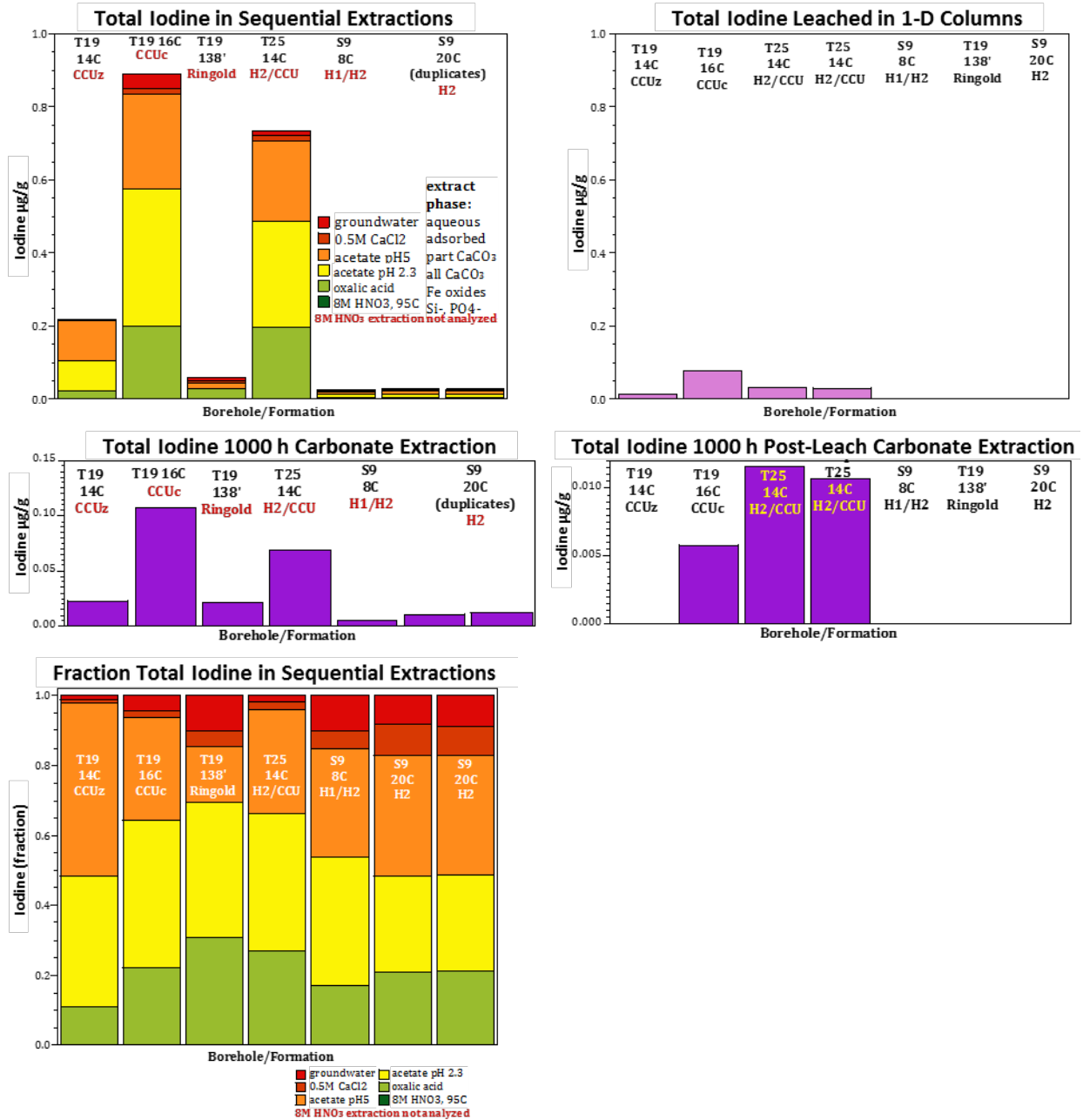
**Figure 20**. Iodine sequential extraction results. Note that leaching experiments were not conducted for samples T-19 Ringold (C9507-B35461), S-9 8C (C9512-B36177), or S-9 20C (C9512-B361F3).
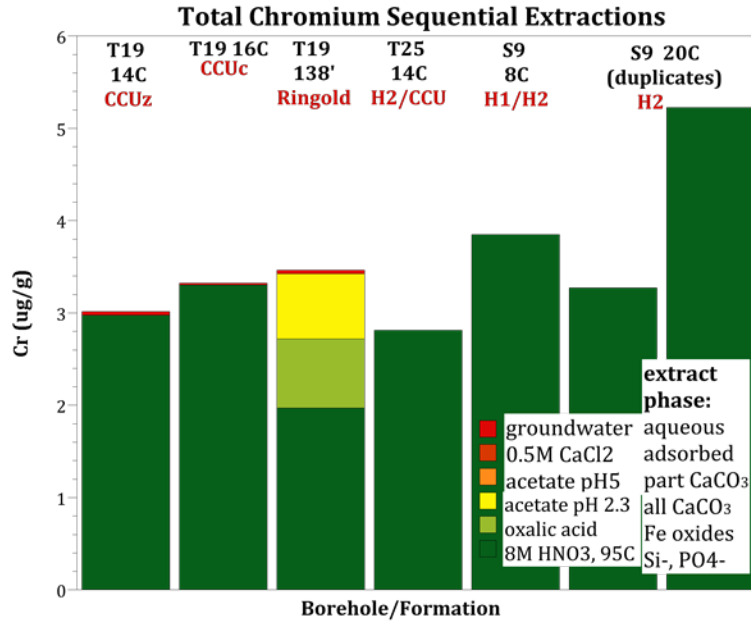
**Figure 21**. Chromium sequential extraction results.

**Table 24**. Iodine speciation.

| Sample Name | Sample Location | Iodate (µg/L) | Iodide (µg/L) | Total Iodine (µg/L) |
|---|---|---|---|---|
| C9507-B35434 | T19 14C (CCUz) | 0.827 | ND | 1.24 |
| C9507-B35443 | T19 16C (CCUc) | 3.76 | 13.4 | 18.6 |
| C9507-B35461 | T19 138' (Ringold) | 0.817 | 4.24 | 5.84 |
| C9510-B361N1 | T25 14C (H2/CCU) | 1.31 | 3.35 | 5.04 |
| C9512-B36177 | S-9 8C (H1/2) | ND | ND | 1.19 |
| C9512-B361F3 | S-9 20C (H2) | ND | ND | 1.3 |
| ND is not detected. | | | | |
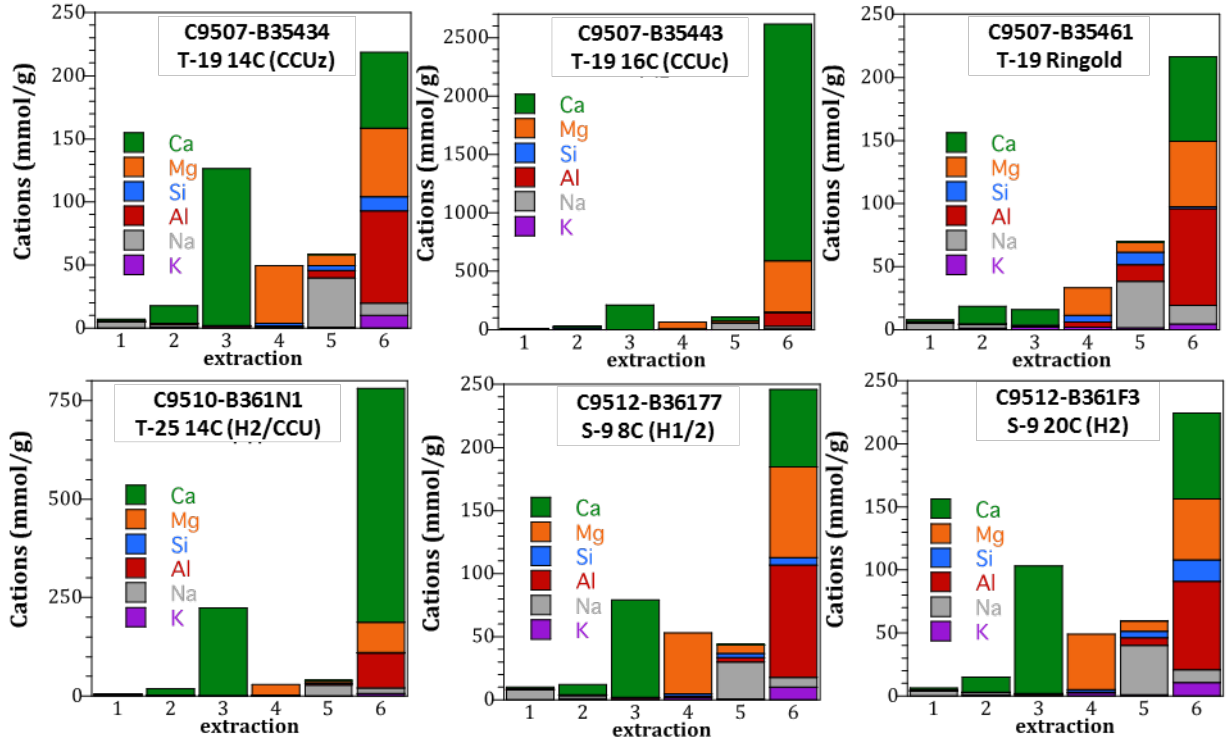
**Figure 22**. Cations measured in sequential extraction solutions. Note that metals are not reported if the extraction solution contained that metal (Ca for extraction 4, Mg for extractions 2 and 3, and Na in extractions 3 and 4).
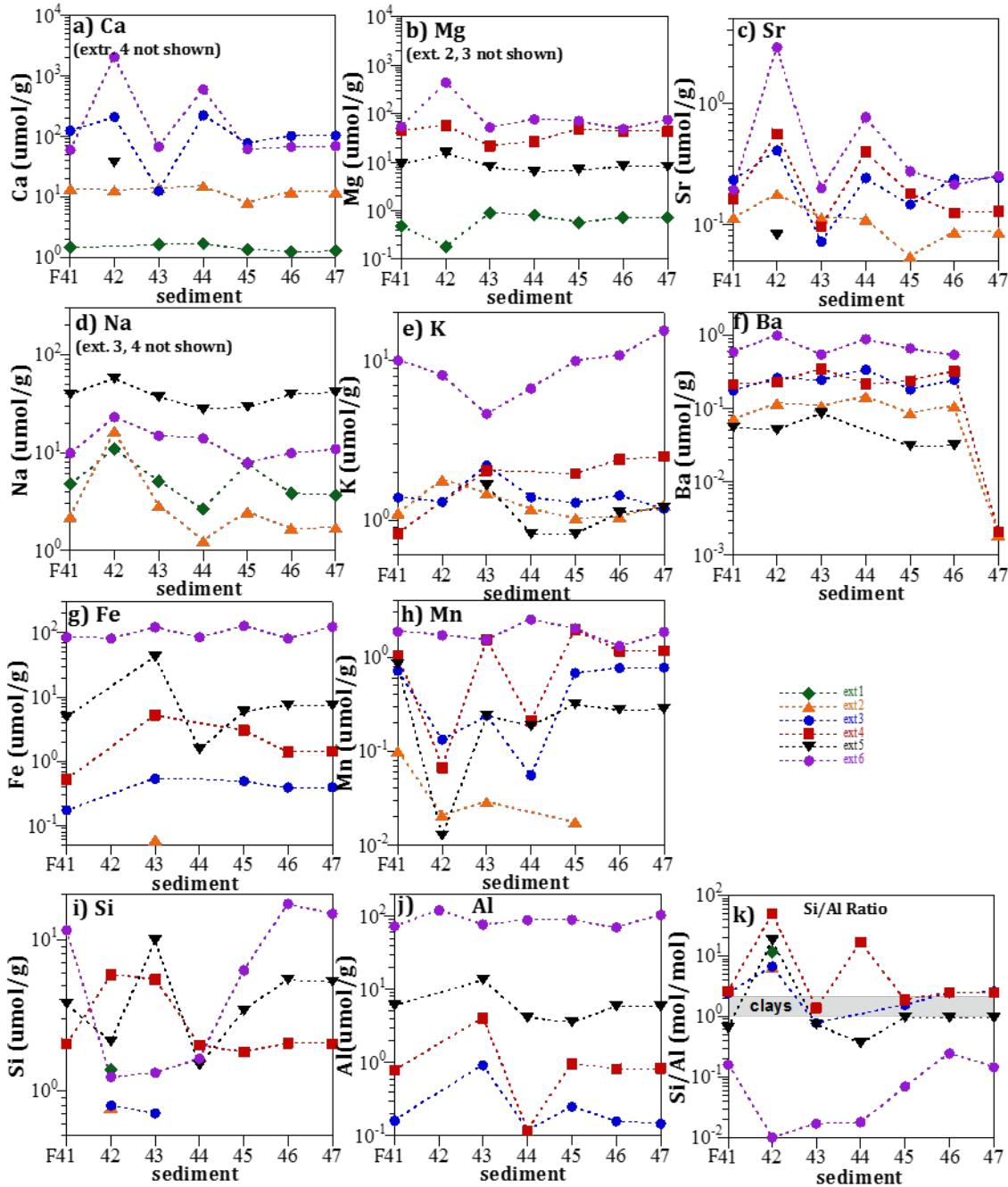
**Figure 23**. Major and trace cations/metals measured in sequential extractions: (a) Ca, (b) Mg, (c) Sr, (d) Na, (e) K, (f) Ba, (g) Fe, (h) Mn, (i) Si, (j) Al, and (k) Si/Al ratio. The sediment sample codes are F41 = C9507-B35434, T19 14C; F42 = C9507-B35443, T19 16C; F43 = C9507-B35461, T19 138'; F44 = C9510-B361N1, T25 14C; F45 = C9512-B36177, S9 8C; and F46 = F47 = C9512-B361F3, S9 20C.

The sequential extraction data for uranium (Table 23, Figure 19) show only a small portion of the uranium mass in the samples is present in the aqueous and sorbed (mobile) phases. In every sample, the highest fraction of uranium mass is in the sixth extraction, likely representing mostly natural uranium. For the B35443 sample of CCU high-carbonate sediment with the highest uranium concentration, the

third and fourth extractions (representing carbonate materials) show relatively high fractions of uranium. In summary, for uranium, a relatively small fraction of the uranium mass in these samples would transport under equilibrium partitioning conditions (i.e., is mobile). Thus, transport analyses should include kinetic transport processes or recognize that a portion of the uranium is functionally immobile. The 1000-hour extraction results, targeted at identifying mobile uranium, are consistent with the sequential extraction results in that the uranium mass extracted in the 1000-hour test is about the same as all of the mass in the first two sequential extractions plus a portion of the mass in the third extraction. Post-soil-column-leaching results show that the uranium mass extracted in the 1000-hour test is reduced dramatically, as expected. Soil-column effluent data analyzed as cumulative mass of uranium leached are consistent with the loss in uranium mass shown in the comparison of pre- and post-soil-column-test uranium mass in the 1000-hour extraction tests and are similar to the uranium mass present in the first two sequential extractions plus a portion of the mass in the third extraction.

The sequential extractions for total iodine (Table 23, Figure 20) also show a low fraction of the iodine in the aqueous and sorbed (mobile) phases. In every sample, the largest fraction of the iodine is in the third and fourth extractions, representing carbonate materials. Iodine is also present in the fifth extraction. Iodine determination in the sixth extractions was hindered by the acidic matrix and was not reportable. Speciation of iodine was only possible in the first extraction (Table 24). Iodide dominated the speciation in first extraction for samples B35443, B361N1, and B35461, which all had relatively high total iodine concentrations. Iodate dominated the speciation in sample B35434. Other samples were non-detect for both iodine species. A significant amount of iodine was present in the third and fourth extractions, which are targeted at determining contaminant concentrations associated with carbonate precipitates. It is most likely that carbonate-associated iodine would be in the iodate form, but speciation was not possible for these extraction solutions. As with uranium, only a small fraction of the iodine mass in these samples would transport under equilibrium partitioning conditions (i.e., is mobile). Thus, transport analyses should include kinetic transport processes or recognize that a portion of the iodine is functionally immobile. This assessment is based on total iodine (which includes both I-127 and I-129), but the behavior of I-129 is expected to be similar to total iodine. The mechanism for the relatively large portion of iodine found in the extractions not associated with equilibrium partitioning may be association of iodate with carbonate precipitates. This type of co-precipitation has been observed in the scientific literature (Zhang et al. 2013; Podder et al. 2016) and is consistent with release of iodine in the third and fourth extractions that are targeted at dissolving carbonate precipitates.

As with uranium, the iodine sequential extraction, 1000-hour extraction, and soil-column data show consistent results (Table 23, Figure 20). The 1000-hour extraction results, targeted at identifying mobile iodine, are consistent with the sequential extraction results in that the iodine mass extracted in the 1000-hour test is about the same as all of the mass in the first two sequential extractions plus a portion of the mass in the third extraction. Post-soil-column-leaching results show that the iodine mass extracted in the 1000-hour test is reduced dramatically, as expected. Soil-column effluent data analyzed as cumulative mass of iodine leached are consistent with the loss in iodine mass shown in the comparison of pre- and post-soil-column-test iodine mass in the 1000-hour extraction tests and are similar to the iodine mass that was present in the first two sequential extractions plus a portion of the mass in the third extraction.

The sequential extraction data for chromium suggest that all of the chromium is natural, as expected based on water, acid, and alkaline extraction chromium results (Section 4.1). Thus, these data are not interpreted in terms of chromium attenuation and transport processes.

Ions released from sequential extractions can be interpreted, although the interpretation must consider the ions present in the extraction solutions (Figure 22 and Figure 23). Samples B35434, B35461, B361F3, and B36177 are similar in the types and amounts of ions released in the extractions, with moderate differences in carbonate concentration (Ca and Mg released in extractions 3 and 4). Samples B35443 and B361N1 have a much higher carbonate content, as indicated by the amount of calcium released, but are otherwise similar to the other samples.

Another important category of experiment that can demonstrate contaminant mobility is a leaching test that can quantify how quickly contaminants are released into the aqueous phase. In this type of test, sediments containing contaminants are exposed to artificial pore water to quantify release of the existing contaminants into the aqueous phase. For a batch leaching test, sediments are contacted with a single aqueous solution for a long time period. Samples of the aqueous phase are analyzed for contaminant concentration. Initial, short-contact-time results are representative of equilibrium partitioning of contaminants from the sediments. Over time, if the contaminant concentration stays stable at near this initial concentration, it can be interpreted that only equilibrium partitioning is controlling contaminant release from the sediments. Concentrations rising over time indicate that some kinetically controlled process such as dissolution of precipitates or diffusion from small pores in the sediments is contributing to contaminant release from the sediments. Both partitioning and kinetically controlled contaminant release attenuate the mobility of contaminants.

Batch leaching results are shown in Figure 24 and Figure 25 for uranium and iodine, respectively. Analysis showed that Cr(VI) and Tc-99 in the artificial pore water were below detection limits in all of the sediments. The aqueous uranium concentration increased in all sediments (Figure 24), indicating slow kinetic release of uranium, likely from a combination of adsorbed U-carbonate species desorption (relatively rapid release) and exchange with uranium in solid phase carbonates (relatively slow release). Sediment uranium concentrations ranged from 0.3 to 30 µg/L initially (at 1 hour), and increased to 0.72 to 44 µg/L by 1000 hours.
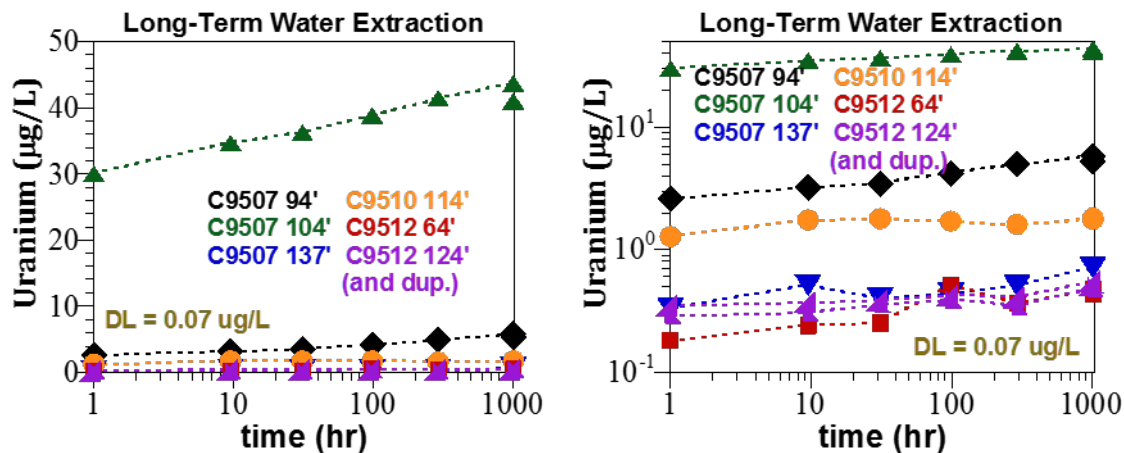


**Figure 24**. Aqueous uranium concentration in long-term batch leaching experiment.
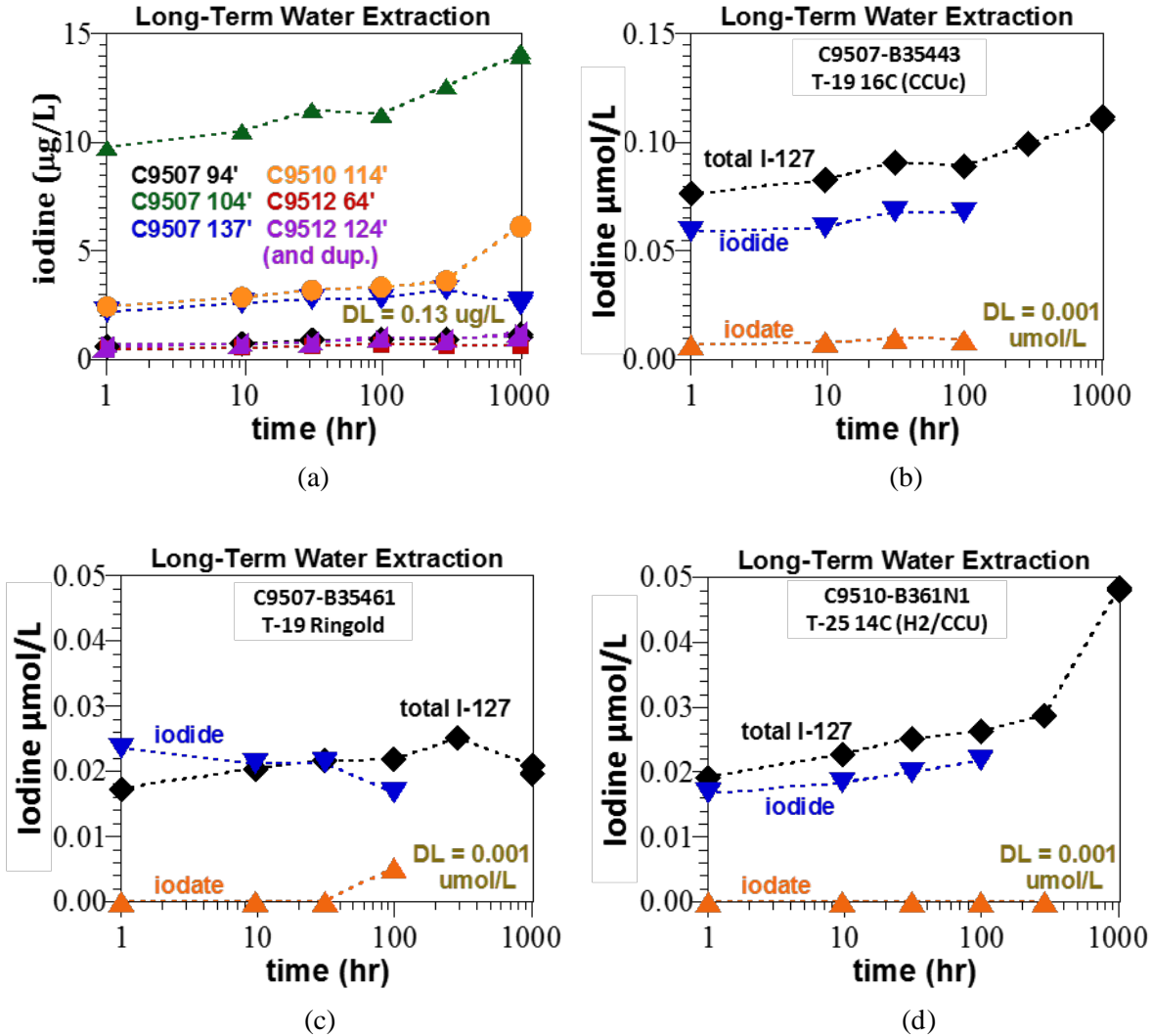
**Figure 25**.  Aqueous total iodine concentration in long-term batch leaching experiment: (a) total iodine for all sediments, (b) iodine species for C9507-B35443, T-19 16C, (c) iodine species for C9507-B35461, T-19 138', and (d) iodine species for C9510-B361N1, T-25 14C.  Iodine speciation for other sediments was below detection limits.

Release of iodine species from sediments was also kinetically controlled (Figure 25), with total iodine concentrations ranging from 0.2 to 10 µg/g initially (at 1 hour), and increasing to 0.3 to 14 µg/g by 1000 hours (Figure 25a).  Iodine speciation was difficult to characterize in sediments at these low concentrations in a matrix of high ion concentration (i.e., mainly Na-nitrate) because the analysis relies on anion separation before iodide or iodate mass analysis.  Three sediments had concentrations of iodine species (Figure 25b to d) above the detection limits, which showed that 75% to 100% of the iodine in the aqueous phase was iodide.  Iodide is more mobile than iodate (about 4 times lower $K_d$), and iodate can be incorporated into carbonates.  Thus, it is expected that iodide would be most susceptible to short-term release from sediments.  Iodate, if present, may be more slowly released if it is incorporated into carbonate precipitates.  Determination of iodine speciation was not possible in all of the sequential extractions.  However, in samples with the highest total iodine concentration, iodide dominated the species in the first water extraction.  For the sequential extractions, a significant amount of total iodine

was present in the third and fourth extractions (contaminant associated with carbonate precipitates). Dissolution rates for iodate-carbonate precipitates may be slow and may not contribute significantly to the iodine concentration in the batch leaching experiment.

Soil-column leaching tests contact sediments with a clean flowing artificial groundwater under saturated flow conditions. Contaminant concentrations in the effluent of the column are controlled by the magnitude of equilibrium partitioning and kinetically controlled contaminant release processes (e.g., dissolution of precipitates or small-pore diffusion). Soil-column tests provide data that can be interpreted in terms of modeling contaminant release and partitioning under one-dimensional transport conditions. Slower release of contaminant mass from the column (i.e., continued release over many pore volumes of water flow through the column) indicates the partitioning and/or kinetically controlled processes are attenuating the mobility of the contaminant. In addition, stop-flow events, where the water flow in the column is stopped for tens to hundreds of hours, can indicate the presence of kinetically controlled contaminant release if the contaminant concentration increases during the stop-flow event.

Soil-column leaching results are shown in Figure 26 through Figure 37. Uranium and iodine show some slow-release behavior in terms of an extended release of contaminants over time from the column. In addition, an increase in uranium and iodine concentration during stop-flow events was observed for all events, though the magnitude varied. Additional analysis of stop-flow events is provided in Section 4.3. Analysis shows that Tc-99 and Cr(VI) in effluent samples were all below detection limits, so these are not shown. Analysis of cations and anions (excluding carbonate) on selected effluent samples shows that Na and nitrate decrease rapidly to near influent artificial groundwater concentrations. Bromide breakthrough shows uniform flow in columns, with average retardation of 0.96 to 1.04. Iodine species analysis on effluent samples was difficult due to the high nitrate concentration because the analysis relies on anion separation before iodide or iodate mass analysis. Only a few samples from the first pore volume of column effluent had iodine concentrations high enough for speciation analysis. Thus, the speciation data are not of value and are not reported.



(a)  (b)
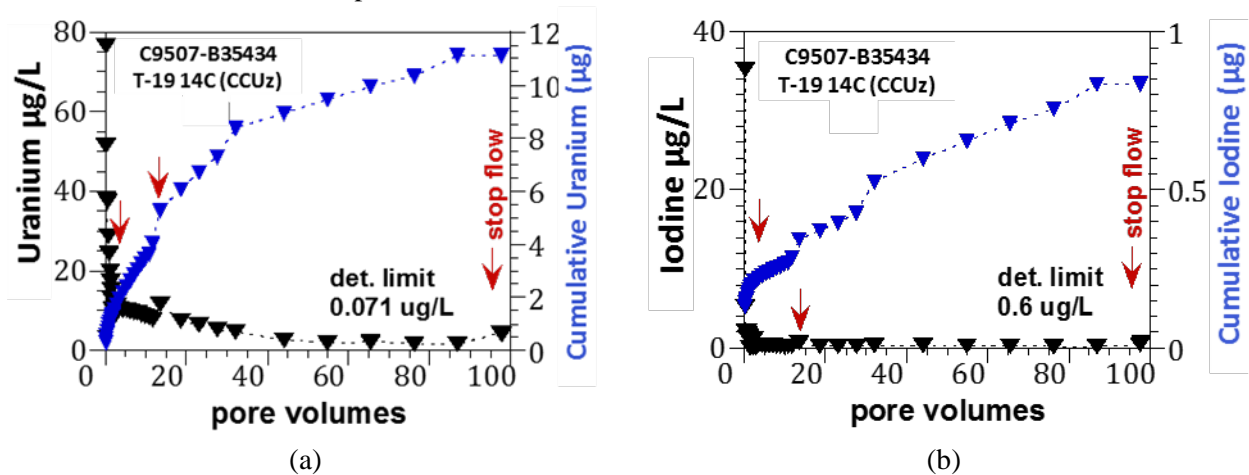
**Figure 26**. Artificial groundwater leaching of the C9507-B35434, T19 14C sample for (a) uranium, and (b) total iodine effluent concentrations. Most iodate and iodide concentrations were below detection limits.
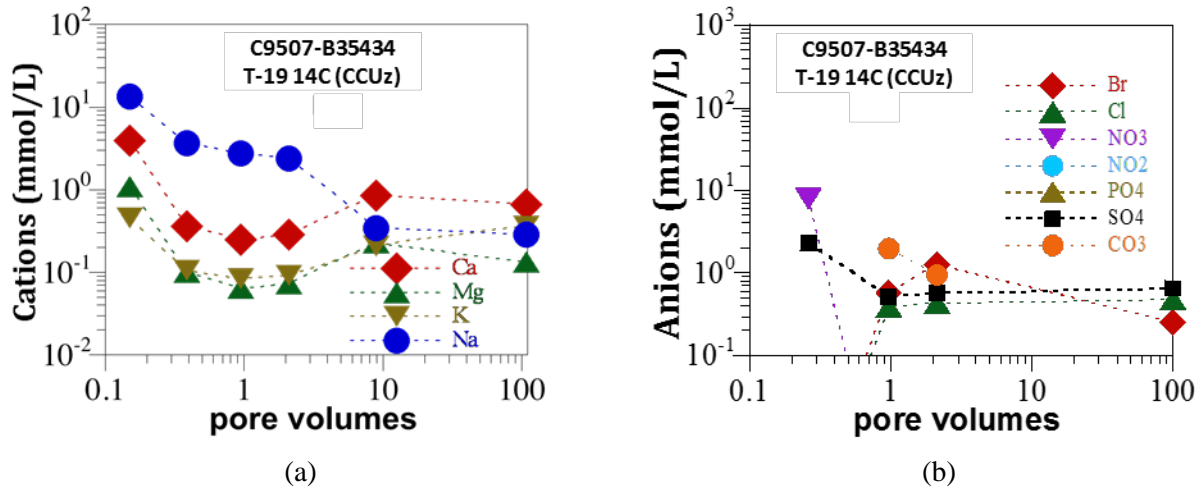
**Figure 27**. Artificial groundwater leaching of the C9507-B35434, T19 14C sample for (a) cation and (b) anion effluent concentrations for selected samples.
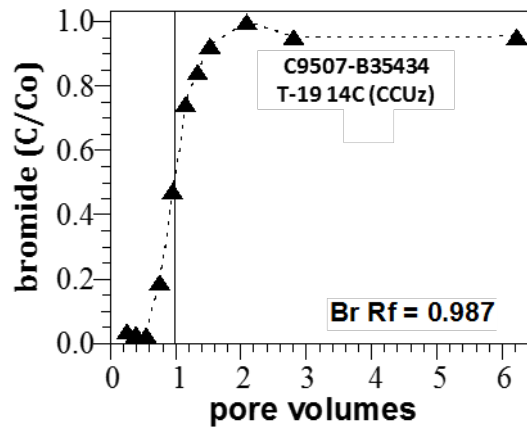


**Figure 28**. Artificial groundwater leaching of the C9507-B35434, T19 14C sample for tracer (bromide) effluent concentration.

(a)

(b)
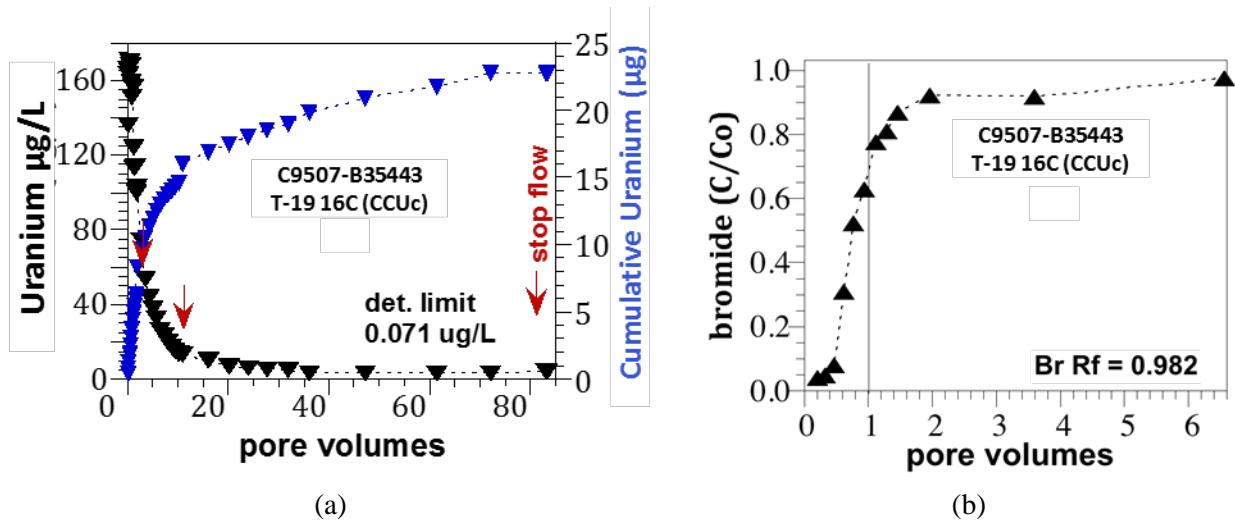
**Figure 29**. Artificial groundwater leaching of the C9507-B35443, T19 16C sample for (a) uranium and (b) tracer (bromide) effluent concentrations.
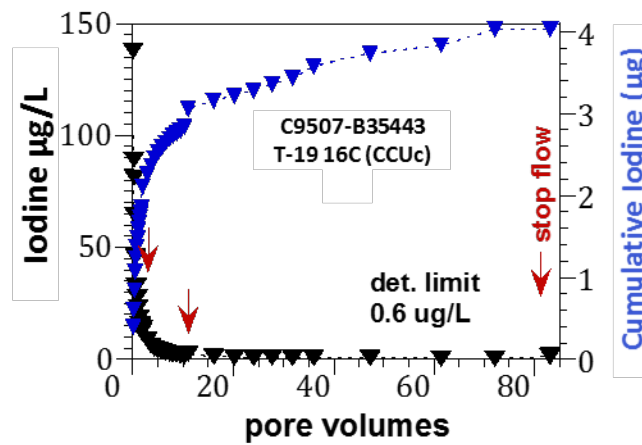


**Figure 30**. Artificial groundwater leaching of the C9507-B35443, T19 16C sample for total iodine data.
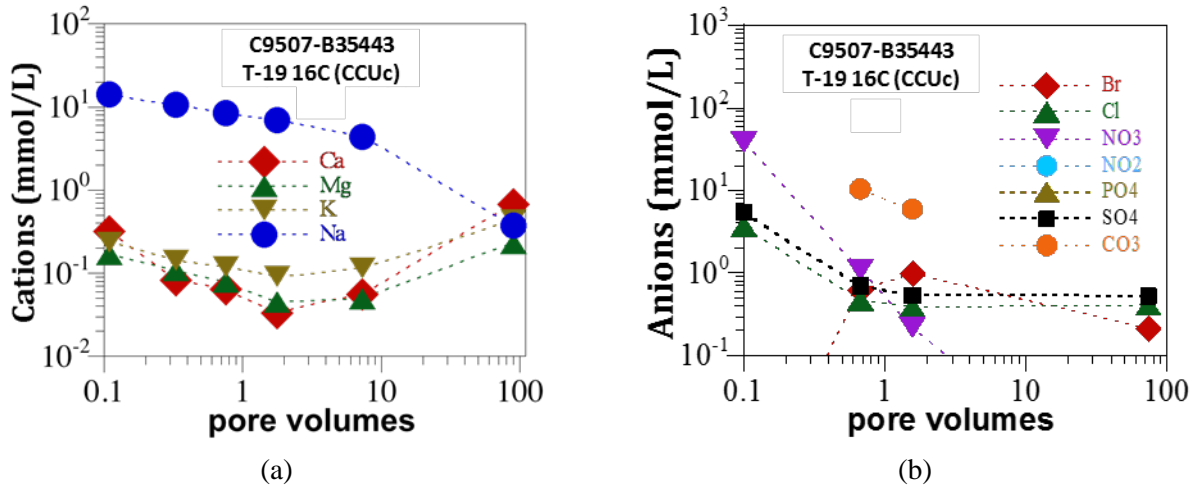
**Figure 31**. Artificial groundwater leaching of the C9507-B35443, T19 16C sample for (a) cation and (b) anion effluent concentrations for selected samples.
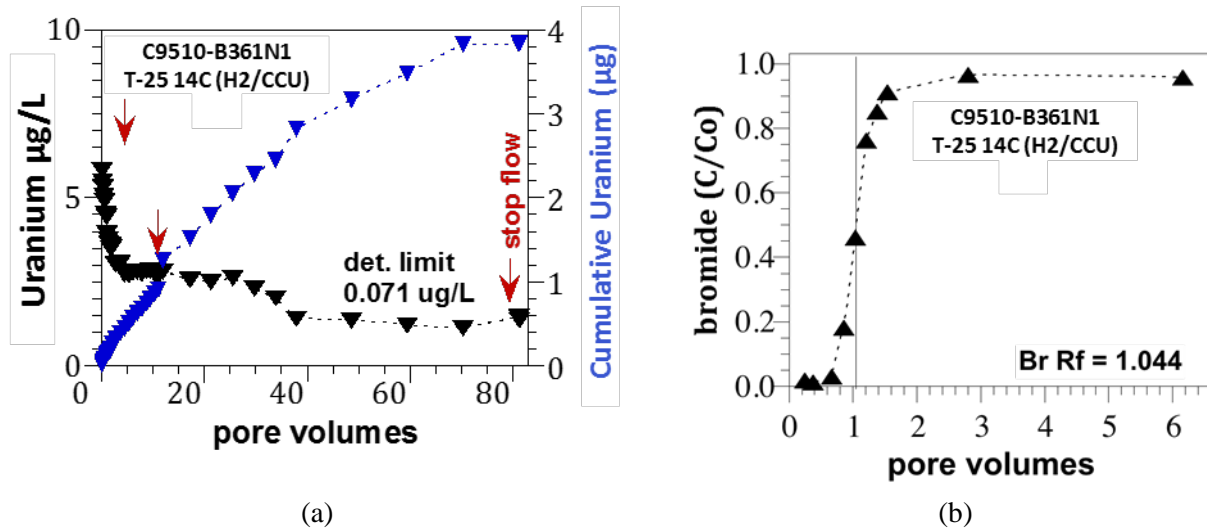


**Figure 32**. Artificial groundwater leaching of the C9510, T25 14C sample for (a) uranium and (b) tracer (bromide) effluent concentrations.
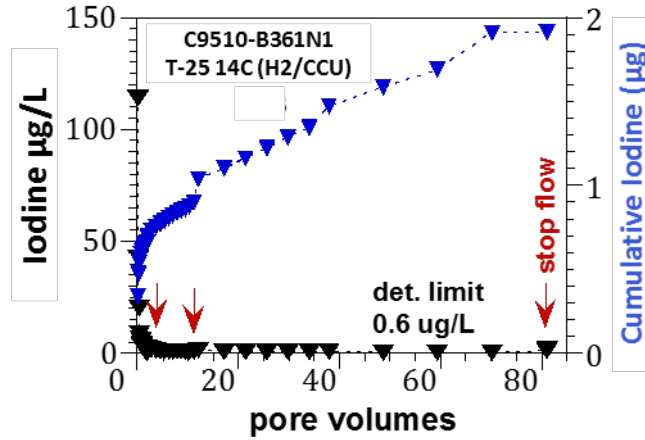
**Figure 33**. Artificial groundwater leaching of the C9510, T25 14C sample for total iodine data.



(a)

(b)
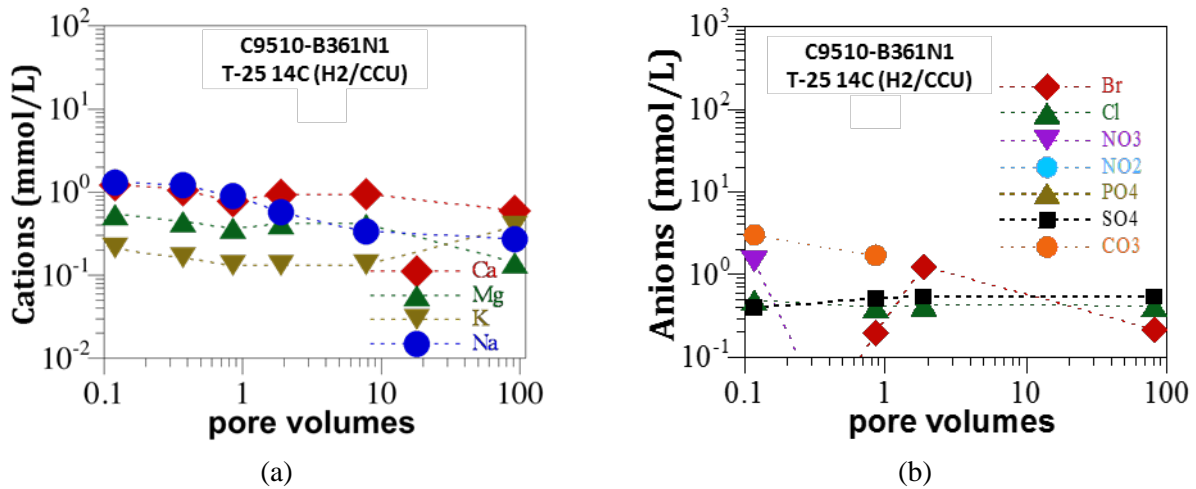
**Figure 34**. Artificial groundwater leaching of the C9510, T25 14C sample for (a) cation and (b) anion
effluent concentrations for selected samples.

(a)

(b)
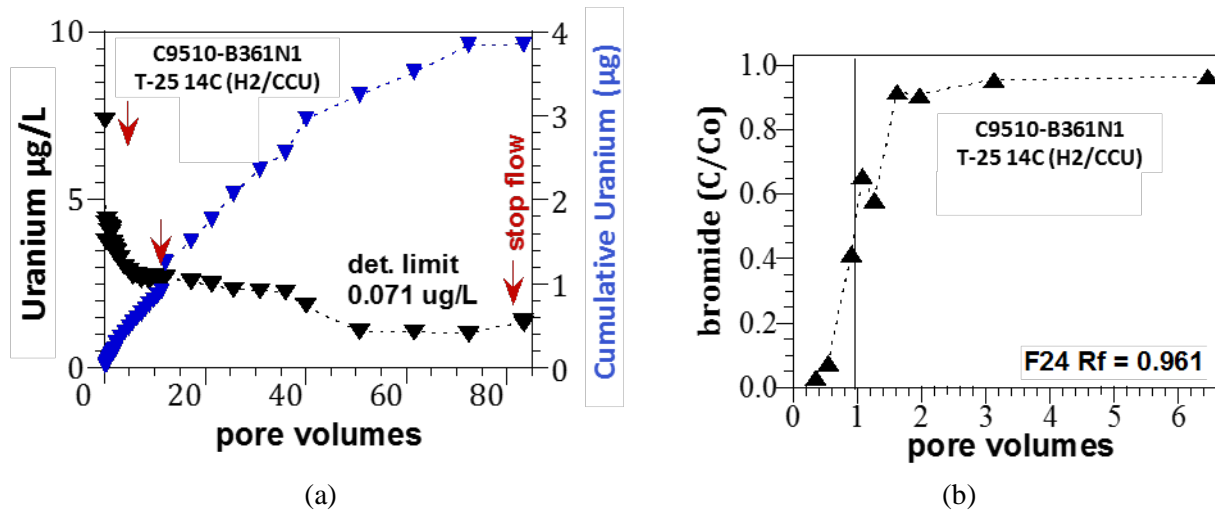
**Figure 35**. Artificial groundwater leaching of the C9510, T25 14C sample (duplicate sample) for (a) uranium and (b) tracer (bromide) effluent concentrations.
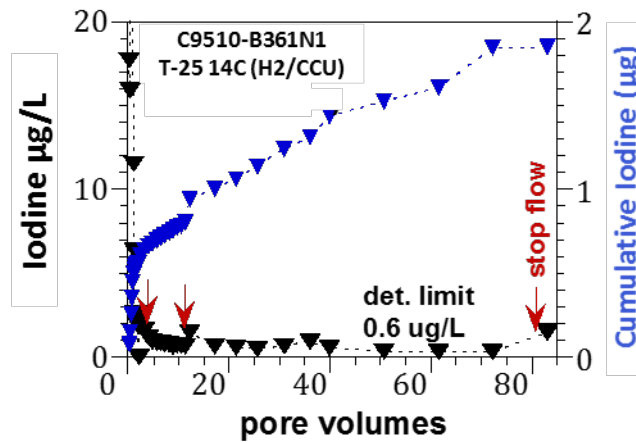


**Figure 36**. Artificial groundwater leaching of the C9510, T25 14C sample (duplicate sample) for total iodine data.
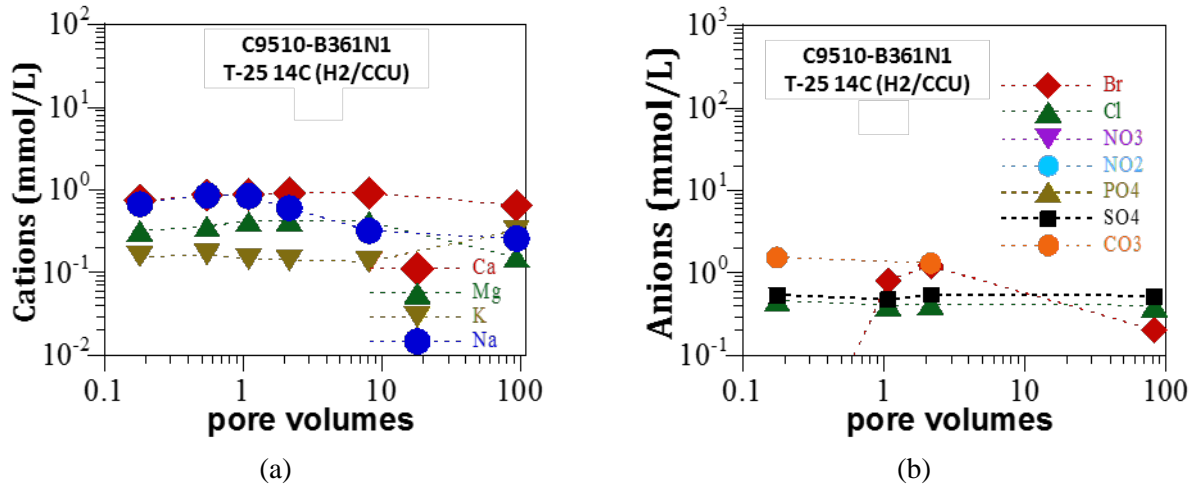
**Figure 37**. Artificial groundwater leaching of the C9510, T25 14C sample (duplicate sample) for (a) cation and (b) anion effluent concentrations for selected samples.

The batch and soil-column leaching tests demonstrate that there is some slow release of uranium and iodine in these samples. This type of release is consistent with attenuation mechanisms associated with sorption properties and dissolution of carbonates over time in the saturated column conditions. Nitrate was released very rapidly, confirming the low sorption properties of this contaminant. Assessment of chromium and Tc-99 was not possible with these leaching experiments due to the low/non-detect contaminant concentrations in the samples (noting that chromium in the sediments was attributed to natural chromium only extractable by acid). Interpretation of the leaching results in terms of transport parameters is provided in Section 4.3.

## 4.3  Quantification of Attenuation and Transport Parameters

Several types of data were collected that can be analyzed to estimate attenuation and transport parameters that are needed for fate and transport assessments. The batch leaching and soil-column leaching experiments presented in Section 4.2 can be interpreted to estimate transport parameters. The concentration trend of batch leaching data can be used to estimate a contaminant release rate. Column effluent data can be modeled to estimate transport parameters, though this type of analysis is not included in this report. Stop-flow data can be used to estimate contaminant release rates based on the observed change in concentration over the stop-flow time interval. Because some of the samples did not contain sufficient contamination for effective application of leaching experiments, spiked-contaminant tests were conducted that can be used to evaluate transport parameters. Batch experiments spiked with contaminants can be analyzed to assess both adsorption and desorption linear equilibrium partitioning coefficients ($K_d$) based on the observed ratio of solid- and solution-phase contaminant concentrations. Spike-contaminant soil-column tests provide breakthrough and elution curves, which, when compared to conservative tracer breakthrough and elution curves, can be used to estimate adsorption and desorption linear equilibrium partitioning coefficients ($K_d$).

Table 25 shows the batch leaching data interpreted as contaminant release rates from the sediment. These rates were calculated for the data collected between 100 and 1000 hours of contact time. The change in concentration from time zero, where the concentration in the aqueous phase would be zero, and the 100-hour sample was interpreted to represent sorption-related contaminant release.

**Table 25**. Post-sorption contaminant release rates calculated for batch leaching experiments.

| Sample Name | Sample Location | Iodine (ug/kg/d) | Uranium (ug/kg/d) |
|---|---|---|---|
| C9507-B35434 | T19 14C (CCUz) | 0.015 | 0.098 |
| C9507-B35443 | T19 16C (CCUc) | 0.261 | 0.261 |
| C9507-B35461 | T19 138' (Ringold) | - | 0.024 |
| C9510-B361N1 | T25 14C (H2/CCU) | 0.247 | 0.010 |
| C9512-B36177 | S-9 8C (H1/2) | - | - |
| C9512-B361F3 | S-9 20C (H2) | 0.022 | 0.010 |

Table 26 shows tabulated data for stop-flow events and the associated calculated contaminant release rates. The computed release rates for uranium and iodine are generally higher for samples with higher total contaminant mass leached. Over time as more pore volumes are passed through the soil-column, release rates of iodine generally declined. Note that release rates are for total iodine; the iodine speciation method was not sensitive enough to provide data during stop-flow events. For uranium, the response was mixed, with a general decline shown in the highest uranium (and carbonate) sample, B35443, but steady to increasing release rates for the other samples.

**Table 26**. Contaminant release rates calculated for stop-flow events during soil-column leaching experiments.

| Sample Name | Sample Location | Stop Flow (pv) | Uranium Rel. Rate (ug/kg/day) | Iodine Rel. Rate (ug/kg/day) | Stop Flow (pv) | Uranium Rel. Rate (ug/kg/day) | Iodine Rel. Rate (ug/kg/day) | Stop Flow (pv) | Uranium Rel. Rate (ug/kg/day) | Iodine Rel. Rate (ug/kg/day) |
|---|---|---|---|---|---|---|---|---|---|---|
| C9507-B35434 | T19 14C (CCUz) | 2.09 | 1.385 | 0.568 | 11.65 | 1.808 | 0.183 | 86.90 | 1.299 | 0.115 |
| C9507-B35443 | T19 16C (CCUc) | 1.78 | 1.951 | 1.106 | 10.20 | 0.195 | 0.585 | 83.10 | 0.501 | 0.442 |
| C9510-B361N1 | T25 14C (H2/CCU) | 1.89 | 0.044 | 1.056 | 11.15 | 0.058 | 0.412 | 81.06 | 0.160 | 0.402 |
| C9510-B361N1 | T25 14C (H2/CCU) | 2.15 | 0.023 | 1.017 | 11.65 | 0.042 | 0.366 | 86.90 | 0.178 | 0.553 |

Table 27 and Table 28 show the adsorption and desorption linear equilibrium partitioning coefficients ($K_d$) from spiked-contaminant batch experiments for pore water and artificial groundwater tests, respectively. Table 29 and Table 30 show the adsorption and desorption linear equilibrium partitioning coefficients ($K_d$) from spiked-contaminant batch experiments conducted at multiple spike concentrations for samples B35434 and B35461 for pore water and artificial groundwater tests, respectively. These results are the average of two replicate experiments. In most cases, replicate results were comparable and the average data are used to interpret the batch partitioning experiment results. Results for individual tests are shown in Appendix B.

**Table 27**. Calculated partitioning coefficients for spiked-contaminant experiments using the pore-water recipe (Table 8).

| | | Uranium | | Tc-99 (pertechnetate) | | Iodate | | Iodide | | Chromate | |
|---|---|---|---|---|---|---|---|---|---|---|---|
| | | adsorption (mL/g) | desorption (mL/g) | adsorption (mL/g) | desorption (mL/g) | adsorption (mL/g) | desorption (mL/g) | adsorption (mL/g) | desorption (mL/g) | adsorption (mL/g) | desorption (mL/g) |
| C9507-B35434 | 1-day | 1.82 | 0.79 | 0.21 | 1.14 | 0.86 | 2.36 | 0.03 | 0 | 0.14 | 2.40 |
| T19 14C (CCUz) | 7-day | 1.57 | 1.14 | 0.21 | 0.72 | 2.69 | 2.89 | 0 | 0 | 0.20 | 2.06 |
| | 28-day | 1.40 | 0.97 | 0.22 | 0.48 | 1.13 | 3.76 | 0 | 0 | 0.56 | 3.30 |
| C9507-B35443 | 1-day | 9.10 | 6.99 | 0.22 | 13.98 | 3.91 | 5.62 | 0 | 0 | 0.25 | 2.41 |
| T19 16C (CCUc) | 7-day | 10.49 | 10.24 | 0.31 | 6.12 | 4.03 | 6.36 | 0 | 0 | 0.28 | 1.71 |
| | 28-day | 8.06 | 10.30 | 0.76 | 9.41 | 3.22 | NR | 0 | 0 | 0.41 | 1.49 |
| C9507-B35461 | 1-day | 1.64 | 0.87 | 0.11 | 0.91 | 0.81 | 1.33 | 0 | 0 | 0.52 | NR |
| T19 138' | 7-day | 1.16 | 0.71 | 0.07 | 0.34 | 1.25 | 2.53 | 0 | 0 | 4.02 | 141.59 |
| (Ringold) | 28-day | 0.56 | 0.71 | 0.25 | 0.77 | 0.77 | 1.97 | 0 | 0 | 8.64 | NR |
| C9510-B361N1 | 1-day | 5.21 | 6.26 | 0.20 | 0.65 | 6.59 | 5.92 | 0 | 0 | 0.18 | 1.81 |
| T25 14C | 7-day | 5.85 | 5.26 | 0.11 | 0.24 | 6.03 | 7.90 | 0 | 0 | 0.20 | 1.07 |
| (H2/CCU) | 28-day | 5.42 | 6.63 | 0.17 | 0.27 | 5.13 | 9.06 | 0 | 0 | 0.65 | 2.52 |
| C9512-B36177 | 1-day | 0.87 | 0.36 | 0.05 | 0.07 | 1.03 | 2.52 | 0 | 0 | 0.10 | 11.27 |
| S-9 8C (H1/2) | 7-day | 0.75 | 0.44 | 0 | 0 | 1.33 | 3.16 | 0.04 | 0.16 | 0.24 | 15.66 |
| | 28-day | 0.43 | 0.38 | 0.03 | 0 | 1.06 | 3.83 | 0.00 | 0 | 0.98 | 11.74 |
| C9512-B361F3 | 1-day | 2.36 | 1.54 | 0.12 | 0.29 | 0.76 | 1.30 | 0.04 | 0 | 0.13 | 1.29 |
| S-9 20C (H2) | 7-day | 2.84 | 2.00 | 0.03 | 0 | 1.66 | 2.24 | 0.04 | 0.04 | 0.29 | 1.43 |
| | 28-day | 1.91 | 2.57 | 0.11 | 0.01 | 0.59 | 1.52 | 0 | 0 | 0.68 | 2.97 |

NR is not reported because concentrations in the desorption solution were below detection.
A value of "0" was assigned to any computed $K_d$ value of less than zero.

**Table 28**. Calculated partitioning coefficients for spiked-contaminant experiments using the artificial groundwater recipe (Table 9).

| | | Uranium | | Tc-99 (pertechnetate) | | Iodate | | Iodide | | Chromate | |
|---|---|---|---|---|---|---|---|---|---|---|---|
| | | adsorption (mL/g) | desorption (mL/g) | adsorption (mL/g) | desorption (mL/g) | adsorption (mL/g) | desorption (mL/g) | adsorption (mL/g) | desorption (mL/g) | adsorption (mL/g) | desorption (mL/g) |
| C9507-B35434 T19 14C (CCUz) | 1-day | NR | NR | 0.04 | 0.26 | 0.98 | 1.89 | 0 | 0 | 0.02 | 0.36 |
| | 7-day | NR | NR | 0.04 | 0 | 1.22 | 1.68 | 0 | 0 | 0.05 | 0.33 |
| | 28-day | NR | NR | 0.04 | 0 | 1.31 | 1.61 | 0.02 | 0 | 0.40 | 2.06 |
| C9507-B35443 T19 16C (CCUc) | 1-day | NR | NR | 0.04 | 1.83 | 2.20 | 4.46 | 0 | 0 | 0.09 | 0.88 |
| | 7-day | NR | NR | 0.32 | 1.55 | 2.61 | 3.75 | 0 | 0 | 0.12 | 0.97 |
| | 28-day | NR | NR | 0.23 | 0.69 | 2.49 | 3.12 | 0 | 0 | 0.26 | 1.06 |
| C9507-B35461 T19 138' (Ringold) | 1-day | NR | NR | 0.13 | 2.43 | 0.61 | 0.99 | 0 | 0 | 0.17 | 18.22 |
| | 7-day | NR | NR | 0.27 | 2.35 | 0.80 | 0.95 | 0 | 0 | 0.73 | 18.35 |
| | 28-day | NR | NR | 0.14 | 0.40 | 0.70 | 0.96 | 0 | 0 | 4.08 | 36.35 |
| C9510-B361N1 T25 14C (H2/CCU) | 1-day | NR | NR | 0.04 | 0.30 | 5.94 | 7.35 | 0 | 0 | 0.09 | 0.59 |
| | 7-day | NR | NR | 0.07 | 0.07 | 5.10 | 4.03 | 0 | 0 | 0.11 | 0.53 |
| | 28-day | NR | NR | 0 | 0 | 4.89 | 9.09 | 0 | 0 | 0.41 | 1.58 |
| C9512-B36177 S-9 8C (H1/2) | 1-day | NR | NR | 0 | 0 | 0.68 | 1.31 | 0 | 0 | 0.01 | 0.26 |
| | 7-day | NR | NR | 0 | 0 | 0.74 | 1.33 | 0 | 0 | 0.15 | 0.79 |
| | 28-day | NR | NR | 0 | 0 | 0.89 | 1.58 | 0 | 0 | 0.23 | 1.57 |
| C9512-B361F3 S-9 20C (H2) | 1-day | NR | NR | 0.05 | 0.26 | 0.79 | 1.12 | 0 | 0 | 0.06 | 0.26 |
| | 7-day | NR | NR | 0.07 | 0.28 | 0.94 | 1.14 | 0 | 0 | 0.19 | 0.61 |
| | 28-day | NR | NR | 0 | 0 | 0.87 | 1.22 | 0.001 | 0 | 0.17 | 0.70 |

NR is not reported: For uranium, the NR is because the no-sediment control showed large concentration decreases.
A value of "0" was assigned to any computed $K_d$ value of less than zero.

**Table 29**. Calculated partitioning coefficients for spiked-contaminant experiments using the pore-water recipe (Table 8) for samples B35434 and B35461 with multiple spiked-contaminant concentrations.

| | | Uranium | | | | | |
|---|---|---|---|---|---|---|---|
| | | adsorption (mL/g) | adsorption (mL/g) | adsorption (mL/g) | desorption (mL/g) | desorption (mL/g) | desorption (mL/g) |
| Initial Concentration | | 100 µg/L | 500 µg/L | 1000 µg/L | 100 µg/L | 500 µg/L | 1000 µg/L |
| C9507-B35434 T19 14C (CCUz) | 1-day | 1.17 | 1.82 | 1.74 | 0 | 0.79 | 0.98 |
| | 7-day | 1.56 | 1.57 | 2.75 | 0.34 | 1.14 | 2.16 |
| | 28-day | 1.34 | 1.40 | 2.99 | 0 | 0.97 | 2.58 |
| C9507-B35461 T19 138' (Ringold) | 1-day | 1.57 | 1.64 | 1.58 | 0 | 0.87 | 0.75 |
| | 7-day | 1.47 | 1.16 | 2.15 | 0.99 | 0.71 | 1.86 |
| | 28-day | 0.94 | 0.56 | 2.74 | 0.56 | 0.71 | 2.66 |

| | | Tc-99 (pertechnetate) | | | | | |
|---|---|---|---|---|---|---|---|
| | | adsorption (mL/g) | adsorption (mL/g) | adsorption (mL/g) | desorption (mL/g) | desorption (mL/g) | desorption (mL/g) |
| Initial Concentration | | 5 µg/L | 10 µg/L | 50 µg/L | 5 µg/L | 10 µg/L | 50 µg/L |
| C9507-B35434 T19 14C (CCUz) | 1-day | 0.04 | 0 | 0.21 | 0.80 | 0.43 | 1.14 |
| | 7-day | 0.55 | 0.45 | 0.21 | 1.16 | 1.61 | 0.72 |
| | 28-day | 0.62 | 0.41 | 0.22 | 1.07 | 0.88 | 0.48 |
| C9507-B35461 T19 138' (Ringold) | 1-day | 0.06 | 0 | 0.11 | 1.82 | 0 | 0.91 |
| | 7-day | 0.71 | 0.45 | 0.07 | 8.01 | 3.10 | 0.34 |
| | 28-day | 0.33 | 0.41 | 0.25 | 1.74 | 5.64 | 0.77 |

| | | Iodate | | | | | |
|---|---|---|---|---|---|---|---|
| | | adsorption (mL/g) | adsorption (mL/g) | adsorption (mL/g) | desorption (mL/g) | desorption (mL/g) | desorption (mL/g) |
| Initial Concentration | | 100 µg/L | 500 µg/L | 1000 µg/L | 100 µg/L | 500 µg/L | 1000 µg/L |
| C9507-B35434 T19 14C (CCUz) | 1-day | 0.86 | 0.95 | 0.52 | 2.36 | 2.08 | 0.88 |
| | 7-day | 2.69 | 0.46 | 0.73 | 2.89 | 1.03 | 1.81 |
| | 28-day | 1.13 | 0.55 | 0.51 | 3.76 | 0.19 | 0.36 |
| C9507-B35461 T19 138' (Ringold) | 1-day | 0.81 | 0.79 | 0.31 | 1.33 | 2.07 | 0.61 |
| | 7-day | 1.25 | 0.32 | 0.65 | 2.53 | 0.41 | 1.65 |
| | 28-day | 0.77 | 0.27 | 0.17 | 1.97 | 0 | 0 |

| | | Iodide | | | | | |
|---|---|---|---|---|---|---|---|
| | | adsorption (mL/g) | adsorption (mL/g) | adsorption (mL/g) | desorption (mL/g) | desorption (mL/g) | desorption (mL/g) |
| Initial Concentration | | 100 µg/L | 500 µg/L | 1000 µg/L | 100 µg/L | 500 µg/L | 1000 µg/L |
| C9507-B35434 T19 14C (CCUz) | 1-day | 0.03 | 0 | 0.08 | 0 | 0 | 0.17 |
| | 7-day | 0 | 0.07 | 0.03 | 0 | 0.09 | 0 |
| | 28-day | 0 | 0.04 | 0.05 | 0 | 0 | 0.01 |
| C9507-B35461 T19 138' (Ringold) | 1-day | 0 | 0 | 0 | 0 | 0 | 0 |
| | 7-day | 0 | 0 | 0 | 0 | 0 | 0 |
| | 28-day | 0 | 0.02 | 0 | 0 | 0.01 | 0 |

| | | Chromate | | | | | |
|---|---|---|---|---|---|---|---|
| | | adsorption (mL/g) | adsorption (mL/g) | adsorption (mL/g) | desorption (mL/g) | desorption (mL/g) | desorption (mL/g) |
| Initial Concentration | | 100 µg/L | 500 µg/L | 1000 µg/L | 100 µg/L | 500 µg/L | 1000 µg/L |
| C9507-B35434 T19 14C (CCUz) | 1-day | 0.09 | 0.14 | 0.03 | 4.49 | 2.40 | 0.41 |
| | 7-day | 0.15 | 0.20 | 0.09 | 3.82 | 2.06 | 0.53 |
| | 28-day | 0.78 | 0.56 | 0.37 | 2.40 | 3.30 | 2.00 |
| C9507-B35461 T19 138' (Ringold) | 1-day | 0.22 | 0.52 | 0.10 | NR | NR | NR |
| | 7-day | 2.07 | 4.02 | 0.68 | 25.70 | 141.59 | 61.87 |
| | 28-day | 18.96 | 8.64 | 11.47 | NR | NR | NR |

NR is not reported because concentrations in the desorption solution were below detection.
A value of "0" was assigned to any computed $K_d$ value of less than zero.

**Table 30**. Calculated partitioning coefficients for spiked-contaminant experiments using the artificial groundwater recipe (Table 9) for samples B35434 and B35461 with multiple spiked-contaminant concentrations.

| | | Uranium | | | | | |
|---|---|---|---|---|---|---|---|
| | | adsorption (mL/g) | adsorption (mL/g) | adsorption (mL/g) | desorption (mL/g) | desorption (mL/g) | desorption (mL/g) |
| | Initial Concentration | 100 µg/L | 500 µg/L | 1000 µg/L | 100 µg/L | 500 µg/L | 1000 µg/L |
| C9507-B35434 T19 14C (CCUz) | 1-day | NR | NR | NR | NR | NR | NR |
| | 7-day | NR | NR | NR | NR | NR | NR |
| | 28-day | NR | NR | NR | NR | NR | NR |
| C9507-B35461 T19 138' (Ringold) | 1-day | NR | NR | NR | NR | NR | NR |
| | 7-day | NR | NR | NR | NR | NR | NR |
| | 28-day | NR | NR | NR | NR | NR | NR |
| | | Tc-99 (pertechnetate) | | | | | |
| | | adsorption (mL/g) | adsorption (mL/g) | adsorption (mL/g) | desorption (mL/g) | desorption (mL/g) | desorption (mL/g) |
| | Initial Concentration | 5 µg/L | 10 µg/L | 50 µg/L | 5 µg/L | 10 µg/L | 50 µg/L |
| C9507-B35434 T19 14C (CCUz) | 1-day | 0 | 0.02 | 0.04 | 0.15 | 0.62 | 0.26 |
| | 7-day | 0.14 | 0.10 | 0.04 | 1.96 | 0.46 | 0 |
| | 28-day | 0.20 | 0.08 | 0.04 | 0.18 | 0 | 0 |
| C9507-B35461 T19 138' (Ringold) | 1-day | 0 | 0 | 0.13 | 0.01 | 1.07 | 2.43 |
| | 7-day | 0.29 | 0.39 | 0.27 | 4.92 | 6.49 | 2.35 |
| | 28-day | 0.20 | 0.10 | 0.14 | 2.41 | 1.13 | 0.40 |
| | | Iodate | | | | | |
| | | adsorption (mL/g) | adsorption (mL/g) | adsorption (mL/g) | desorption (mL/g) | desorption (mL/g) | desorption (mL/g) |
| | Initial Concentration | 100 µg/L | 500 µg/L | 1000 µg/L | 100 µg/L | 500 µg/L | 1000 µg/L |
| C9507-B35434 T19 14C (CCUz) | 1-day | 0.98 | 0.60 | 0.18 | 1.89 | 1.44 | 0.22 |
| | 7-day | 1.22 | 0.82 | 0.61 | 1.68 | 1.18 | 1.07 |
| | 28-day | 1.31 | 1.08 | 0.62 | 1.61 | 1.66 | 0.98 |
| C9507-B35461 T19 138' (Ringold) | 1-day | 0.61 | 0.28 | 0.12 | 0.99 | 0.83 | 0.05 |
| | 7-day | 0.80 | 0.38 | 0.28 | 0.95 | 0.67 | 0.66 |
| | 28-day | 0.70 | 0.50 | 0.33 | 0.96 | 1.21 | 0.83 |
| | | Iodide | | | | | |
| | | adsorption (mL/g) | adsorption (mL/g) | adsorption (mL/g) | desorption (mL/g) | desorption (mL/g) | desorption (mL/g) |
| | Initial Concentration | 100 µg/L | 500 µg/L | 1000 µg/L | 100 µg/L | 500 µg/L | 1000 µg/L |
| C9507-B35434 T19 14C (CCUz) | 1-day | 0 | 0.02 | 0.02 | 0 | 0 | 0 |
| | 7-day | 0 | 0.02 | 0.03 | 0 | 0.01 | 0 |
| | 28-day | 0.02 | 0.06 | 0.06 | 0 | 0.17 | 0.09 |
| C9507-B35461 T19 138' (Ringold) | 1-day | 0 | 0 | 0 | 0 | 0 | 0 |
| | 7-day | 0 | 0.01 | 0.01 | 0 | 0 | 0 |
| | 28-day | 0 | 0.01 | 0.01 | 0 | 0 | 0 |
| | | Chromate | | | | | |
| | | adsorption (mL/g) | adsorption (mL/g) | adsorption (mL/g) | desorption (mL/g) | desorption (mL/g) | desorption (mL/g) |
| | Initial Concentration | 100 µg/L | 500 µg/L | 1000 µg/L | 100 µg/L | 500 µg/L | 1000 µg/L |
| C9507-B35434 T19 14C (CCUz) | 1-day | 0.02 | 0.02 | 0.03 | 3.75 | 0.36 | 0.22 |
| | 7-day | 0.21 | 0.05 | 0.09 | 6.94 | 0.33 | 0.42 |
| | 28-day | 0.17 | 0.40 | 0.21 | 5.39 | 2.06 | 0.97 |
| C9507-B35461 T19 138' (Ringold) | 1-day | 0.13 | 0.17 | 0.05 | 8.73 | 18.22 | 5.39 |
| | 7-day | 2.61 | 0.73 | 0.37 | NR | 18.35 | 8.06 |
| | 28-day | NR | 4.08 | 12.59 | NR | 36.35 | 97.93 |

NR is not reported: For uranium, the NR is because the no-sediment control showed large concentration decreases; for chromate, because concentrations in the desorption solution were below detection.
A value of "0" was assigned to any computed $K_d$ value of less than zero.

.

Table 31 shows the adsorption and desorption linear equilibrium partitioning coefficients ($K_d$) from spiked-contaminant soil-column experiments. Figure 38 through Figure 40 depict the breakthrough and elution curves for the spiked-contaminant soil-column tests. Batch and soil-column experiments provide different types of data that can be used to estimate $K_d$. There was good agreement between the 1-day batch and the soil-column adsorption $K_d$ estimates in this study for Tc-99, iodine, and chromium. The 1-day batch data were selected for this comparison because of the short residence time used for the soil-column tests. Because batch desorption $K_d$ tests were over a long duration, they are less suitable for comparison to soil-column desorption $K_d$ estimates. Batch experiments with uranium for the simulated groundwater medium were not reportable because the uranium concentration decreased significantly in the no-sediment controls. soil-column experiments with uranium were also problematic, and effluent concentrations did not show breakthrough or elution responses that could be analyzed for $K_d$.

**Table 31**. Calculated partitioning coefficients for spiked-contaminant column experiments.

| | | Adsorption | | | Desorption | | |
| | | Tc-99 | | | Tc-99 | | |
| | | Chromate | (Pertechnetate) | Iodate | Chromate | (Pertechnetate) | Iodate |
| Sample Name | Sample Location | $K_d$ (mL/g) | $K_d$ (mL/g) | $K_d$ (mL/g) | $K_d$ (mL/g) | $K_d$ (mL/g) | $K_d$ (mL/g) |
|---|---|---|---|---|---|---|---|
| C9507-B35434 | T19 14C (CCUz) | 0.030 | 0.086 | 0.708 | 0.045 | 0.192 | 0.859 |
| C9507-B35461 | T19 138' (Ringold) | 0.017 | 0.000 | 0.677 | 0.023 | 0.006 | 0.529 |
| C9512-B361F3 | S-9 20C (H2) | 0.025 | 0.037 | 0.707 | 0.028 | 0.037 | 0.877 |
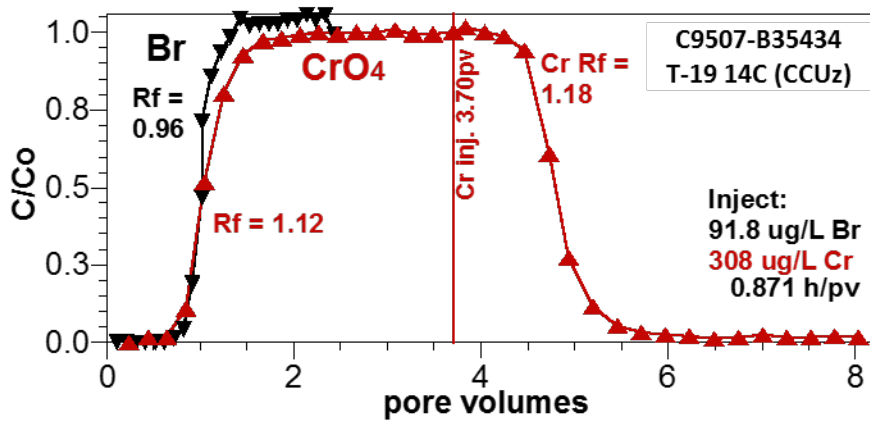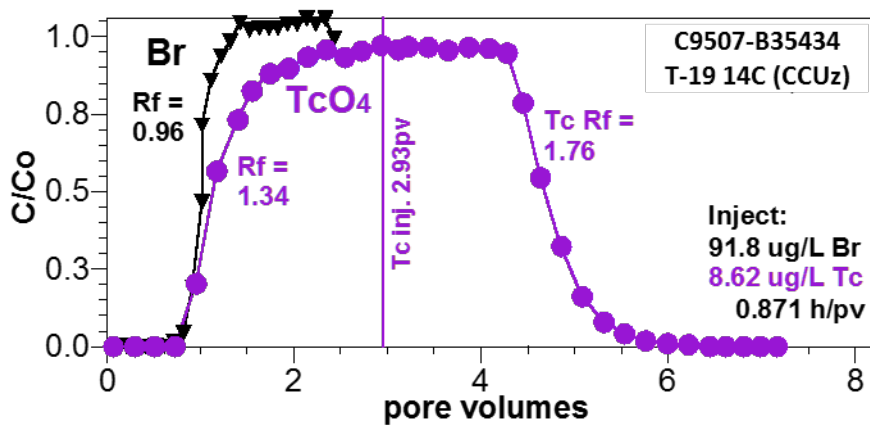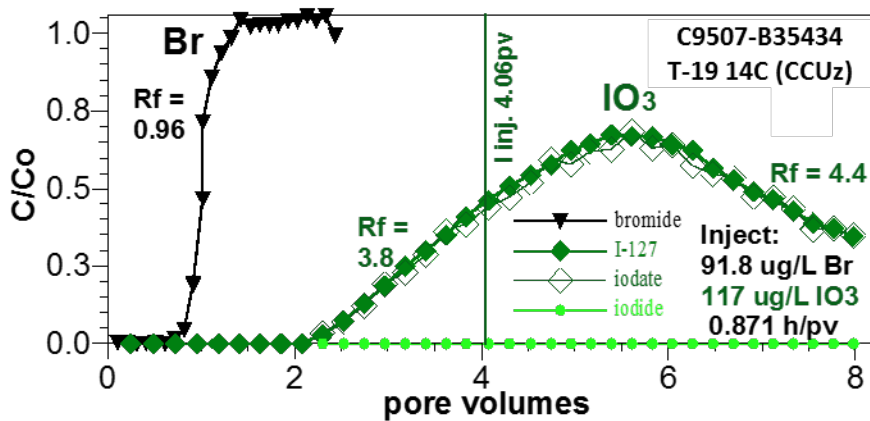
**Figure 38**. Breakthrough and elution responses for spiked-contaminant soil-column experiments with the C9507-B35434, T19 14C sample for (a) bromide (tracer) and chromate, (b) bromide and pertechnetate, and (c) bromide and iodate.
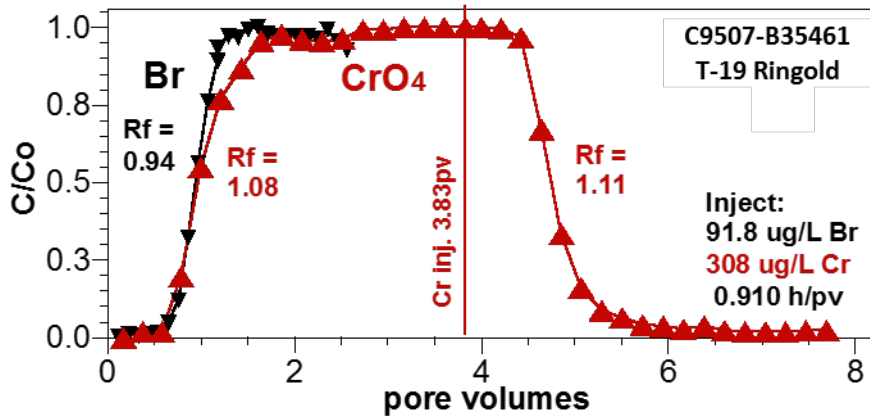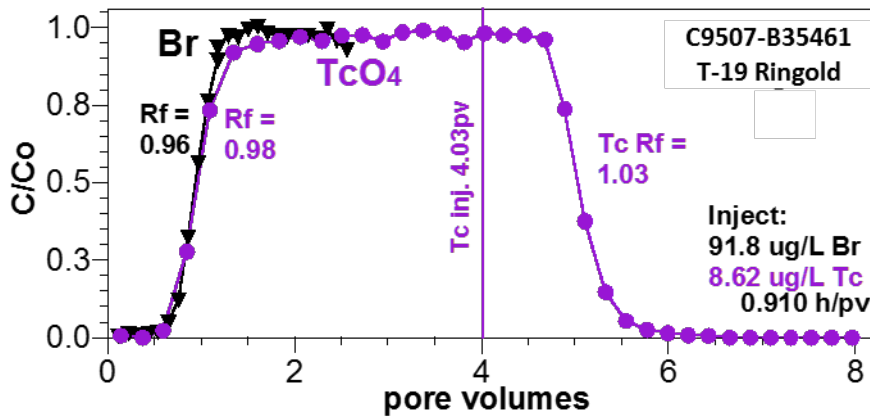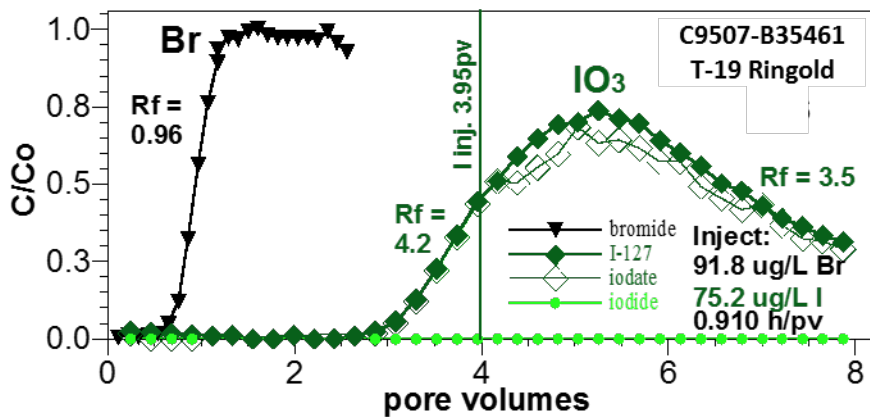
**Figure 39**. Breakthrough and elution responses for spiked-contaminant soil-column experiments with the C9507-B35461, T19 138' sample for (a) bromide (tracer) and chromate, (b) bromide and pertechnetate, and (c) bromide and iodate.
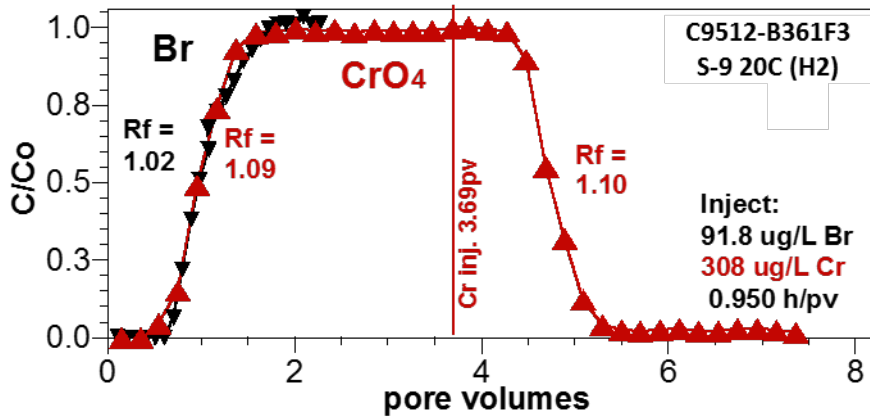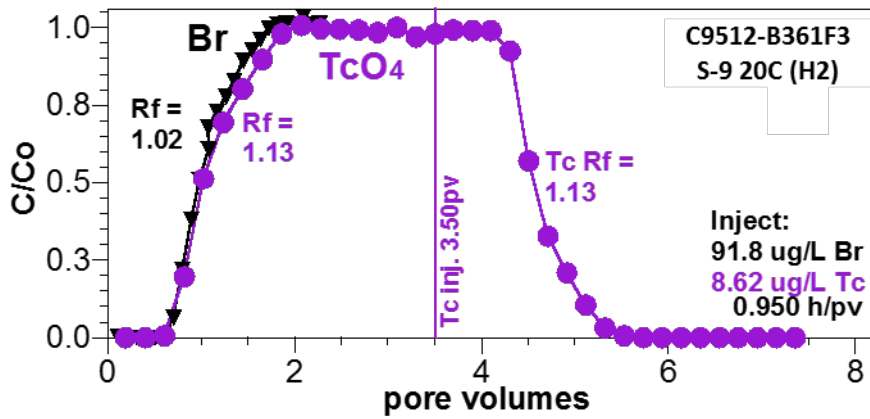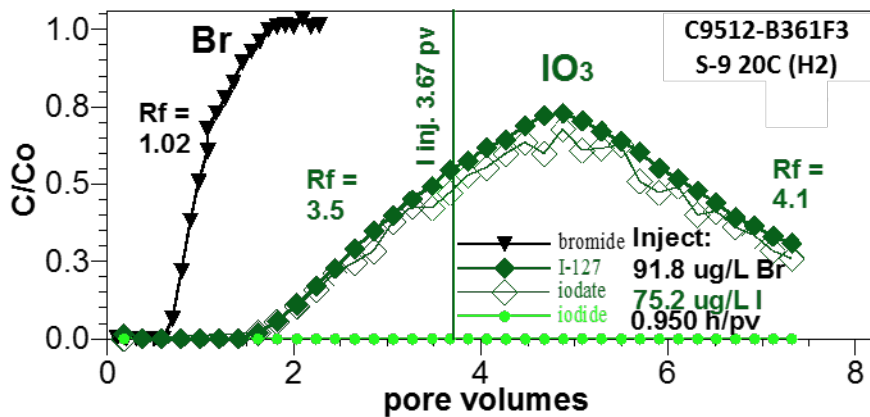
**Figure 40**. Breakthrough and elution responses for spiked-contaminant soil-column experiments with the C9510-B361F3, S-9 20C sample for (a) bromide (tracer) and chromate, (b) bromide and pertechnetate, and (c) bromide and iodate.

The batch experiments provide a larger experimental matrix than the soil-column experimental matrix for assessment of variability in $K_d$ across the sample types and for comparison of adsorption and desorption $K_d$ estimates.  For both uranium and iodate, adsorption and desorption were highest for samples B35443 and B361N1, where both samples have a high carbonate content.  The remaining samples showed moderate $K_d$ values for uranium and iodate.  Chromate, iodide, and Tc-99 (pertechnetate) $K_d$ values were all low, except for chromate, where adsorption for days 7 and 28 and desorption (a 28-day test) $K_d$ values were all much higher than the 1-day values.  Reduction of chromate in laboratory experiments has been observed over these timeframes for other soil samples (Truex et al. 2015b).  Thus, interpretation and use of later-time data for chromate $K_d$ values should consider the possibility that chemical reduction occurred during the test.  The effect of potential reduction may have also affected some of the Tc-99 and iodate results, though increases in $K_d$ over time were less dramatic than observed with the chromate data.  The desorption $K_d$ values for Tc-99 (pertechnetate), iodate, and chromate are all generally higher than adsorption $K_d$ values.  The comparison of adsorption and desorption $K_d$ values for uranium shows a mixed result of higher, lower, and similar values.

Tests for selected samples at multiple spiked-contaminant concentrations provide data to assess the concentration range suitable for use of a $K_d$-type sorption parameter.  Results showing comparable $K_d$ values for each concentration condition indicate use of a $K_d$-type sorption parameter is reasonable.  In some cases, the $K_d$ value decreases as the spiked-contaminant concentration increases, notably for iodate.  This result may indicate that sorption sites are limited and a sorption isotherm may be needed to model sorption for higher concentrations.  In some treatments, the $K_d$ value increased with increased spiked-contaminant concentration, notably for some uranium treatments.  This result may indicate some precipitation is occurring in the treatment.

Soil-column tests show well-behaved breakthrough curves for bromide, chromate, Tc-99 (pertechnetate), and iodate, but not for uranium, as discussed above.  Speciation data for iodine shows that injected iodate was not reduced to iodide during the experimental timeframe.  The observation that breakthrough of concentrations of chromate and Tc-99 (pertechnetate) are nearly the same as the injected concentrations also suggests no (or very limited) contaminant reduction occurred during the experimental timeframe.  For these short-duration soil-column tests, there is minimal difference between measured adsorption and desorption $K_d$ values, in contrast to the batch results.  However, batch adsorption (7- and 28-day) and desorption (28-day) tests included much longer contact time of the contaminant and the sediment.

# 5.0   Recommendations

The laboratory study provided useful data to identify and quantify attenuation and transport processes for the targeted contaminants and the biogeochemical and physical context for these processes.  For future laboratory studies of attenuation and transport processes with similar samples, several adjustments can be considered to enhance the laboratory study.

- A number of samples contained low levels of the targeted contaminants.  Thus, it is important to quickly analyze sediment intervals for contaminant concentrations and use these data to define the appropriate next analyses.  This approach will enable consideration of contaminant concentrations relative to subsequent testing approaches and analysis sensitivity.  For the study reported herein, this approach was appropriately applied to limit the number of soil-column leaching experiments and emphasize spiked-contaminant partitioning experiments.  Future efforts should implement a first step to evaluate water- and acid-extractable contaminant concentrations and conduct sequential extractions for the sample.  These data would be compared to results reported herein to assess leaching potential based on high total contaminant concentrations and high fractions of the contaminants distributed in the first three sequential extraction solutions.  These samples would be candidates for batch and soil-column leaching tests.  Samples not suitable for leaching would be considered for spiked-contaminant tests as discussed below.  Grab samples (e.g., samples other than those originally targeted for attenuation testing) can also be considered to augment the number of samples available for assessing leaching characteristics as described below.

- Some types of attenuation and transport information are best determined from contaminated samples (i.e., as opposed to spiked-contaminant tests).  One option for each borehole would be to collect grab samples throughout the borehole at the vertical locations where contaminant of concern analyses are being conducted (i.e., by CHPRC).  For those locations with high contaminant levels, a subset of attenuation studies (e.g., repacked column tests, batch leaching tests, sequential extractions, and the basic suite of contaminant and geochemical analyses) could be conducted.  These tests do not require an intact sample.  While the full suite of analyses for the attenuation laboratory study could not be obtained at these locations, the additional grab-sample data set could provide important information about mobility of contaminants for field-contaminated sediments.  Field-contaminated sediments are unique in that they reflect contaminant conditions caused by the history of the waste disposal, contaminant transport, and attenuation processes that have occurred.  Thus, these field-contaminated sediments best represent the starting point for future contaminant transport.  For this reason, it is important to evaluate additional locations within the borehole that provide this type of representative conditions for evaluating contaminant behavior.

- There were several instances where the sample conditions (e.g., nitrate concentration) limited the applicability of laboratory analyses.  Notably, iodine speciation was limited for some of the sample matrices.  In addition, iodine speciation was hampered by the ionic strength and acidity of some of the extraction solution properties.  Thus, the results reported herein can be used to indicate when matrix interference will occur for iodine speciation.

Based on evaluation of the data collected in this study, several types of additional data collection should be considered for these samples or for future samples.

- Measure the specific surface area of sediments for use in interpreting the partitioning data set.  This analysis will be conducted for the existing samples and reported along with the hydraulic and physical

properties in a separate report.  It provides another measure of sediment properties beyond just texture and geochemical properties that can be used to assess correlations of partitioning and sediment characteristics.

- The spiked-contaminant studies conducted for the samples in the study reported herein provided a useful set of information for contaminant transport parameters.  These data demonstrated that there is variability in these parameters across the different types of samples.  Thus, future studies should consider augmenting this set of partitioning information with partitioning studies on samples from other lithologic zones of importance to the 200-DV-1 OU.  Candidate samples for additional partitioning tests include those samples that have lithologic and geochemical properties significantly different from the samples included in the large experimental matrix reported herein.  These data would augment the current data set to enable evaluate variations in partitioning for a broader set of sediment types.

The data generated in this laboratory study provide a technical basis for updating the site CSMs and transport analyses.  The laboratory study was structured to address the information requirements for considering MNA as all or part of a remedy (i.e., EPA 2015) by identifying and quantifying processes that affect contaminant fate and transport.  As outlined in the conclusions section, attenuation was demonstrated as contaminant-specific and waste-site specific outcomes of this study.  The attenuation processes and transport parameters reported herein and can be used as part of the technical defensibility for identifying attenuated transport through the vadose zone within the remedial investigation and feasibility study for the 200-DV-1 OU.

# 6.0   Quality Assurance

The PNNL Quality Assurance (QA) Program is based upon the requirements as defined in DOE Order 414.1D, *Quality Assurance*, and 10 CFR 830, "Energy/Nuclear Safety Management, Subpart A, Quality Assurance Requirements.  PNNL has chosen to implement the following consensus standards in a graded approach:

- ASME NQA-1-2000, *Quality Assurance Requirements for Nuclear Facility Applications*, Part 1, Requirements for Quality Assurance Programs for Nuclear Facilities.

- ASME NQA-1-2000, Part II, Subpart 2.7, Quality Assurance Requirements for Computer Software for Nuclear Facility Applications, including problem reporting and corrective action.

- ASME NQA-1-2000, Part IV, Subpart 4.2, Guidance on Graded Application of Quality Assurance (QA) for Nuclear-Related Research and Development.

The procedures necessary to implement the requirements are documented through PNNL's "How Do I...?  (HDI), a system for managing the delivery of laboratory-level policies, requirements, and procedures.

The *DVZ-AFRI Quality Assurance Plan* (QA-DVZ-AFRI-001) was applied as the applicable QA document for this work under the NQA-1 QA program.  This QA plan conforms to the QA requirements of DOE Order 414.1D and 10 CFR 830, Subpart A.  This effort is subject to the *Price Anderson Amendments Act*.

The implementation of the Deep Vadose Zone – Applied Field Research Initiative QA program is graded in accordance with NQA-1-2000, Part IV, Subpart 4.2, Guidance on Graded Application of Quality Assurance (QA) for Nuclear-Related Research and Development.  The technology level defined for this effort is Development Research, which consists of developing information that will be used directly by the Hanford Site to support remediation decisions.

This work was conducted under the Development Research level to ensure the reproducibility and defensibility of these experimental results.  As such, reviewed calculation packages are available upon request except where experimental information is denoted as a scoping or preliminary study.

This work used PNNL's Environmental Sciences Laboratory (ESL) for chemical analyses.  The ESL operates under a dedicated QA plan that complies with the *Hanford Analytical Services Quality Assurance Requirements Document* (HASQARD; DOE 2007), Rev. 3.  ESL implements HASQARD through *Conducting Analytical Work in Support of Regulatory Programs* (CAWSRP).  Data quality objectives established in CAWSRP were generated in accordance with HASQARD requirements. Chemical analyses of testing samples and materials were conducted under the ESL QA Plan.

QA reviews of data and analyses were conducted for this work in accordance with the QA plan. There were no reportable QA issues with the data included in this report.

# 7.0 Conclusions

The data collected in this laboratory study addressed the following three objectives:

- Define the contaminant distribution and the hydrologic and biogeochemical setting.

- Identify attenuation processes and describe the associated attenuation mechanisms.

- Quantify attenuation and transport parameters for use in evaluating remedies.

These objectives are elements of the framework identified in EPA guidance (EPA 2015) for evaluating MNA of inorganic contaminants, and they directly support updating the CSM for these waste sites (and generally for the Hanford Central Plateau). Importantly, the information supports defining suitable contaminant transport parameters that are needed to evaluate transport of contaminants through the vadose zone and to the groundwater. This type of transport assessment supports a coupled analysis of groundwater and vadose zone contamination. The laboratory study information, in conjunction with transport analyses, can be used as input to evaluate the feasibility of remedies for the 200-DV-1 OU. This remedy evaluation will be enhanced by considering these study results that improve the understanding of controlling features and processes for transport of contaminants through the vadose zone to the groundwater.

Interpretation of this laboratory study can be considered from several perspectives relevant to supporting 200-DV-1 OU activities. Results for each contaminant were evaluated across all of the samples to identify contaminant-specific conclusions and to enable consideration of how results from this study may be relevant to other waste sites. Results are also evaluated with respect to conclusions relevant to the specific waste sites included in the study. Lastly, study results were evaluated with respect to updating CSMs and future evaluation of remedies, including the associated fate and transport assessment needed as a basis for remedy evaluation.

The data and information from these attenuation and transport studies were interpreted to support the following conclusions about contaminant behavior observed across the waste sites sampled in this study.

- Uranium

  – Uranium concentrations were low in most samples; therefore, a significant fraction of the uranium may be associated with natural background concentrations.

  – The dominant form of uranium was U(VI), supporting the conclusion that little uranium reduction has occurred in these samples.

  – For samples where uranium concentrations were elevated, only a small fraction of the uranium was present in the aqueous phase or in a form that would be transported in the aqueous phase under equilibrium partitioning conditions. Most of the uranium was associated with precipitates, and transport of uranium would be controlled by dissolution processes. This type of slow-release transport behavior was observed in the batch and soil-column leaching experiments for samples with higher uranium concentrations (B35434, B35443, and B361N1).

  – Uranium $K_d$ values were varied across the different samples tested, with the highest $K_d$ value associated with the sample of the high carbonate CCU material (B35443). Thus, in transport assessments, selection of a $K_d$ value for uranium should consider spatial variation of the $K_d$ value

based on lithologic units and carbonate content. The CCU samples show the highest $K_d$ values for uranium. Thus, carbonate content and smaller particle sizes are important to consider for uranium $K_d$. Organic carbon content did not appear to be important, but was generally low in all samples. In terms of desorption versus adsorption $K_d$ values, there was no clear trend across all of the samples. However, only the pore-water (Table 10) $K_d$ tests provided useful data, not the tests with artificial groundwater (Table 11).

- Iodine

  – I-129 concentrations in the vadose zone were non-detect for all samples. Total iodine concentrations were moderate and suitable for conducting attenuation and transport studies. Because total iodine and I-129 form the same chemical species, attenuation and transport behavior for total iodine and I-129 will be the same.

  – Total iodine speciation in the aqueous phase was mostly dominated by iodide. However, sequential extractions showed only a small fraction of the iodine was present in the aqueous phase or in a form that would be transported in the aqueous phase under equilibrium partitioning conditions. Most of the iodine was associated with precipitates (likely carbonates), and transport of iodine in these precipitates would be controlled by dissolution processes. Speciation was not possible in the carbonate precipitate extractions for the sequential extraction procedure, but it is likely that the iodine present in these extractions was iodate. Scientific literature has shown co-precipitation of iodate and carbonates (Zhang et al. 2013; Podder et al. 2016) The leaching experiments showed some slow-release behavior of iodine that may be associated with these carbonate precipitates.

  – Total iodine $K_d$ values show minimal sorption of iodide and moderate sorption of iodate. Iodate $K_d$ values varied across the different samples tested, with the highest $K_d$ values associated with the samples with high carbonate concentrations (B35443 and B361N1). Thus, in transport assessments, selection of a $K_d$ value for iodate should consider spatial variation of the $K_d$ value based on carbonate content. Unlike uranium, the higher iodate $K_d$ values are not all associated with CCU material (smaller particle sizes). Organic carbon content did not appear to be important, but was generally low in all samples. Transport of iodide and iodate through the vadose zone will be different, and speciation should be considered when conducting transport assessments. Desorption $K_d$ values were mostly higher than adsorption $K_d$ values in the batch experiments that were conducted.

- Tc-99

  – Tc-99 was not detected in any of the samples.

  – Tc-99 $K_d$ values determined in spiked-contaminant tests were minimal to low, and values varied slightly across the different samples tested. However, the nominal retardation value for Tc-99 from these data would be close to 1. In batch testing, some of the desorption $K_d$ values for Tc-99 were higher than the corresponding adsorption $K_d$ values. Chemical reduction during the experimental timeframe (up to 56 days total) may have contributed to the higher apparent desorption $K_d$ values, noting that reduction of Tc-99 by Hanford sediments has been observed in the laboratory (Szecsody et al. 2014).

- Chromium

  - Cr(VI) was not detected in most samples and, when detected, was present at a low concentration. Total chromium measured in acid extractions was likely from natural background.

  - Cr(VI) $K_d$ values determined in spiked-contaminant tests were low, and values varied slightly across the different samples tested. The measured $K_d$ values generally increased with experiment time (from 1 to 28 days). It is possible that all or some of this increase was due to Cr(VI) reduction, which has been observed in laboratory experiments with Hanford sediment. Desorption $K_d$ values from batch experiments were all higher than adsorption values. However, some of the concentration changes in the batch desorption experiments (up to 56-day duration) may have been due to some Cr(VI) reduction (Truex et al. 2015b).

- Nitrate

  - Nitrate concentrations were high in all of the samples. Two samples showed very low nitrite concentrations as a potential indicator of denitrification. However, nitrite concentrations were 4 to 5 orders-of-magnitude lower than nitrate concentrations, indicating that minimal reduction had occurred.

  - Nitrate behavior in leaching experiments showed rapid elution, consistent with a minimal $K_d$ value. The nominal retardation value for nitrate from these data would be close to 1.

  - Nitrate is a dominant electron acceptor and has influenced the microbial ecology in the samples.

The following conclusions were developed for the specific boreholes/waste sites analyzed in this study.

- T-19

  - Samples for the laboratory study from the T-19 waste site (borehole C9507) were of CCU silt, CCU caliche, and Ringold (silty, sandy gravel) materials. These samples were from locations well below the historical waste discharge and did not show signs of altered biogeochemistry induced by the waste discharge, other than the presence of contaminants. Nitrate concentrations were similar in all of the samples, indicating that waste fluids had penetrated to at least the depth of the lowest sample. The pore-water pH was consistent with a carbonate-saturated system. The highest uranium and (total) iodine concentrations were in the CCU caliche (high carbonate) material, suggesting that uranium and iodine accumulated in this zone as the waste solution passed through. Accumulation could be expected based on the observed high $K_d$ value in this unit and the potential formation of uranium- and iodine-carbonate precipitates. Thus, the CCU is an important unit at this waste site for controlling contaminant transport. Tc-99 was not detected in any of these samples. Cr(VI) was only detected at a very low concentration near the detection limit in the CCU caliche sample.

  - Based on the data collected in this laboratory study, the following attenuation processes are important at this waste site. Sorption processes are important for uranium and iodate, and to a lesser extent for chromate and Tc-99. Formation of uranium- and iodate-carbonate precipitates also appears to be an attenuation mechanism in T-19 borehole samples. Minor indications of reduction were observed in one T-19 sample, and the potential for reduction through biotic (by the microbes found in the samples) or abiotic (e.g., ferrous iron) mechanisms is present, though it would likely have limited effect on future contaminant migration.

- T-25

  - The sample for the laboratory study from the T-25 waste site (borehole C9510) was of CCU silt materials. The sample was from a location well below the historical waste discharge and did not show signs of altered biogeochemistry induced by the waste discharge, other than the presence of contaminants. The presence of high nitrate concentration indicates that waste fluids had penetrated to at least the depth of the sample. The pore-water pH was consistent with a carbonate-saturated system. The CCU silt had high carbonate content, though not as high as the CCU caliche sample from the T-19 site. Uranium and total iodine were present at low concentrations, though concentrations were sufficient for assessment of leachability. High $K_d$ values were measured for uranium and iodine, similar to the high $K_d$ values measured for the T-19 CCU caliche sample that also had a large fraction of carbonate. Accumulation could be expected based on the high observed $K_d$ value in this unit and the potential formation of uranium- and iodine-carbonate precipitates. Thus, the CCU silt is an important unit at this waste site controlling contaminant transport. Tc-99 and Cr(VI) were not detected in any of the samples.

  - Based on the data collected in this laboratory study, the following attenuation processes are important at this waste site. Sorption processes are important for uranium and iodate, and to a lesser extent for chromate and Tc-99. Formation of uranium- and iodate-carbonate precipitates also appears to be an attenuation mechanism in T-25 borehole samples. The potential for reduction through biotic (by the microbes found in the samples) or abiotic (e.g., ferrous iron) mechanisms is present, though it would likely have limited effect on future contaminant migration.

- S-9

  - Samples for the laboratory study from the S-9 waste site (borehole C9512) were of sandy Hanford Formation and transition from Hanford to CCU silt materials. These samples were deep below the historical waste discharge and did not show significant signs of altered biogeochemistry induced by the waste discharge, other than the presence of contaminants. However, the upper sample showed indication of potential reductive activity that, along with the very high nitrate concentration, may indicate some waste solution effects at this depth. Nitrate concentration was very high in the upper sample (the highest concentration of all samples in the laboratory study), and was at a moderately high concentration in the lower sample, indicating that waste fluids had penetrated to at least the depth of the lowest sample. The pore-water pH was consistent with a carbonate-saturated system. The uranium concentration in the lower sample was low, but was an order of magnitude higher than the uranium concentration in the upper sample. Neither sample appeared to be elevated in carbonate. Tc-99 and Cr(VI) were not detected in any of the samples.

  - Based on the data collected in this laboratory study, the following attenuation processes are important at this waste site. Sorption processes are important for uranium and iodate, and to a lesser extent for chromate and Tc-99. Formation of uranium- and iodate-carbonate precipitates also appears to be an attenuation mechanism in S-9 borehole samples. Minor indications of reduction were observed in one S-9 sample and the potential for reduction through biotic (by the microbes found in the samples) or abiotic (e.g., ferrous iron) is present, though it would likely have limited effect on future contaminant migration.

The study provided a set of data that addressed the study objectives and can support future evaluation of remedies, including MNA and the associated fate and transport assessment that is needed as a basis for remedy evaluations. The first objective was to jointly evaluate contaminant concentrations and the biogeochemical and hydrologic setting for these data. This information provides a baseline for interpreting attenuation and transport studies. As noted, there were significant variations in transport parameter values and some attenuation mechanisms linked to specific sediment characteristics (e.g., carbonate content). For scaling and use of this information in fate and transport assessments, these variations should be considered in light of the sample properties. For this study, the sample properties were strongly linked to the sediment units sampled rather than waste stream properties. Thus, scaling and use in future efforts can translate the attenuation and transport information from this laboratory study to other waste sites based on the distribution of similar sediment units (e.g., the CCU silt and CCU caliche).

Another objective of the study was to identify attenuation processes that appear to be active in these samples and that will affect contaminant transport through the vadose zone. Sorption processes are important for uranium and iodate, and to a lesser extent for chromate and Tc-99. Carbonate content appeared to be important for uranium and iodate $K_d$. Accumulation in carbonate precipitates was identified as an attenuation mechanism for uranium and iodate. Slow release of uranium and total iodine was evident in leaching experiments. Geochemical signatures of reducing conditions were minimal or non-existent in the samples. However, there was indication of potential catalysts for reductive processes, including the presence of microbes and reduced iron and manganese phases. These reductive catalysts may be responsible for some of the difficult-to-extract contaminant phases (e.g., precipitated phases) observed in sequential extraction analysis. Attenuation mechanisms relevant to chromium and Tc-99 (other than sorption) could not be fully assessed because of the low/non-detect concentrations of these contaminants.

A key objective of the study was to quantify attenuation and transport parameters to support parameterization of fate and transport assessments. This type of assessment will be needed to evaluate transport of contaminants through the vadose zone, to evaluate the coupled vadose zone-groundwater system, and to assess the need for, magnitude of, and/or design of remediation. The contaminant- and sample-specific values from stop-flow portions of soil-column experiments, batch leaching, and $K_d$ experiments provide a set of information that can be directly used to develop transport parameters. Soil-column effluent concentration data can also be compared to one-dimensional simulations to assess fate and transport model configurations for $K_d$ or for surface complexation models.

Collectively, the information from this laboratory study can be considered in terms of updating the CSM for contaminants in the vadose zone. It can also provide input to describing the coupled vadose zone-groundwater system that needs to be considered for remedy determinations. CSM elements from this laboratory study are listed below. These elements will need to be incorporated with other data collected during the 200-DV-1 OU remedial investigation as part of updating the CSMs for the 200-DV-1 OU component waste sites.

- Sequential extraction experiments (and more coarsely indicated by comparison of water- and acid-extraction contaminant data) show that only a small fraction of the uranium and iodine mass in samples is in a mobile form that would transport under equilibrium-partitioning conditions. Leaching experiment results confirmed that slow-release processes affect the transport of these contaminants. The relative amount of uranium and iodine mass in the mobile versus functionally immobile phases affects the potential for future mass discharge from the vadose zone to the groundwater.

- Laboratory data suggest that formation and dissolution of uranium- and iodate-carbonate precipitates is a potential attenuation mechanism affecting the relative mobile and immobile mass fractions and the transport characteristics of uranium and iodine.

- Attenuation and sorption are not uniform in the vadose zone, especially for uranium and the iodate form of iodine. Lithology (e.g., the presence and extent of layers such as the CCU) and carbonate content affected the transport parameter values for these contaminants.

- For the waste sites included in this study, the effects of waste chemistry (e.g., altered sediment pH or biogeochemistry), other than contaminant concentrations, did not penetrate deep into the vadose zone. The biogeochemical signature of samples shows that a transport evaluations at these waste sites will not need to include properties modified by waste chemistry for the deep portion of the vadose zone.

- While the CSM should acknowledge the potential for transformation processes (e.g., biotic or abiotic reduction), minimal evidence was observed that these processes are active. However, biotic and abiotic transformation may have occurred in the past and contributed to the currently observed contaminant distribution within the sediment and pore water.

- Oxygen and hydrogen isotope data were collected and primarily show correlation to regional precipitation with some variations from evaporative and condensation processes.

- It will be important to incorporate variations in physical property data into the CSM to augment existing data and correlate to indirect measures of lithology (e.g., geophysical logging). Some additional hydraulic property data were collected for this laboratory study and will be documented in a separate report.

This laboratory study extended the characterization of the 200-DV-1 OU to include identification and quantification of contaminant attenuation processes and parameters that will be needed to evaluate transport of contaminants through the vadose zone into the groundwater. This type of site-specific information enhances the technical basis to support remedy evaluation. Quantifying transport of contaminants in the vadose zone in terms of a source to groundwater under existing and future conditions without additional intervention is a basic element of remedy evaluation for the vadose zone. This type of evaluation and the supporting laboratory data describing the factors that affect transport (i.e., attenuation processes) are used in the process of considering MNA as all or part of a remedy. For cases where future contaminant discharge from the vadose zone will create or continue plumes of concern in the groundwater, the transport behavior and magnitude of the source discharge are used to define the target for vadose remediation (i.e., the extent of an engineered remedy needed in addition to natural attenuation) and assess potential remedy options. Thus, the information in this laboratory study was included in the 200-DV-1 OU characterization efforts to support the upcoming remedy evaluation in the feasibility study.

# 8.0   References

10 CFR 830, "Energy/Nuclear Safety Management," Subpart A, Quality Assurance Requirements. *Code of Federal Regulations*, as amended.

ASME NQA-1-2000, *Quality Assurance Requirements for Nuclear Facility Applications*.  American Society of Mechanical Engineers, New York, New York.

Beckett P.  1989.  "The use of extractants in studies on trace metals in soils, sewage sludges, and sludge-treated soils."  In *Advances in Soil Science*, Volume 9, Springer-Verlag, New York, New York, pp. 144-176.

Benson DA, K Clark, I Karsch-Mizrachi, DJ Lipman, J Ostell, and EW Sayers.  2015.  "GenBank." *Nucleic Acids Research* 43(Database issue): D30-D35.

Brina R and AG Miller.  1992.  "Direct detection of trace levels of uranium by laser induced kinetic phosphorimetry."  *Analytical Chemistry* 64(13):1413-1418.

Callos Y, F Mornet, A Sciandra, N Waser, A Larson, and PJ Harrison.  1999.  "An optical method for the rapid measurement  of micromolar concentrations of nitrate in marine phytoplankton cultures."  *Journal of Applied Phycology* 11(2):179-184.

Chao T and L Zhou.  1983.  "Extraction techniques for selective dissolution of amorphous iron oxides from soils and sediments."  *Soil Science Society of America Journal* 47(2):225-232.

CHPRC.  2015a.  *Conceptual Site Models for the 200-DV-1 Operable Unit Waste Sites in the T Complex Area, Central Plateau, Hanford, Washington*.  SGW-49924, Rev. 0, CH2M Hill Plateau Remediation Company, Richland, Washington.

CHPRC.  2015b.  *Conceptual Site Models for the 200-DV-1 Operable Unit Waste Sites in the S Complex Area, Central Plateau, Hanford, Washington*.  SGW-50280, Rev. 1, CH2M Hill Plateau Remediation Company, Richland, Washington.

Cole JR et al.  2013.  "Ribosomal  Database Project: data and tools for high throughput rRNA analysis." *Nucleic Acids Research*: gkt1244.

Craig H.  "1961 Isotopic variations in meteoric waters."  *Science* 133:1702-1703.

DePaolo DJ, ME Conrad, K Maher, and GW Gee.  2004.  "Evaporation effects on oxygen and hydrogen isotopes in deep vadose zone pore fluids at Hanford, Washington."  *Vadose Zone Journal* 3:220-232.

DOE.  1992.  *Hanford Site Groundwater Background*.  DOE/RL-92-23, U.S. Department of Energy, Richland Operations Office, Richland, Washington.

DOE.  2007.  *Hanford Analytical Services Quality Assurance Requirements Document*.  DOE/RL-96-68, Rev. 3, U.S. Department of Energy, Richland, Washington.

DOE. 2012. *Characterization Sampling and Analysis Plan for the 200-DV-1 Operable Unit*. DOE/RL-2011-104, U.S. Department of Energy, Richland Operations Office, Richland, Washington.

DOE. 2016. *Remedial Investigation/Feasibility Study and RCRA Facility Investigation/Corrective Measures Study Work Plan for the 200-DV-1 Operable Unit*. DOE/RL-2011-102, U.S. Department of Energy, Richland Operations Office, Richland, Washington.

DOE Order 414.1D, *Quality Assurance*. U.S. Department of Energy, Washington, D.C.

EPA. 2004. *Quality Assurance/Quality Control Guidance for Laboratories Performing PCR Analyses on Environmental Samples*. EPA/815/B-04/001, U.S. Environmental Protection Agency, Washington, D.C.

EPA. 2007a. *Monitored Natural Attenuation of Inorganic Contaminants in Ground Water- Volume 1, Technical Basis for Assessment*. EPA/600/R-07/139, U.S. Environmental Protection Agency, Washington, D.C.

EPA. 2007b. *Monitored Natural Attenuation of Inorganic Contaminants in Ground Water- Volume 2, Assessment for Non-Radionuclides Including Arsenic, Cadmium, Chromium, Copper, Lead, Nickel, Nitrate, Perchlorate, and Selenium*. EPA/600/R-07/140, U.S. Environmental Protection Agency, Washington, D.C.

EPA. 2010. *Monitored Natural Attenuation of Inorganic Contaminants in Ground Water- Volume 3, Assessment for Radionuclides Including Tritium, Radon, Strontium, Technetium, Uranium, Iodine, Radium, Thorium, Cesium, and Plutonium-Americium*. EPA/600/R-101093, U.S. Environmental Protection Agency, Washington, D.C.

EPA. 2015. *Use of Monitored Natural Attenuation for Inorganic Contaminants in Groundwater at Superfund Sites*. OSWER Directive 9283.1-36, U.S. Environmental Protection Agency, Office of Solid Waste and Emergency Response, Washington, D.C.

Gould W, M Stichbury, M Francis, L Lortie, and D Blowes. 2003. "An MPN method for the enumeration of iron-reducing bacteria." In *14th International Symposium on Environmental Biogeochemistry: Mining and the Environment Conference*.

Graham DL. 1983. *Stable isotopic composition of precipitation from the Rattlesnake Hills area of south-central Washington State*. RHO-BW-ST-44 P, Rockwell Hanford Operations, Richland, Washington.

Grebel JE, JA Charbonnet, and DL Sedlak. 2016. "Oxidation of organic contaminants by manganese oxide geomedia for passive urban stormwater treatment systems." *Water Research* 88:481-491.

Gleyzes C, S Tellier, and M Astruc. 2002. "Fractionation studies of trace elements in contaminated soils and sediments: a review of sequential extraction procedures." *Trends in Analytical Chemistry* 21:(6 & 7):451-467.

Goebel TS and RJ Lascano. 2012. System for high throughput water extraction from soil material for stable isotope analysis of water. *Journal of Analytical Sciences, Methods and Instrumentation* 2:203-207.

Hall G, J Vaive, R Beer, and N Hoashi. 1996. "Selective leaches revisited, with emphasis on the amorphous Fe oxyhydroxides phase extraction." *Journal of Geochemical Exploration* 56:59-78.

Hearn PP Jr., WC Steinkampf, DG Horton, GC Solomon, LD White, and JR Evans. 1989. "Oxygen-isotope composition of ground water and secondary minerals in Columbia Plateau basalts: Implications for the paleohydrology of the Pasco Basin." *Geology* 17:606-610.

Heron G, C Crozet, AC Bourg, and TH Christensen. 1994. "Speciation of Fe(II) and Fe(III) in contaminated aquifer sediments using chemical extraction techniques." *Environmental Science and Technology* 28:1698-1705.

Kohler M, DP Curtis, DE Meece, and JA Davis. 2004. "Methods for estimating adsorbed uranium (VI) and distribution coefficients of contaminated sediments." *Environmental Science and Technology* 38: 240-247.

Larner B, A Seen, and A Townsend. 2006. "Comparative study of optimized BCR sequential extraction scheme and acid leaching of elements in certified reference material NIST 2711." *Analytica Chimica Acta* 556:444-449.

Lee BD, JJ Moran, MK Nims, and DL Saunders. 2017. *Stable Hydrogen and Oxygen Isotope Analysis of B-Complex Perched Water Samples*. PNNL-26341, Pacific Northwest National Laboratory, Richland, Washington.

McKinney CR, JM McCrea, S Epstein, HA Allen, and HA Urey. 1950. "Improvements in mass spectrometers for the measurement of small differences in isotope abundance ratios." *Review of Scientific Instruments* 21:724-730.

O'Leary NA, MW Wright, JR Brister, S Ciufo, D Haddad, R McVeigh, B Rajput, B Robbertse, B Smith-White, D Ako-Adjei, A Astashyn, A Badretdin, Y Bao, O Blinkova, V Braver, V Chetvernin, J Choi, E Cox, O Ermolaeva, CM Farrell, T Goldfarb, T Gupta, D Haft, E Hatcher, W Hlavina, VS Joardar, VK Kodali, W Li, D Maglott, P Masterson, KM McGarvey, MR Murphy, K O'Neill, S Pujar, SH Rangwala, D Rausch, LD Riddick, C Schoch, A Shkeda, SS Storz, H Sun, F Thibaud-Nissen, I Tolstoy, RE Tully, AR Vatsan, C Wallin, D Webb, W Wu, MJ Landrum, A Kimchi, T Tatusova, M DiCuccio, P Kitts, TD Murphy, and KD Pruitt. 2015. "Reference sequence (RefSeq) database at NCBI: current status, taxonomic expansion, and functional annotation." *Nucleic Acids Research*: gkvll89.

Podder J, J Lin, W Sun, SM Botis, J Tse, N Chen, Y Hu, D Li, J Seaman, and Y Pan. 2016. "Iodate in calcite and vaterite: Insights from synchrotron X-ray absorption spectroscopy and first-principles calculations." *Geochimica et Cosmochimica Acta*, doi: http://dx.doi.org/10.1016/j.gca.2016.11.032

Prudic D, D Stonestrom, and R Streigl. 1997. *Tritium, Deuterium, and Oxygne-18 in Water Collected from Unsaturated Sediments near a Low-Level Radioactive-Waste Burial Site South of Beatty, Nevada*. Water Resources Investigations Report 97-4062, U.S. Geological Survey, Reston, Virginia.

Qafoku NP, CC Ainsworth, JE Szecsody, and OS Qafoku. 2004. "Transport-controlled kinetics of dissolution and precipitation in the sediments under alkaline and saline conditions." *Geochimica et Cosmochimica Acta* 68(14):2981-2995.

Rehm HL, SJ Bale, P Bayrak-Toydemir, JS Berg, KK Brown, JL Deignan, MJ Friez, BH Funke, MR Hegde, E Lyon, and the Working Group of the American College of Medical Genetics. 2013. "ACMG clinical laboratory standards for next-generation sequencing." *Genetics in Medicine* 15(9):733-747.

Rice EW, RB Baird, AD Eaton, and LS Clesceri (eds). 2012. *Standard Methods for the Examination of Water and Wastewater*, 22nd Edition. American Public Health Association, Washington, D.C.; American Water Works Association, Denver, Colorado; and Water Environment Federation, Alexandria, Virginia.

Serne RJ, BN Bjornstad, JM Keller, PD Thorne, DC Lanigan, JN Christensen, and GS Thomas. 2010. *Conceptual Models for Migration of Key Groundwater Contaminants Through the Vadose Zone and Into the Upper Unconfined Aquifer Below the B-Complex*. PNNL-19277, Pacific Northwest National Laboratory, Richland, Washington.

Serne RJ, JH Westsik, Jr, BD Williams, HB Jung, and G Wang. 2015. *Extended Leach Testing of Simulated LAW Cast Stone Monoliths*. PNNL-24297, Pacific Northwest National Laboratory, Richland, Washington.

Singleton MJ, EL Sonnenthal, ME Conrad, DJ DePaolo, and GW Gee. 2004. "Multiphase reactive transport modeling of seasonal infiltration events and stable isotope fractionation in unsaturated zone pore water and vapor at the Hanford site." *Vadose Zone Journal* 3:775-785.

Spane FA Jr. 1999. *Effects of Barometric Fluctuations on Well Water-Level Measurements and Aquifer Test Data*. PNNL-13078, Pacific Northwest National Laboratory, Richland, Washington.

Spane FA Jr. and WD Webber. 1995. *Hydrochemistry and Hydrogeologic Conditions within the Hanford Site Upper Basalt Confined Aquifer System*. PNL-10817, Pacific Northwest National Laboratory, Richland, Washington.

Sutherland R and F Tack. 2002. "Determination of Al, Cu, Fe, Mn, Pb, and Zn in certified reference materials using the optimized BCR sequential extraction procedure." *Analytica Chimica Acta* 454:249-257.

Szecsody JE, BD Lee, MJ Truex, CE Strickland, JJ Moran, MMV Snyder, CT Resch, AR Lawter, L Zhong, BN Gartman, DL Saunders, SR Baum, II Leavy, JA Horner, B Williams, BB Christiansen, EM McElroy, MK Nims, RE Clayton, and D Appriou. 2017. *Geochemical, Microbial, and Physical Characterization of 200-DV-1 Operable Unit Cores from Boreholes C9552, C9487, and C9488, Hanford Site Central Plateau*. PNNL-26266, Pacific Northwest National Laboratory, Richland, Washington.

Szecsody J, J Zachara, and P Bruckhart. 1994. "Adsorption-Dissolution Reactions Affecting the Distribution and Stability of Co(II)-EDTA in Fe-oxide Sand." *Environmental Science and Technology* 28:1706-1716.

Szecsody J, M Truex, N Qafoku, D Wellman, T Resch, and L Zhong. 2013. "Influence of acidic and alkaline co-contaminants on uranium migration in vadose zone sediments." *Journal of Contaminant Hydrology* 151:155-175.

Szecsody JE, D Jansik, JP McKinley, and N Hess. 2014. "Influence of alkaline waste on technetium mobility in Hanford formation sediments." *Journal of Environmental Radioactivity* 135:147-160.

Truex MJ and KC Carroll. 2013. *Remedy Evaluation Framework for Inorganic, Non-Volatile Contaminants in the Deep Vadose Zone*. PNNL-21815, Pacific Northwest National Laboratory, Richland, Washington.

Truex MJ, JE Szecsody, N Qafoku, and JR Serne. 2014. *Conceptual Model of Uranium in the Vadose Zone for Acidic and Alkaline Wastes Discharged at the Hanford Site Central Plateau*. PNNL-23666, Pacific Northwest National Laboratory, Richland, Washington.

Truex MJ, M Oostrom, and GD Tartakovsky. 2015a. *Evaluating Transport and Attenuation of Inorganic Contaminants in the Vadose Zone for Aqueous Waste Disposal Sites*. PNNL-24731, Pacific Northwest National Laboratory, Richland, Washington.

Truex MJ, JE Szecsody, NP Qafoku, R Sahajpal, L Zhong, AR Lawter, and BD Lee. 2015b. *Assessment of Hexavalent Chromium Natural Attenuation for the Hanford Site 100 Area*. PNNL-24705, Pacific Northwest National Laboratory, Richland, Washington.

Truex MJ, BD Lee, CD Johnson, NP Qafoku, GV Last, MH Lee, and DI Kaplan. 2016. *Conceptual Model of Iodine Behavior in the Subsurface at the Hanford Site*. PNNL-24709, Rev. 1., Pacific Northwest National Laboratory, Richland, Washington.

Um W, J Serne, M Truex, A Ward, M Valenta, C Brown, C Iovin, K Geiszler, I Kutnyakov, E Clayton, H Chang, S Baum, R Clayton, and D Smith. 2009. *Characterization of Sediments from the Soil Desiccation Pilot Test (SDPT) Site in the BC Cribs and Trenches Area*. PNNL-18800, Pacific Northwest National Laboratory, Richland, Washington.

West AG, SJ Patrickson, and JR Ehleringer. 2006. "Water extraction times for plant and soil materials used in stable isotope analysis." *Rapid Communication in Mass Spectrometry* 20:1317-1321.

Xue Y, C Murray, G Last, and R Mackley. 2003. *Mineralogical and Bulk-Rock Geochemical Signatures of Ringold and Hanford Formation Sediments*. PNNL-14202, Pacific Northwest National Laboratory, Richland, Washington.

Zachara J, C Liu, C Brown, S Kelly, J Christensen, J McKinley, J Davis, J Serne, E Dresel, and W Um. 2007. *A Site-Wide Perspective on Uranium Geochemistry at the Hanford Site*. PNNL-17031, Pacific Northwest National Laboratory, Richland, Washington.

Zhang S, C Xu, D Creeley, Y-F Ho, H-P Li, R Grandbois, KA Schwehr, DI Kaplan, CM Yeager, D Wellman, and PH Santschi. 2013. "Iodine-129 and Iodine-127 Speciation in Groundwater at the Hanford Site, US: Iodate Incorporation into Calcite." *Environmental Science & Technology* 47(17):9635-9642.

# Appendix A

# Geologist Descriptions of Samples

# Appendix A

# Geologist Descriptions of Samples

The following files show the geologist description of the samples used in this study.

| Well ID: C9507 | Well Name: | Location: |
|---|---|---|

| Project: FY16 200-DV-1 Characterization | Reference Measure Point: Ground Surface |
|---|---|

| Depth (ft) | Sample | Graphic Log MISIG | Sample Description: Sediment Classification, Grain Size Distribution, Color, Moisture Content, Sorting, Angularity, Mineralogy, Particle Size, Reaction to HCl, Other | Comments: Depth of Casing, Drilling Method, Sampling Method, Sampler Size, Water Level, Other |
|---|---|---|---|---|
| 92 | 14A | | | |
| 93 | 14B | | | |
| 94 | 14C | | 94.1-94.47: Sand (S) v. well-sorted vf-f SA-SR, lt. brownish gray (2.5y 6.5/2), >90% S, <10% M, mostly vf S, v. weakly cons., mod. rxn w/ HCl, sl. moist -94.35-94.47: vf (<½ mm) lt. color finer mS laminations | Core #14C: 94.1-95.1 HEIS# B335434 |
| 95 | 14D | | 94.47-94.65: Sand (S) f-mu (75% m, 25% f), SA-SR, 25% mafic, 75% felsic, (v. heterolithic), well-sort., mod. rxn w/ HCl, lt. brownish gray (2.5y 6/2). 94.65-94.67: Silty Sand (mS) <70% S (vf) >30% M, sl. moist, st. cohesive when pressed, non-plastic, mod. rxn w/ HCl, lt. brownish gray (2.5y 6/2) | |
| 96 | 14E | | 94.67-95.1: Sand (S) >90% vf-f, <10% M, v. well-sort, SA-SR, v. weakly cons., sl. moist, mod. rxn w/ HCl, lt. brownish gray (2.5y 6.5/2) | |
| 97 | | | | |
| 98 | | | | |

| Reported By: | | | |
|---|---|---|---|
| Jake Horner | Geologist | John Horner | 8-11-16 |
| Print Name | Title | Signature | Date |

| Reviewed By: | | | |
|---|---|---|---|
| | | | |
| Print Name | Title | Signature | Date |

| OR Doc Type: | WMU Code(s): |
|---|---|

A-6003-642 (REV 1)

| Well ID: C9507 | Well Name: | Location: 8-29-16 |
|---|---|---|
| Project: FY16 200-DV-1 Characterization | | Reference Measure Point: Ground Surface |

| Depth (ft) | Sample | Graphic Log M,S,G | Sample Description: Sediment Classification, Grain Size Distribution, Color, Moisture Content, Sorting, Angularity, Mineralogy, Particle Size, Reaction to HCl, Other | Comments: Depth of Casing, Drilling Method, Sampling Method, Sampler Size, Water Level, Other |
|---|---|---|---|---|
| 103 | | | 103.4'-103.9': Gravelly Sand (gS) 5%M, 20%G (wR pebbles & caliche nodules up to 5mm), 75% S (70% vf-f, 20%m, 10% c-vc), well-cons. wk. cem. v. st. rxn w/ HCl, sl. moist, mod.-sort., lt. ol. brn. (2.5y 5.5/3) S is ≥80% felsic | Core #16B 103.4'-104.4' HEIS# 335422 |
| 104 | Core #16B | | 103.9'-104.0': Sandy Gravel (sG) 60% S (vf-vc; 40% vf-f, 30%m, 30% c-vc), 35% G (vf-f mafic-dom. peb.) S - 80% felsic, mod. cons, nm-cem, st. rxn w/ HCl, lt grey (2.5y 7/2), v. sl. moist. 104.0'-104.3': Sandy Gravel (sG) as above but w/ well-cem. caliche nodules. 104.3-104.4': Gravel fraction ↑ 40% with abundant caliche nodules. | |
| 105 | Core #16C | | 104.4'-104.57': Sandy Gravel (sG) 10% vf-f mafic-dom. pebbles, 45% well-cem. caliche nodules (v. st. rxn w/ HCl, contains vf-f G in cemented matrix-supported M), ≠ 40% vf-m felsic-dom. Sand, 5% M, more nodules=2.5cm, lt. yellowish brn. (2.5y 7.5/3), dry 104.57'-105.05': gravelly silty Sand (gmS) 10-20% caliche nodules, 30-40% M, 40-60% Sand (vf-vc; 90% vf-f, 10%m-vc) ≥75% felsic Mottled zones 10YR 7/2 - 10YR 8/2, M-rich zones of mS (2.5y 6/2) lt. brn. 10YR zones have a pinkish rim, sl. moist, mod. cons., mod. rxn w/ HCl. 105.05-105.4': Sandy Gravel (sG) >60% caliche nodules, sR-sA, up to 2cm, 35% vf-vc S, 5% M, poorly sorted, wk-mod. consolidated, pale yellow (2.5y 6.5/4), st. rxn w/ HCl, Sand is felsic-dom. | Core #16C 104.4-105.4' HEIS# 335443 |
| 106 | | | | |

| Reported By: | | | |
|---|---|---|---|
| Jake Horner | Geologist | [signature] | 8-29-16 |
| Print Name | Title | Signature | Date |

| Reviewed By: | | | |
|---|---|---|---|
| | | | |
| Print Name | Title | Signature | Date |
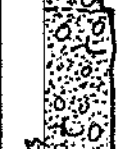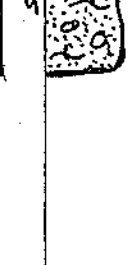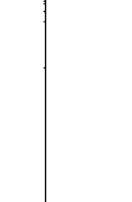
For Office Use Only

| OR Doc Type: | WMU Code(s): |
|---|---|

Well ID: C9507
Well Name:
Location:

Project: FY16 200-DV-1 Characterization
Reference Measure Point: Ground Surface

| Depth (ft) | Sample | Graphic Log | Sample Description:<br>Sediment Classification, Grain Size Distribution, Color, Moisture Content, Sorting, Angularity, Mineralogy, Particle Size, Reaction to HCl, Other | Comments:<br>Depth of Casing, Drilling Method, Sampling Method, Sampler Size, Water Level, Other |
|---|---|---|---|---|
| 137 | | | 137.6 - 139.6' examined at end caps. 138.1' (bottom of "A", top of "B") Silty Sandy Gravel (msG), 60-70% G, 2-5 cm, max = 7 cm, R-WR w/ broken clasts 25-35% S (60% m, 20% c-vc, 20% f-vf, R-SR 5-10% M, secondary alteration appears as mottled clay-rich zones Sand matrix is dom. pale yellow (2.5y 7/3) S is felsic-dom. mottled colors range from grayish-brn. (2.5y 5/2) to pale yellow (2.5y 7/3) & some white (2.5y 8/1). mostly dark brn. on M-rich cobble rinds Dry to v. sl. moist, no rxn w/ HCl. well-cons. cobbles compacted, but matrix breaks up & crumbles easily. | HEIS#s #B35461/B36H08 @ 8-2-16 |
| 138 | A | | | |
| | B | | | |
| | C | | | |
| 139 | | | 139.1' - 139.6' (liner "D"): Silty Sandy Gravel (msG) 65% G, 25-30% S, 5-10% M. Same as above. | |
| | D | | | |
| 140 | | | | |

Reported By:
Jake Horner — Print Name
Geologist — Title
Signature
8-2-16 — Date

Reviewed By:
Print Name
Title
Signature
Date

**For Office Use Only**

OR Doc Type:
WMU Code(s):

A-6003-642 (REV 1)

# BOREHOLE LOG

| Well ID: C9510 | Well Name: | Location: |
|---|---|---|
| Project: FY16 200-DV-1 Characterization | | Reference Measure Point: Ground Surface |

| Depth (ft) | Sample | Graphic Log MBIG | Sample Description: Sediment Classification, Grain Size Distribution, Color, Moisture Content, Sorting, Angularity, Mineralogy, Particle Size, Reaction to HCl, Other | Comments: Depth of Casing, Drilling Method, Sampling Method, Sampler Size, Water Level, Other |
|---|---|---|---|---|
| 113 | Core #14B | | 113.3'-114.3': Sand (S) 85% vf-f S 5-10% M, 5% vf pebbles, well-cons., wk-cemented, felsic-dom., ol. brn. (2.5 4/4), strong rxn. w/ HCl, well-sorted, sl. moist, sparse pebbles & white caliche nodules up to 5mm, lg. pebbles/ nodules v. sparse. -113.8-113.9' 10-15% caliche nodules. | Core #14B 113.3'-114.3' HEIS#B361M9 |
| 114 | | | | |
| 115 | Core #14C | | 114.3'-115.3': Sand (S) 95% S (>80% f-vf, 10% m, 10% c-vc), 5% v.f pebbles. Pebbles are 50% mafic-dom., S is >75% felsic, SA-SR, st. rxn w/ HCl, mod. consolidated, mod. cem., sl. moist, dk grayish brn. (2.5y 4/2, moist) & lt. gray (2.5y 7/2) when dry. sparse caliche nodules up to 1cm. | Core #14C 114.3'-115.3' HEIS#B361N1 |
| 116 | | | | |

Reported By:

| Jake Horner | Geologist | | 8-29-16 |
|---|---|---|---|
| Print Name | Title | Signature | Date |

Reviewed By:

| | | | |
|---|---|---|---|
| Print Name | Title | Signature | Date |

| OR Doc Type: | WMU Code(s): |
|---|---|

A-6003-642 (REV 1)

# BOREHOLE LOG

| Well ID: C9512 | | Well Name: | | Location: | |
|---|---|---|---|---|---|
| Project: FY16 200-DV-1 Characterization | | | | Reference Measure Point: Ground Surface | |

| Depth (ft) | Sample | Graphic Log | Sample Description: Sediment Classification, Grain Size Distribution, Color, Moisture Content, Sorting, Angularity, Mineralogy, Particle Size, Reaction to HCl, Other | Comments: Depth of Casing, Drilling Method, Sampling Method, Sampler Size, Water Level, Other |
|---|---|---|---|---|
| 63 | Core #8B | | 63.2 - 64.2: Sand (S) 99% S (upper fn. - lower crs; 15% f, 70% m, 15% crs), 70% felsic, SA-SR, wk. cons, non-cem, no rxn w/ HCl, 1% M, lt. gray (2.5Y 7/2). | Core BPS @ 8-29-16 Core #8B HEIS #B36175 |
| 64 | | | -63.83' - 63.85': thin gS layer, 80% S (fn-v.c.) 15% f, 45% m, 40% c-vc), up to 20% G (vf-f, up to 4 mm pebbles, SA-A, mafic-dominated). -63.85' - a thin ±1mm layer of lt ol. brown (2.5Y 5/6), sl. moist M. -63.85'- 63.97': Sand (S) 90% med. S as above G/M stringers grading to coarser S. -63.97 - 64.2' Sand (S) 95% S (10% f, 50% m, 40% c-vc), 60-70% felsic, A, ≤5% vf peb, unconsolidated, dry, lt. grayish brn. (2.5Y 6/2.5). | |
| 65 | Core #8C | | 64.2' - 65.2': Sand (S) 98% S (3% f, 90% m-c, 5% vc) 2% pebbles up to 2 cm, well-sorted, SA sand, 70% felsic, uncons., non-cemented, v. weak to no rxn w/ HCl, lt. yellowish brn. (2.5Y 6/3) | Core #8C HEIS #B36177 |
| 66 | | | | |

| Reported By: | | | |
|---|---|---|---|
| Jake Horner | Geologist | [signature] | 8-29-16 |
| Print Name | Title | Signature | Date |

| Reviewed By: | | | |
|---|---|---|---|
| | | | |
| Print Name | Title | Signature | Date |

**For Office Use Only**

| OR Doc Type: | WMU Code(s): |
|---|---|

A-6003-642 (REV 1)

| Well ID: C9512 | | Well Name: | | Location: | |
|---|---|---|---|---|---|
| Project: FY 200 @ 8-29-16 | | FY16 200-DV-1 Char. | | Reference Measure Point: Ground Surface | |

| Depth (ft) | Sample | Graphic Log | Sample Description: Sediment Classification, Grain Size Distribution, Color, Moisture Content, Sorting, Angularity, Mineralogy, Particle Size, Reaction to HCl, Other | Comments: Depth of Casing, Drilling Method, Sampling Method, Sampler Size, Water Level, Other |
|---|---|---|---|---|
| 123 | Core #B20 | | 123.0'-123.25': Sand (S) 100% well-sorted Sand (10%f, 60%m, 30%c), SA, uncons., v.wk. rxn w/ HCl, 50% mafic, sl. moist, lt. yellowish brn. (2.5y, 6/3). | Core #20B 123'-124' HEIS#B361F1 |
| | | | 123.25'-123.35': Sand (S) cont... grain size decreases to 40% vf-f, 50% m, 10% c, sl. moist, (2.5y, 6/3), v.wk. rxn HCl. | |
| 124 | Core #C20 | | 123.35'-123.55': Sand (S) ↑ G.S. 10% f, 50% m, 40% c-vc, 60% felsic, v.wk rxn w/ HCl, SA, lt. brn. gray (2.5y, 6/2), v.sl. moist, clean, no M. | Core #20C 124'-125' HEIS#B361F3 |
| | | | 123.55'-124.0' 125.0' @8-29-16: Sand (S) >95% vf-f Sand, <5% M, v.wk. cons., wk cem, moist, felsic-dom. (90%), lt. ol. brn., (2.5y, 5/4), sl. moldable sand with very little silt, well-sorted. | |
| 125 | | | -124.4' ~1cm thick layer of sl. coarser (mostly ~~som~~ fine) sand. -124.5' ~1cm thick layer of coarser fn. sand. | |
| 126 | | | | |

| Reported By: | | | | |
|---|---|---|---|---|
| Jake Horner | Geologist | | John Horner | 8-29-16 |
| Print Name | Title | | Signature | Date |

| Reviewed By: | | | | |
|---|---|---|---|---|
| | | | | |
| Print Name | Title | | Signature | Date |

# Appendix B

# Spiked-Contaminant Batch Experiments
# Individual Treatment Results

# Appendix B

# Spiked-Contaminant Batch Experiments
# Individual Treatment Results

The table below shows the individual treatment results for spiked-contaminant batch tests conducted to estimate the linear equilibrium partitioning coefficient ($K_d$). For this table, some data show negative computed $K_d$ values. Negative $K_d$ values are interpreted as indicating and estimate of zero for the $K_d$ value.

| Sample Name/Spike/Duration | Uranium | | Tc-99 (pertechnetate) | | Iodate | | Iodide | | Chromate | |
|---|---|---|---|---|---|---|---|---|---|---|
| | Adsorption $K_d$ (mL/g) | Desorption $K_d$ (mL/g) | Adsorption $K_d$ (mL/g) | Desorption $K_d$ (mL/g) | Adsorption $K_d$ (mL/g) | Desorption $K_d$ (mL/g) | Adsorption $K_d$ (mL/g) | Desorption $K_d$ (mL/g) | Adsorption $K_d$ (mL/g) | Desorption $K_d$ (mL/g) |
| Base Concentration Results in Pore-Water Matrix (Table 8) | | | | | | | | | | |
| PW-B35434 Spike-A-1d | 1.89 | 0.61 | 0.16 | 0.72 | 0.78 | 3.33 | 0.03 | -0.04 | 0.18 | 2.04 |
| PW-B35434 Spike-B-1d | 1.75 | 0.98 | 0.27 | 1.56 | 0.94 | 1.39 | 0.02 | -0.15 | 0.11 | 2.75 |
| PW-B35443 Spike-A-1d | 8.67 | 6.46 | 0.19 | 10.43 | 3.77 | 4.51 | -0.26 | -1.63 | 0.25 | 2.21 |
| PW-B35443 Spike-B-1d | 9.52 | 7.53 | 0.25 | 17.52 | 4.05 | 6.73 | -0.27 | -1.58 | 0.25 | 2.62 |
| PW-B361N1 Spike-A-1d | 5.06 | 5.73 | 0.21 | 0.72 | 6.73 | 7.59 | -0.07 | -0.78 | 0.20 | 1.74 |
| PW-B361N1 Spike-B-1d | 5.35 | 6.79 | 0.19 | 0.58 | 6.45 | 4.26 | -0.11 | -1.10 | 0.16 | 1.89 |
| PW-B35461 Spike-A-1d | 1.81 | 0.73 | 0.13 | 1.12 | 0.88 | 1.39 | -0.05 | -0.42 | 0.76 | NR |
| PW-B35461 Spike-B-1d | 1.46 | 1.02 | 0.08 | 0.70 | 0.75 | 1.26 | -0.06 | -0.56 | 0.28 | NR |
| PW-B361F3 Spike-A-1d | 2.49 | 1.53 | 0.10 | 0.20 | 0.78 | 1.30 | 0.08 | 0.06 | 0.12 | 1.34 |
| PW-B361F3 Spike-B-1d | 2.23 | 1.56 | 0.13 | 0.38 | 0.74 | 1.30 | 0.01 | -0.13 | 0.15 | 1.23 |
| PW-B36177 Spike-A-1d | 0.86 | 0.39 | 0.07 | 0.13 | 0.89 | 2.52 | 0.00 | -0.06 | 0.09 | 11.49 |
| PW-B36177 Spike-B-1d | 0.88 | 0.33 | 0.04 | 0.00 | 1.18 | 2.51 | -0.03 | -0.17 | 0.12 | 11.05 |
| PW-B35434 Spike-A-7d | 1.56 | 1.23 | 0.14 | 0.64 | 2.17 | 2.65 | -0.31 | -1.63 | 0.21 | 2.63 |
| PW-B35434 Spike-B-7d | 1.59 | 1.06 | 0.28 | 0.80 | 3.22 | 3.13 | 0.01 | 0.00 | 0.20 | 1.49 |
| PW-B35443 Spike-A-7d | 9.83 | 11.40 | 0.33 | 3.15 | 3.86 | 5.12 | -0.24 | -1.63 | 0.15 | 1.25 |
| PW-B35443 Spike-B-7d | 11.14 | 9.08 | 0.29 | 9.08 | 4.20 | 7.61 | -0.25 | -1.79 | 0.40 | 2.18 |
| PW-B361N1 Spike-A-7d | 5.73 | 4.98 | 0.14 | 0.40 | 5.79 | 6.17 | -0.09 | -0.93 | 0.30 | 1.64 |
| PW-B361N1 Spike-B-7d | 5.97 | 5.55 | 0.08 | 0.08 | 6.27 | 9.64 | -0.09 | -0.74 | 0.10 | 0.51 |
| PW-B35461 Spike-A-7d | 1.26 | 0.65 | 0.11 | 0.60 | 0.97 | 1.90 | -0.03 | -0.31 | 2.44 | 141.59 |
| PW-B35461 Spike-B-7d | 1.06 | 0.77 | 0.02 | 0.08 | 1.53 | 3.16 | -0.07 | -0.57 | 5.60 | NR |
| PW-B361F3 Spike-A-7d | 2.95 | 2.13 | 0.00 | -0.12 | 1.57 | 2.25 | 0.05 | 0.12 | 0.29 | 1.24 |
| PW-B361F3 Spike-B-7d | 2.74 | 1.87 | 0.06 | -0.03 | 1.75 | 2.22 | 0.02 | -0.05 | 0.29 | 1.62 |
| PW-B36177 Spike-A-7d | 0.69 | 0.66 | -0.04 | -0.48 | 1.39 | 3.37 | 0.06 | 0.29 | 0.21 | 17.88 |
| PW-B36177 Spike-B-7d | 0.80 | 0.21 | -0.01 | -0.06 | 1.28 | 2.95 | 0.03 | 0.03 | 0.27 | 13.44 |
| PW-B35434 Spike-A-28d | 1.23 | 0.91 | 0.16 | 0.36 | 1.23 | 3.70 | -0.03 | -0.27 | 0.64 | 3.54 |
| PW-B35434 Spike-B-28d | 1.57 | 1.03 | 0.28 | 0.60 | 1.03 | 3.83 | 0.00 | -0.16 | 0.48 | 3.07 |
| PW-B35443 Spike-A-28d | 8.00 | 9.87 | 1.01 | 8.35 | 3.50 | 3.23 | -0.34 | -1.18 | 0.34 | 1.25 |
| PW-B35443 Spike-B-28d | 8.12 | 10.73 | 0.51 | 10.47 | 2.95 | 3.79 | -0.35 | -1.08 | 0.49 | 1.73 |
| PW-B361N1 Spike-A-28d | 5.99 | 6.93 | 0.23 | 0.55 | 5.30 | 7.75 | -0.14 | -0.99 | 0.71 | 2.93 |
| PW-B361N1 Spike-B-28d | 4.85 | 6.34 | 0.11 | -0.01 | 4.95 | 10.37 | -0.10 | -0.86 | 0.59 | 2.11 |
| PW-B35461 Spike-A-28d | 0.34 | 0.43 | 0.19 | 0.65 | 0.79 | 1.74 | -0.10 | -0.40 | NR | NR |
| PW-B35461 Spike-B-28d | 0.78 | 0.98 | 0.30 | 0.88 | 0.75 | 2.20 | -0.11 | -0.55 | 8.64 | NR |
| PW-B361F3 Spike-A-28d | 1.56 | 3.54 | 0.14 | 0.04 | 0.60 | 0.90 | 0.00 | -0.13 | 0.72 | 3.47 |
| PW-B361F3 Spike-B-28d | 2.27 | 1.59 | 0.07 | -0.03 | 0.59 | 2.15 | -0.02 | -0.20 | 0.63 | 2.47 |
| PW-B36177 Spike-A-28d | 0.41 | 0.25 | 0.06 | -0.12 | 1.16 | 5.25 | -0.02 | -0.18 | 0.96 | 11.40 |
| PW-B36177 Spike-B-28d | 0.46 | 0.51 | 0.00 | -0.25 | 0.97 | 2.40 | 0.01 | 0.02 | 0.99 | 12.08 |

| Sample Name/Spike/Duration | Uranium | | Tc-99 (pertechnetate) | | Iodate | | Iodide | | Chromate | |
|---|---|---|---|---|---|---|---|---|---|---|
| | Adsorption $K_d$ (mL/g) | Desorption $K_d$ (mL/g) | Adsorption $K_d$ (mL/g) | Desorption $K_d$ (mL/g) | Adsorption $K_d$ (mL/g) | Desorption $K_d$ (mL/g) | Adsorption $K_d$ (mL/g) | Desorption $K_d$ (mL/g) | Adsorption $K_d$ (mL/g) | Desorption $K_d$ (mL/g) |
| Base Concentration Results in Artificial Groundwater Matrix (Table 9) | | | | | | | | | | |
| AGW-B35434 Spike-A-1d | NR | NR | -0.06 | -0.27 | 0.91 | 1.86 | -0.04 | -0.41 | 0.03 | 0.44 |
| AGW-B35434 Spike-B-1d | NR | NR | 0.14 | 0.79 | 1.06 | 1.92 | -0.07 | -0.52 | 0.01 | 0.27 |
| AGW-B35443 Spike-A-1d | NR | NR | 0.09 | 2.81 | 2.23 | 5.19 | -0.40 | -2.01 | 0.14 | 1.21 |
| AGW-B35443 Spike-B-1d | NR | NR | -0.01 | 0.86 | 2.18 | 3.72 | -0.40 | -2.19 | 0.03 | 0.56 |
| AGW-B361N1 Spike-A-1d | NR | NR | 0.04 | 0.25 | 5.81 | 7.31 | -0.17 | -1.22 | 0.11 | 0.65 |
| AGW-B361N1 Spike-B-1d | NR | NR | 0.05 | 0.35 | 6.07 | 7.40 | -0.20 | -1.47 | 0.07 | 0.53 |
| AGW-B35461 Spike-A-1d | NR | NR | 0.03 | 0.98 | 0.60 | 1.06 | -0.13 | -1.00 | 0.21 | 16.93 |
| AGW-B35461 Spike-B-1d | NR | NR | 0.23 | 3.88 | 0.62 | 0.93 | -0.11 | -0.99 | 0.13 | 19.51 |
| AGW-B361F3 Spike-A-1d | NR | NR | 0.05 | 0.25 | 0.80 | 1.25 | -0.04 | -0.36 | 0.05 | 0.22 |
| AGW-B361F3 Spike-B-1d | NR | NR | 0.06 | 0.27 | 0.78 | 1.00 | -0.03 | -0.29 | 0.07 | 0.31 |
| AGW-B36177 Spike-A-1d | NR | NR | -0.11 | -0.58 | 0.65 | 1.28 | -0.11 | -0.82 | 0.01 | 0.22 |
| AGW-B36177 Spike-B-1d | NR | NR | -0.01 | -0.14 | 0.70 | 1.33 | -0.08 | -0.57 | 0.01 | 0.29 |
| AGW-B35434 Spike-A-7d | NR | NR | 0.01 | -0.04 | 1.25 | 1.65 | -0.03 | -0.37 | 0.06 | 0.29 |
| AGW-B35434 Spike-B-7d | NR | NR | 0.07 | -0.01 | 1.19 | 1.71 | -0.05 | 0.28 | 0.05 | 0.37 |
| AGW-B35443 Spike-A-7d | NR | NR | 0.34 | 1.69 | 2.67 | 4.59 | -0.42 | -1.97 | 0.13 | 0.99 |
| AGW-B35443 Spike-B-7d | NR | NR | 0.29 | 1.40 | 2.55 | 2.90 | -0.40 | -2.14 | 0.12 | 0.94 |
| AGW-B361N1 Spike-A-7d | NR | NR | 0.07 | 0.10 | 5.90 | 4.67 | -0.22 | -1.36 | 0.09 | 0.50 |
| AGW-B361N1 Spike-B-7d | NR | NR | 0.06 | 0.05 | 4.30 | 3.40 | -0.17 | -1.29 | 0.14 | 0.56 |
| AGW-B35461 Spike-A-7d | NR | NR | 0.33 | 2.51 | 0.88 | 1.01 | -0.10 | -0.85 | 0.95 | 21.84 |
| AGW-B35461 Spike-B-7d | NR | NR | 0.20 | 2.19 | 0.72 | 0.89 | -0.12 | -0.93 | 0.51 | 14.85 |
| AGW-B361F3 Spike-A-7d | NR | NR | 0.10 | 0.23 | 0.93 | 1.04 | 0.01 | -0.23 | 0.22 | 0.67 |
| AGW-B361F3 Spike-B-7d | NR | NR | 0.05 | 0.33 | 0.96 | 1.23 | -0.03 | -0.32 | 0.16 | 0.55 |
| AGW-B36177 Spike-A-7d | NR | NR | -0.04 | -0.40 | 0.72 | 1.27 | -0.06 | -0.43 | 0.25 | 1.11 |
| AGW-B36177 Spike-B-7d | NR | NR | -0.01 | NR | 0.77 | 1.38 | -0.04 | -0.40 | 0.05 | 0.47 |
| AGW-B35434 Spike-A-28d | NR | NR | 0.04 | -0.43 | 1.33 | 1.64 | 0.04 | -0.05 | 0.40 | 1.64 |
| AGW-B35434 Spike-B-28d | NR | NR | 0.03 | 0.07 | 1.29 | 1.58 | -0.01 | -0.32 | 0.41 | 2.48 |
| AGW-B35443 Spike-A-28d | NR | NR | 0.25 | 0.54 | 2.62 | 3.83 | -0.40 | -1.90 | 0.16 | 0.83 |
| AGW-B35443 Spike-B-28d | NR | NR | 0.21 | 0.83 | 2.36 | 2.40 | -0.41 | -1.95 | 0.36 | 1.30 |
| AGW-B361N1 Spike-A-28d | NR | NR | -0.06 | -0.36 | 5.09 | 9.91 | -0.21 | -1.25 | 0.44 | 1.67 |
| AGW-B361N1 Spike-B-28d | NR | NR | -0.06 | -0.21 | 4.69 | 8.27 | -0.21 | -1.38 | 0.39 | 1.49 |
| AGW-B35461 Spike-A-28d | NR | NR | 0.23 | 0.99 | 0.70 | 1.06 | -0.09 | -0.88 | 3.03 | 31.81 |
| AGW-B35461 Spike-B-28d | NR | NR | 0.05 | -0.19 | 0.70 | 0.85 | -0.12 | -0.93 | 5.13 | 40.88 |
| AGW-B361F3 Spike-A-28d | NR | NR | -0.05 | -0.01 | 0.87 | 1.25 | 0.02 | -0.16 | 0.18 | 0.93 |
| AGW-B361F3 Spike-B-28d | NR | NR | -0.02 | -0.26 | 0.88 | 1.20 | -0.02 | -0.39 | 0.16 | 0.46 |
| AGW-B36177 Spike-A-28d | NR | NR | -0.11 | -0.70 | 0.85 | 1.53 | 0.01 | -0.04 | 0.11 | 1.06 |
| AGW-B36177 Spike-B-28d | NR | NR | -0.09 | -1.14 | 0.93 | 1.62 | -0.04 | -0.44 | 0.34 | 2.08 |

| Sample Name/Spike/Duration | Uranium | | Tc-99 (pertechnetate) | | Iodate | | Iodide | | Chromate | |
|---|---|---|---|---|---|---|---|---|---|---|
| | Adsorption $K_d$ (mL/g) | Desorption $K_d$ (mL/g) | Adsorption $K_d$ (mL/g) | Desorption $K_d$ (mL/g) | Adsorption $K_d$ (mL/g) | Desorption $K_d$ (mL/g) | Adsorption $K_d$ (mL/g) | Desorption $K_d$ (mL/g) | Adsorption $K_d$ (mL/g) | Desorption $K_d$ (mL/g) |
| Alternate Concentration Results (Spike 2 and Spike 3) in Pore-Water Matrix (Table 8) | | | | | | | | | | |
| PW-B35434 Spike 2-A-1d | 1.04 | -0.95 | -0.07 | 0.17 | 0.57 | 1.27 | 0.00 | -0.26 | 0.10 | 4.49 |
| PW-B35434 Spike 2-B-1d | 1.31 | -0.88 | 0.15 | 1.43 | 1.34 | 2.89 | -0.02 | -0.46 | 0.08 | NR |
| PW-B35461 Spike 2-A-1d | 1.35 | -0.44 | 0.14 | 3.63 | 0.57 | 1.34 | -0.05 | -0.68 | 0.21 | NR |
| PW-B35461 Spike 2-B-1d | 1.80 | 0.41 | -0.02 | 0.01 | 1.01 | 2.79 | -0.01 | -0.38 | 0.24 | NR |
| PW-B35434 Spike 3-A-1d | 2.03 | 0.51 | -0.03 | 0.51 | 0.31 | 0.49 | 0.08 | 0.15 | 0.04 | 0.38 |
| PW-B35434 Spike 3-B-1d | 1.46 | 1.46 | -0.03 | 0.35 | 0.74 | 1.27 | 0.08 | 0.20 | 0.02 | 0.44 |
| PW-B35461 Spike 3-A-1d | 1.64 | 0.80 | -0.10 | -0.89 | 0.25 | 0.37 | 0.00 | -0.23 | 0.09 | NR |
| PW-B35461 Spike 3-B-1d | 1.52 | 0.70 | 0.04 | 0.54 | 0.37 | 0.85 | -0.01 | -0.21 | 0.11 | NR |
| PW-B35434 Spike 2-A-7d | 1.87 | 0.99 | 0.58 | 1.29 | 0.68 | 1.39 | 0.16 | 0.35 | 0.14 | 3.82 |
| PW-B35434 Spike 2-B-7d | 1.25 | -0.32 | 0.53 | 1.04 | 0.25 | 0.67 | -0.01 | -0.17 | 0.17 | NR |
| PW-B35461 Spike 2-A-7d | 1.79 | 1.16 | 0.67 | 7.68 | 0.30 | 0.63 | -0.03 | -0.38 | 1.68 | NR |
| PW-B35461 Spike 2-B-7d | 1.15 | 0.81 | 0.76 | 8.35 | 0.34 | 0.20 | -0.07 | -0.60 | 2.45 | 25.70 |
| PW-B35434 Spike 3-A-7d | 2.77 | 2.30 | 0.46 | 1.72 | 0.62 | 1.11 | 0.06 | 0.01 | 0.06 | 0.37 |
| PW-B35434 Spike 3-B-7d | 2.73 | 2.03 | 0.45 | 1.51 | 0.85 | 2.51 | 0.01 | -0.09 | 0.11 | 0.68 |
| PW-B35461 Spike 3-A-7d | 1.65 | 1.49 | 0.32 | 2.08 | 0.71 | 1.66 | -0.01 | -0.23 | 0.85 | 92.31 |
| PW-B35461 Spike 3-B-7d | 2.64 | 2.22 | 0.51 | 4.11 | 0.59 | 1.63 | 0.01 | -0.07 | 0.51 | 31.43 |
| PW-B35434 Spike 2-A-28d | 1.15 | -0.37 | 0.67 | 1.09 | 0.52 | 0.17 | 0.05 | -0.06 | 0.65 | 6.01 |
| PW-B35434 Spike 2-B-28d | 1.53 | -0.28 | 0.56 | 1.04 | 0.59 | 0.21 | 0.03 | 0.03 | 0.92 | -1.21 |
| PW-B35461 Spike 2-A-28d | 1.18 | 1.32 | 0.39 | 2.08 | 0.13 | -0.48 | 0.01 | -0.01 | 20.59 | NR |
| PW-B35461 Spike 2-B-28d | 0.70 | -0.21 | 0.27 | 1.40 | 0.42 | 0.23 | 0.03 | 0.03 | 17.33 | NR |
| PW-B35434 Spike 3-A-28d | 1.69 | 1.56 | 0.39 | 0.90 | 0.43 | 0.21 | 0.13 | 0.25 | 0.32 | 1.74 |
| PW-B35434 Spike 3-B-28d | 4.30 | 3.60 | 0.43 | 0.87 | 0.59 | 0.50 | -0.02 | -0.23 | 0.42 | 2.25 |
| PW-B35461 Spike 3-A-28d | 3.63 | 2.50 | 2.04 | 10.12 | 0.04 | -0.59 | -0.01 | -0.18 | 18.80 | NR |
| PW-B35461 Spike 3-B-28d | 1.84 | 2.83 | 0.20 | 1.16 | 0.29 | 0.16 | 0.01 | -0.04 | 4.13 | NR |
| Alternate Concentration Results (Spike 2 and Spike 3) in artificial Groundwater Matrix (Table 9) | | | | | | | | | | |
| AGW-B35434 Spike 2-A-1d | NR | NR | 0.04 | 0.50 | 0.67 | 1.56 | 0.01 | -0.12 | 0.01 | 3.75 |
| AGW-B35434 Spike 2-B-1d | NR | NR | -0.06 | -0.20 | 0.54 | 1.32 | 0.04 | 0.02 | 0.03 | NR |
| AGW-B35461 Spike 2-A-1d | NR | NR | -0.10 | 0.12 | 0.24 | 0.72 | -0.05 | -0.58 | 0.21 | 8.73 |
| AGW-B35461 Spike 2-B-1d | NR | NR | -0.06 | -0.10 | 0.33 | 0.93 | -0.04 | -0.37 | 0.04 | NR |
| AGW-B35434 Spike 3-A-1d | NR | NR | 0.04 | 0.86 | 0.22 | 0.41 | 0.02 | -0.03 | 0.05 | 0.48 |
| AGW-B35434 Spike 3-B-1d | NR | NR | 0.00 | 0.37 | 0.13 | 0.02 | NR | NR | 0.01 | -0.05 |
| AGW-B35461 Spike 3-A-1d | NR | NR | -0.08 | 0.95 | 0.12 | -0.05 | -0.03 | -0.19 | 0.04 | 6.35 |
| AGW-B35461 Spike 3-B-1d | NR | NR | 0.02 | 1.20 | 0.13 | 0.15 | -0.02 | -0.13 | 0.06 | 4.42 |
| AGW-B35434 Spike 2-A-7d | NR | NR | 0.12 | 3.46 | 0.90 | 1.11 | 0.04 | 0.02 | 0.29 | 7.12 |
| AGW-B35434 Spike 2-B-7d | NR | NR | 0.16 | 0.45 | 0.75 | 1.25 | 0.01 | 0.00 | 0.14 | 6.77 |
| AGW-B35461 Spike 2-A-7d | NR | NR | 0.30 | 2.71 | 0.39 | 0.69 | 0.02 | 0.12 | 2.84 | NR |
| AGW-B35461 Spike 2-B-7d | NR | NR | 0.28 | 7.13 | 0.38 | 0.65 | -0.01 | -0.14 | 2.39 | NR |
| AGW-B35434 Spike 3-A-7d | NR | NR | 0.09 | 0.35 | 0.59 | 0.93 | 0.04 | 0.01 | 0.05 | 0.25 |
| AGW-B35434 Spike 3-B-7d | NR | NR | 0.11 | 0.57 | 0.63 | 1.20 | 0.02 | -0.06 | 0.11 | 0.59 |

B.4

| | Uranium | | Tc-99 (pertechnetate) | | Iodate | | Iodide | | Chromate | |
|---|---|---|---|---|---|---|---|---|---|---|
| Sample Name/Spike/Duration | Adsorption $K_d$ (mL/g) | Desorption $K_d$ (mL/g) | Adsorption $K_d$ (mL/g) | Desorption $K_d$ (mL/g) | Adsorption $K_d$ (mL/g) | Desorption $K_d$ (mL/g) | Adsorption $K_d$ (mL/g) | Desorption $K_d$ (mL/g) | Adsorption $K_d$ (mL/g) | Desorption $K_d$ (mL/g) |
| AGW-B35461 Spike 3-A-7d | NR | NR | 0.51 | 8.76 | 0.27 | 0.66 | 0.02 | 0.00 | 0.37 | 7.77 |
| AGW-B35461 Spike 3-B-7d | NR | NR | 0.28 | 4.22 | 0.28 | 0.67 | 0.00 | -0.11 | 0.37 | 8.35 |
| AGW-B35434 Spike 2-A-28d | NR | NR | 0.23 | 0.24 | 1.09 | 1.61 | 0.07 | 0.26 | 0.42 | 8.52 |
| AGW-B35434 Spike 2-B-28d | NR | NR | 0.17 | 0.12 | 1.06 | 1.72 | 0.06 | 0.08 | -0.09 | 2.27 |
| AGW-B35461 Spike 2-A-28d | NR | NR | -0.06 | -0.21 | 0.54 | 1.35 | 0.00 | -0.14 | NR | NR |
| AGW-B35461 Spike 2-B-28d | NR | NR | 0.46 | 5.03 | 0.47 | 1.08 | 0.01 | -0.03 | NR | NR |
| AGW-B35434 Spike 3-A-28d | NR | NR | 0.13 | 0.15 | 0.65 | 1.01 | 0.08 | 0.18 | 0.18 | 0.81 |
| AGW-B35434 Spike 3-B-28d | NR | NR | 0.03 | -0.21 | 0.59 | 0.95 | 0.05 | 0.00 | 0.25 | 1.13 |
| AGW-B35461 Spike 3-A-28d | NR | NR | 0.11 | 1.02 | 0.33 | 0.83 | 0.02 | 0.05 | 3.44 | 97.93 |
| AGW-B35461 Spike 3-B-28d | NR | NR | 0.09 | 1.24 | 0.34 | 0.83 | 0.00 | -0.14 | 21.75 | NR |

# Distribution

**No. of**
**Copies**

**No. of**
**Copies**

1 **External Distribution**
CH2M Hill Plateau Remediation
Company
   Mark Byrns       (PDF)

24 **Local Distribution**
Pacific Northwest National Laboratory

| | |
|---|---|
| MJ Truex | (PDF) |
| JE Szecsody | (PDF) |
| NP Qafoku | (PDF) |
| CE Strickand | (PDF) |
| JJ Moran | (PDF) |
| BD Lee | (PDF) |
| MM Snyder | (PDF) |
| AR Lawter | (PDF) |
| CT Resch | (PDF) |
| BN Gartman | (PDF) |

| | |
|---|---|
| L Zhong | (PDF) |
| MK Nims | (PDF) |
| DL Saunders | (PDF) |
| BD Williams | (PDF) |
| JA Horner | (PDF) |
| II Leavy | (PDF) |
| SR Baum | (PDF) |
| BB Christiansen | (PDF) |
| RE Clayton | (PDF) |
| EM McElroy | (PDF) |
| D Appriou | (PDF) |
| KJ Tyrrell | (PDF) |
| ML Striluk | (PDF) |
| Information Release | (PDF) |